



*Global-scale Observations of the
Limb and Disk (GOLD)*

Public Science Data Products Guide

[Revision 4.4 – August 5, 2022]

Changes

| Revision | Date | Changes |
|-----------------|-------------|--|
| 1.0 | 2/28/2019 | Initial Release (Level 1 data only) |
| 2.0 | 6/3/2019 | Added information on Level 2 data |
| 3.0 | 9/16/2019 | Updated sections 3.1.6.2 (Flatfield Correction) and 3.5.5 (Level 1C Background Subtraction) |
| 4.0 | 4/2/2021 | Reformatted and added additional information to Section 3 (Level 1 Data Products) Updated Section 3 (Level 1 Data Products) and Section 4 (Level 2 Data Products) to reflect changes in latest versions of data products. |
| 4.1 | 5/20/2021 | Added additional information about L1B data product generation and file contents (sections 3.2 and 3.3) |
| 4.2 | 8/5/2021 | Added additional information about L0 Science data format (Section 3) |
| 4.3 | 11/17/2021 | Updated L2 O2DEN file contents (section 5.2.2) |
| 4.4 | 8/5/2022 | Corrected variable names in table 4-10: Level 1C Stellar Occultation Disk File Contents. Corrected units in table 5-2: NMAX File Contents. |

Table of Contents

| | | |
|----------|--|-----------|
| 1 | STARTING MATERIAL | 8 |
| 1.1 | REFERENCE DOCUMENTS | 8 |
| 1.2 | ACRONYMS/ABBREVIATIONS | 8 |
| 1.3 | DEFINITIONS | 9 |
| 1.4 | SCOPE | 9 |
| 2 | DATA OVERVIEW | 10 |
| 2.1 | DATA PRODUCT DEFINITIONS | 10 |
| 2.2 | DATA PRODUCT DETAILS | 11 |
| 2.3 | FILE NAMING CONVENTIONS | 12 |
| 2.4 | DATA BINNING | 14 |
| 2.5 | SLIT INFORMATION | 14 |
| 2.6 | NOMINAL DAILY OBSERVING PLAN | 15 |
| 3 | LEVEL 0 SCIENCE DATA | 17 |
| 3.1 | LEVEL 0 SCIENCE DATA FORMAT | 17 |
| 3.2 | LEVEL 0 CCSDS PACKET DESCRIPTION | 18 |
| 4 | LEVEL 1 DATA PRODUCTS | 24 |
| 4.1 | GENERATING LEVEL 1A DATA | 24 |
| 4.1.1 | <i>Time Adjustment</i> | 24 |
| 4.1.2 | <i>Telemetry Coefficients</i> | 25 |
| 4.1.3 | <i>NetCDF File Format</i> | 25 |
| 4.2 | GENERATING LEVEL 1B DATA | 25 |
| 4.2.1 | <i>Detector and Photon Event Data Description</i> | 25 |
| 4.2.2 | <i>Stim Pulse Location Correction</i> | 25 |
| 4.2.3 | <i>Geometric Correction</i> | 26 |
| 4.2.4 | <i>Optical Correction</i> | 26 |
| 4.2.5 | <i>Pulse Height Filtering</i> | 26 |
| 4.2.6 | <i>Spatial/Spectral/Temporal Binning</i> | 26 |
| 4.2.7 | <i>Global Dead Time Correction</i> | 27 |
| 4.2.8 | <i>Local Dead Time Correction</i> | 27 |
| 4.2.9 | <i>Geolocation Information</i> | 27 |
| 4.3 | L1B DATA FILE CONTENTS | 31 |
| 4.3.1 | <i>Generic L1B Metadata</i> | 31 |
| 4.3.2 | <i>L1B File Content for Atmosphere Observations</i> | 34 |
| 4.3.3 | <i>L1B File Content for Occultation Observations</i> | 38 |
| 4.4 | GENERATING LEVEL 1C DATA | 41 |
| 4.4.1 | <i>Disk and Limb Observations</i> | 41 |
| 4.4.1.1 | Flatfield Correction | 43 |
| 4.4.1.2 | 2-D Sensitivity Correction | 43 |
| 4.4.1.3 | Particle Background Subtraction | 44 |
| 4.4.1.4 | Spatial Binning | 44 |
| 4.4.1.5 | Wavelength Registration | 44 |
| 4.4.1.6 | Residual Background and Scattered Light Subtraction | 44 |
| 4.4.1.7 | Radiometric Calibration | 46 |

| | | |
|----------|--|-----------|
| 4.4.1.8 | Uncertainty Definitions | 46 |
| 4.4.2 | <i>Occultation Observations</i> | 46 |
| 4.4.2.1 | Flatfield Correction | 46 |
| 4.4.2.2 | 2-D Sensitivity Correction | 46 |
| 4.4.2.3 | Particle Background Subtraction | 46 |
| 4.4.2.4 | Background Subtraction | 46 |
| 4.4.2.5 | Wavelength Registration | 47 |
| 4.4.2.6 | Radiometric Calibration | 48 |
| 4.5 | GENERIC L1C METADATA..... | 48 |
| 4.6 | L1C AND L1D DAY DISK SCAN DATA PRODUCTS..... | 51 |
| 4.6.1 | <i>Day Disk Scan Observations</i> | 51 |
| 4.6.2 | <i>Level 1C Data File Structure and Content</i> | 53 |
| 4.6.3 | <i>Level 1D Data File Structures</i> | 55 |
| 4.7 | L1C AND L1D LIMB SCAN DATA PRODUCTS..... | 56 |
| 4.7.1 | <i>Limb Scan Observations</i> | 56 |
| 4.7.2 | <i>Level 1C Data File Structure and Contents</i> | 57 |
| 4.7.3 | <i>Level 1D Data File Structures</i> | 60 |
| 4.8 | L1C AND L1D NIGHT DISK SCAN DATA PRODUCTS..... | 62 |
| 4.8.1 | <i>Night Disk Scan Observations</i> | 62 |
| 4.8.2 | <i>Level 1C Data File Content</i> | 63 |
| 4.8.3 | <i>Level 1D Data File Structures</i> | 64 |
| 4.9 | L1C AND L1D STELLAR OCCULTATION DATA PRODUCTS..... | 66 |
| 4.9.1 | <i>Stellar Occultation Observations</i> | 66 |
| 4.9.2 | <i>Level 1C Data File Structures</i> | 67 |
| 4.9.3 | <i>Level 1D Data File Structures</i> | 68 |
| 5 | LEVEL 2 DATA PRODUCTS | 70 |
| 5.1 | NMAX DATA PRODUCT..... | 70 |
| 5.1.1 | <i>Algorithm Description</i> | 70 |
| 5.1.2 | <i>Data File Structures</i> | 72 |
| 5.1.2.1 | NMAX File Contents | 72 |
| 5.1.2.2 | NMAX Data Quality Index | 73 |
| 5.2 | O2DEN DATA PRODUCT..... | 74 |
| 5.2.1 | <i>Algorithm Description</i> | 74 |
| 5.2.2 | <i>Data File Structures</i> | 75 |
| 5.2.2.1 | O2DEN File Contents | 75 |
| 5.2.2.2 | O2DEN Data Quality Index Definitions | 77 |
| 5.3 | ON2 DATA PRODUCT..... | 77 |
| 5.3.1 | <i>Algorithm Description</i> | 77 |
| 5.3.2 | <i>Data File Structures</i> | 79 |
| 5.3.2.1 | ON2 File Contents | 79 |
| 5.3.2.2 | ON2 Data Quality Index | 80 |
| 5.4 | QEUV DATA PRODUCT..... | 80 |
| 5.4.1 | <i>Algorithm Description</i> | 80 |
| 5.4.2 | <i>Data File Structures</i> | 82 |
| 5.4.2.1 | QEUV File Contents | 82 |
| 5.4.2.2 | QEUV Data Quality Index | 83 |
| 5.5 | TDISK DATA PRODUCT..... | 84 |
| 5.5.1 | <i>Algorithm Description</i> | 84 |

| | | |
|---------|------------------------------------|----|
| 5.5.2 | <i>Data File Structures</i> | 85 |
| 5.5.2.1 | TDISK File Contents | 85 |
| 5.5.2.2 | TDISK Data Quality Index | 86 |
| 5.6 | TLIMB DATA PRODUCT..... | 86 |
| 5.6.1 | <i>Algorithm Description</i> | 86 |
| 5.6.2 | <i>Data File Structures</i> | 88 |
| 5.6.2.1 | TLIMB File Contents | 88 |
| 5.6.2.2 | TLIMB Data Quality Index | 89 |

Table of Figures

| | | |
|-------------|---|----|
| Figure 2-1 | Typical Daily Observations..... | 15 |
| Figure 3-1 | Level 0 Data Structure | 17 |
| Figure 3-2 | CCSDS Packet Header (12) | 18 |
| Figure 3-3 | Det A photons – FPGA (32)..... | 19 |
| Figure 3-4 | Det B photons – FPGA (30)..... | 20 |
| Figure 3-5 | Det A/B Scan Mirror – FPGA (6)..... | 21 |
| Figure 3-6 | S/C – SW (8)..... | 21 |
| Figure 3-7 | Det A - SW (36)..... | 22 |
| Figure 3-8 | Det A - SW (36)..... | 23 |
| Figure 4-1 | Level 0 to Level 1B Processing | 24 |
| Figure 4-2 | Geolocation geometry for day and night disk observations..... | 28 |
| Figure 4-3 | Geolocation geometry for limb scan observations..... | 29 |
| Figure 4-4 | Geolocation geometry for occultation observations. | 30 |
| Figure 4-5 | Level 1B to Level 1C Processing..... | 43 |
| Figure 4-6 | Reference Wavelengths for Background | 45 |
| Figure 4-7 | Wavelength Dependence of Background at one 1C Spatial Location | 45 |
| Figure 4-8 | Occultation background subtraction algorithm. The image is total spectral counts as a function of time for a total of 300 seconds and of L1B row..... | 47 |
| Figure 4-9 | Day Disk Scan Observation | 52 |
| Figure 4-10 | GOLD Field of View | 52 |
| Figure 4-11 | Level 1C Bins..... | 53 |
| Figure 4-12 | Example Level 1D Combined Day Disk File | 56 |
| Figure 4-13 | Limb Scan | 57 |
| Figure 4-14 | Grid for Limb Scan | 58 |
| Figure 4-15 | Fixed Grid for Limb Scan | 59 |

| | |
|---|----|
| Figure 4-16 Example Level 1D Combined Limb File | 62 |
| Figure 4-17 Night Disk Scan - Low Resolution Slit (NI1) | 63 |
| Figure 4-18 Example Level 1D Combined Night 1 File..... | 65 |
| Figure 4-19 Occultation Observation..... | 66 |
| Figure 4-20 Example Level 1D Combined Occultation File | 69 |

Table of Tables

| | |
|--|----|
| Table 2-1 Data Product Definition..... | 10 |
| Table 2-2 Data Product Details..... | 12 |
| Table 2-3 File Naming Conventions..... | 13 |
| Table 2-4 Data Binning..... | 14 |
| Table 2-5 Slit Geometry..... | 14 |
| Table 4-1 Generic L1B Metadata | 34 |
| Table 4-2 L1B File Content for Atmosphere Observations..... | 38 |
| Table 4-3 L1B File Content for Occultation Observations..... | 41 |
| Table 4-4 L1C Generic Metadata | 51 |
| Table 4-5 Variances from the generic metadata | 51 |
| Table 4-6 Level 1C Day Disk File Content | 55 |
| Table 4-7 L1D Radiance Band Definitions | 56 |
| Table 4-8 Level 1C Limb File Content..... | 60 |
| Table 4-9 Level 1C Night Disk Scan File Content | 64 |
| Table 4-10 Level 1C Stellar Occultation Disk File Contents | 68 |
| Table 4-11 Occultation L1D Spectral Bins..... | 68 |
| Table 4-12 Occultation L1D Altitude Bins..... | 68 |
| Table 5-1 Level 2 data products and L1C dependence..... | 70 |
| Table 5-2 NMAX File Content..... | 73 |
| Table 5-3 NMAX Data Quality Index | 73 |
| Table 5-4 O2DEN File Contents..... | 76 |
| Table 5-5 O2DEN Data Quality Index | 77 |
| Table 5-6 ON2 File Content | 80 |
| Table 5-7 ON2 Data Quality Index..... | 80 |
| Table 5-8 QEUV File Content | 83 |

| | |
|---|----|
| Table 5-9 QEUV Data Quality Index | 83 |
| Table 5-10 TDISK File Content | 86 |
| Table 5-11 TDISK Data Quality Index..... | 86 |
| Table 5-12 TLIMB File Contents | 89 |
| Table 5-13 TLIMB Data Quality Index | 90 |

1 Starting Material

1.1 Reference Documents

| Title | Reference |
|---|---|
| GOLD Release Notes | Latest release notes are available on the GOLD website: http://gold.cs.ucf.edu/documentation/ |
| Global-Scale Observations of the Limb and Disk Mission: 1. Instrument Design and Early Flight Performance | https://doi.org/10.1029/2020JA027809 . Available at http://gold.cs.ucf.edu/publications/ |
| Global-Scale Observations of the Limb and Disk Mission: 2. Observations, Data Pipeline, and Level 1 Data Products | https://doi.org/10.1029/2020JA027797 . Available at http://gold.cs.ucf.edu/publicatins/ |

1.2 Acronyms/Abbreviations

| Acronym | Meaning |
|---------|--|
| CHA | Channel A |
| CHB | Channel B |
| DAY | Daytime Disk Observations using the HR slit |
| DLR | Daytime Disk Observations using the LR slit |
| DQI | Data Quality Index |
| FOV | Field of View |
| GOLD | Global-scale Observations of the Limb and Disk |
| GSFC | Goddard Space Flight Center |
| GYM | Grating Yaw Mechanism |
| HR | High Resolution |
| LASP | Laboratory for Atmospheric and Space Physics |
| LIM | Limb Observations using the HR slit |
| LR | Low Resolution |
| MCP | Microchannel Plate |
| NetCDF | Network Common Data Format |

| | |
|-------|--|
| NII | Nighttime Disk Observations (Equatorial Arcs) |
| OCC | Occultation Observations using the OCC slit |
| SDC | Science Data Center |
| SOC | Science Operations Center |
| SPDF | Space Physics Data Facility |
| SPICE | Spacecraft, Planet, Instrument, C-matrix, and Events |
| TDB | Barycentric Dynamical Time |
| UCF | University of Central Florida |

1.3 Definitions

Archive – Where the GOLD science data is kept in order to be preserved.

Data Quality Index – Flags to indicate quality of the data.

1.4 Scope

This document describes the publicly available science data products for the Global-scale Observations of the Limb and Disk (GOLD) mission.

2 Data Overview

2.1 Data Product Definitions

| Level | Brief Description | Publicly Available? |
|-----------------|---|--------------------------------|
| 0 | GOLD telemetry as received from the GOLD Ground Station (GGS). Consultative Committee on Space Data Standards (CCSDS) Coded Virtual Channel Data Unit (CVCDUs) [fill VCDUs removed] contained in Cortex Data Transfer format. Binary files on 1-minute cadence. | No |
| 1A | Time-tagged series of photon detection events, including detector location and pulse heights. Data numbers converted to engineering units. (Time in Coordinated Universal Time (UTC)) Separate A and B channel NetCDF files on 1-minute cadence. | No |
| 1B | Data binned and mapped in GOLD coordinates, with geolocation information included. Retain highest resolution conceivably required for all downstream data products. Converts time series of photon events into an image data cube. Separate A and B channel NetCDF files on 1-minute cadence. | Via SPDF |
| 1C | Geolocated data sampled on fixed spatial grids in both counts and radiance or irradiance (calibrated) units. Includes backgrounds and radiance/irradiance error estimates. Data are binned spatially and spectrally, as required for each OBS_TYP and Level 2 algorithm. Separate A and B channel Network Common Data Form (NetCDF) files for each observation, cadence dependent on observation type. | Via the GOLD web site and SPDF |
| Quicklook (L1D) | Images of disk radiance at key wavelengths. Separate A and B channel PNG files for each disk scan. | Via the GOLD web site and SPDF |
| L2 | Daily files produced for each geophysical data product. | Via the GOLD web site and SPDF |

Table 2-1 Data Product Definition

2.2 Data Product Details

| Level 1C | |
|-------------|---|
| Calibration | <ul style="list-style-type: none"> • Geolocated data on fixed spatial grids in both counts and calibrated (radiance for atmosphere emission or irradiance for occultations) units. Includes backgrounds and radiance/irradiance error estimates. • Data are binned spatially and spectrally, as required for each OBS_TYP and Level 2 algorithm. • Separate files for CH A/B and each OBS_TYP (DAY, DLR, NI1, LIM, OCC) |
| Definition | <p>Day (disk images): OBS_TYP = DAY and DLR</p> <ul style="list-style-type: none"> • 0.2° x 0.2° spatial sampling (125×125 km² at nadir). • 0.04 nm spectral sampling. • Data cube: 104 x 92 x 800 pixels (N/S x E/W x spectral). • Cadence: ~ 30 minutes <p>Night 1 (disk images): OBS_TYP = NI1</p> <ul style="list-style-type: none"> • 0.15°×0.15° spatial resolution. • 0.04 nm spectral sampling. • Data cube: N/S and E/W dimensions vary, 800 pixels spectral. • Cadence: ~ 20 minutes <p>Limb (profiles): OBS_TYP = LIM</p> <ul style="list-style-type: none"> • 16 km tangent altitude x 1.25° latitude resolution. • 0.04 nm spectral sampling. • Data cube: 30 x 32 x 800 pixels (tangent altitude x latitude x spectral) • Cadence : ~ 30 minutes <p>Occultations: OBS_TYP = OCC</p> <ul style="list-style-type: none"> • altitude resolution: 0.9 km at 0° latitude, 0.45 km at 60° latitude • 0.12 nm spectral sampling. • Data dimensions: 980 x 266 (E/W-altitude x spectral) • Cadence: ~10 per day at irregular cadence |
| Level 1D | |
| Definition | Quick-look products generated from L1C. Will consist of images or profiles of radiance at key wavelengths. One or more files per L1C file. |
| Details | Images only. |

| Level 2 | | |
|------------|---|--|
| Definition | Retrieved geophysical parameters | |
| | Day Disk | ON2 - O/N ₂ column density ratio (Includes OI and LBH integrated radiance) QEUV - Solar EUV proxy TDISK - Neutral temperature |
| | Night Disk | NMAX - Peak electron density (Includes crest locations and intensities & OI radiance) |
| | Limb (day) | TLIMB - Exospheric temperature, T _{exo} . |
| | Occultation (day & night) | O2DEN - O ₂ density profile |
| Details | Daily files produced for each geophysical data product. Contains each individual specific observation type data taken throughout the corresponding day. | |

Table 2-2 Data Product Details

2.3 File Naming Conventions

| Data Level | Description |
|------------|--|
| L1C | <p>GOLD_L1C_CHX_TYP_yyyy_ddd_hh_mm_vAA_rBB_cCC.nc</p> <p>X = "A" or "B"</p> <p>TYP is the type of observation: "LIM", "OCC", "DAY", "NI1", "NI2", "DLR", "SP1", "SP2", "SP3" to correspond respectively with Limb, Occultation, Day Disk, Night Disk 1, Night Disk 2, Disk Low Resolution, Special Observation 1, Special Observation 3, Special Observation 3, in the OBS_TYP field, as done in the Level 1B files.</p> <p>yyyy_ddd_hh_mm is the year, day of year, hour and minute corresponding to the start of this observation event.</p> <p>AA is the file version number, 2 decimal characters from 01 to 99, which increments by 1 when a full-mission reprocessing is required for the given data product. Each data product version, revision and cycle numbers may be independent of the other data product types.</p> <p>BB is the file revision number, 2 decimal characters from 01 to 99, which increments by 1 when there is a new input configuration or calibration file is used, or when the change does not require full-mission reprocessing. Each data product version, revision and cycle numbers may be independent of the other data product types.</p> <p>CC is the file cycle number, 2 decimal characters from 01 to 99, which increments when a data product must be regenerated due to a loss of data or interruption that can be remedied without new code delivery. Each data product version, revision and cycle numbers may be independent of the other data product types.</p> <p>Example: GOLD_L1C_CHA_OCC_2015_222_23_00_v01_r01_c01.nc</p> |

| Data Level | Description |
|------------------------------|--|
| <p>L1D</p> | <p>The file naming convention for combined Level 1D data file is: GOLD_L1D_CHX_TYP_yyyy_ddd_hh_mm_vAA_rBB_cCC.png</p> <p>X = "A" or "B"</p> <p>TYP is the type of observation: "LIM", "OCC", "DAY", "NI1", "NI2", "DLR", "SP1", "SP2", "SP3" to correspond respectively with Limb, Occultation, Day Disk, Night Disk 1, Night Disk 2, Disk Low Resolution, Special Observation 1, Special Observation 3, Special Observation 3 in the OBS_TYP field, as done in the Level 1C files.</p> <p>yyyy_ddd_hh_mm is the year, day of year, hour and minute corresponding to the start of this observation event.</p> <p>AA is the file version number, 2 decimal characters from 01 to 99, which increments by 1 when a full-mission reprocessing is required for the given data product. Each data product version, revision and cycle numbers may be independent of the other data product types.</p> <p>BB is the file revision number, 2 decimal characters from 01 to 99, which increments by 1 when there is a new input configuration or calibration file is used, or when the change does not require full-mission reprocessing. Each data product version, revision and cycle numbers may be independent of the other data product types.</p> <p>CC is the file cycle number, 2 decimal characters from 01 to 99, which increments when a data product must be regenerated due to a loss of data or interruption that can be remedied without new code delivery. Each data product version, revision and cycle numbers may be independent of the other data product types.</p> <p>Example: GOLD_L1D_CHA_OCC_2015_222_23_00_v01_r01_c01.nc</p> |
| <p>L2</p> <p>Daily Files</p> | <p>GOLD_L2_PROD_yyyy_ddd_vAA_rBB.nc</p> <p>PROD is the Level 2 data product: "ON2", "QEUV", "TDISK", "TLIMB", "O2DEN" or "NMAX"</p> <p>yyyy_ddd is the year and day of year covered by data in the file.</p> <p>AA is the file version number, 2 decimal characters from 01 to 99, which increments by 1 when a full-mission reprocessing is required for the given data product. Each data product version, revision and cycle numbers may be independent of the other data product types.</p> <p>BB is the file revision number, 2 decimal characters from 01 to 99, which increments by 1 when there is a new input configuration or calibration file is used, or when the change does not require full-mission reprocessing. Each data product version, revision and cycle numbers may be independent of the other data product types.</p> <p>CC is the file cycle number, 2 decimal characters from 01 to 99, which increments when a data product must be regenerated due to a loss of data or interruption that can be remedied without new code delivery. Each data product version, revision and cycle numbers may be independent of the other data product types.</p> <p>Example: GOLD_L2_TDISK_2015_222_v01_r01_c01.nc</p> |

Table 2-3 File Naming Conventions

2.4 Data Binning

| OBS_TYPE | L1C Binning |
|---|---|
| Day Disk | <ul style="list-style-type: none"> Angular spacing (E-W, N-S) x spectral sampling (nm): 0.2° x 0.2° x 0.04nm array size: [92 bins E-W, 104 bins N-S, 800 spectral bins] HR slit: 125km x 125km with ~ 0.2 nm spectral resolution (DAY) LR slit: 125km x 125km with ~ 0.4 nm spectral resolution (DLR) |
| Limb | <ul style="list-style-type: none"> Angular spacing (radial, azimuthal) x x spectral sampling (nm): 0.022° x 1.25° x 0.04nm array size: [30 tangent altitude (from -44 to 436 km), 32 latitude, 800 spectral bins] HR slit: 16km tangent altitude x 1.25° latitude with ~ 0.2 nm spectral resolution |
| Occultation | <ul style="list-style-type: none"> Temporal spacing (seconds) x spectral sampling (nm): 300ms x 0.12 nm array size: [980 time steps x 266 spectral bins] OCC slit: 0.9 km at 0° latitude to 0.45 km at 60° latitude with ~ 0.12 nm spectral resolution (set by stellar image diameter) |
| Night Disk - Low Resolution Slit (OBS_TYPE = NI1) | <ul style="list-style-type: none"> Angular spacing (E-W, N-S) x spectral sampling (nm) 0.15° x 0.15° x 0.04nm Unchanged L1B bins summed to dwell time for each mirror position. E-W binning and spectral resolution determined by slit width; N-S binning to approximate the same angular resolution. No further binning is done (does not map to fixed lat-lon grid). LR slit: ~ 0.4 nm spectral resolution |

Table 2-4 Data Binning

2.5 Slit Information

| Slit | Width | Height |
|-----------------|-----------------------------------|-----------------------|
| High Resolution | 0.0764°, ~47.7 km (nadir) | 11°, ~6956 km (nadir) |
| Low Resolution | 0.1528°, ~95.4 km (nadir) | 11°, ~6956 km (nadir) |
| Occultation | 1°, ~740 km (limb at the equator) | 10°, ~6310 km (nadir) |

Table 2-5 Slit Geometry

2.6 Nominal Daily Observing Plan

Figure 2-1 summarizes a typical daily sequence of GOLD observations.

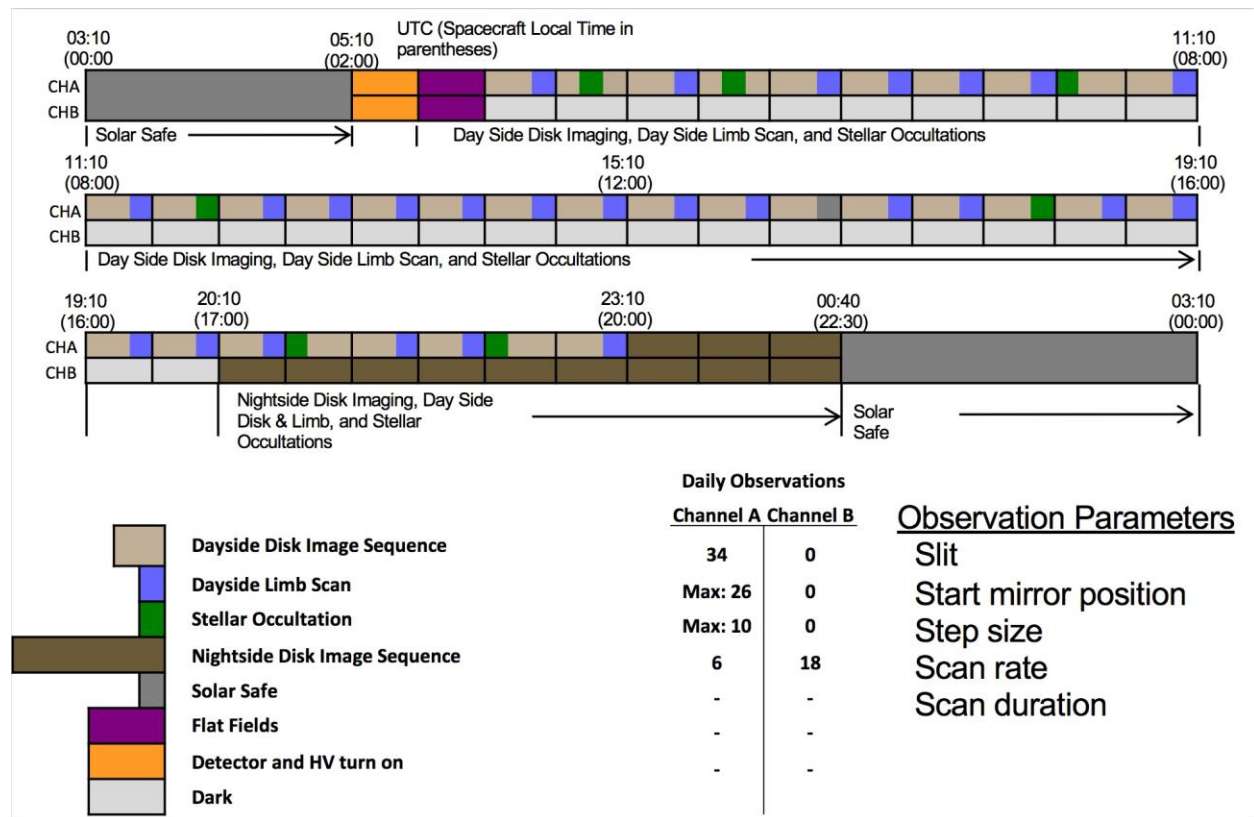


Figure 2-1 Typical Daily Observations

Each GOLD instrument channel consists of a telescope and imaging spectrograph. The telescope makes an instantaneous image of the Earth the spectrograph entrance slit, which is 11.2° tall and cover slightly more than half of the Earth’s 17° wide disk in the north-south direction. A scan mirror within each channel moves the image of the Earth across its spectrograph entrance slit east – west in a series of 345 steps, each 0.0522° wide, resulting in a step-to-step motion of 32.6 km at nadir in order to build up 3-dimensional image cubes. Each step includes a 2-second dwell during which the channel acquires a single spectral-spatial image. Two swaths, one covering the northern hemisphere and the other covering the southern hemisphere, provide a full disk image cube. Each swath requires ~12 minutes to complete (24 minutes for a complete disk map).

Following the disk observation, the channels scan both the north and south hemispheres of the dayside limb. The limb scans begin on the disk at a limb-height of -50 km at the equator and scan to a limb height of ~430 km with a step size of 0.011° (8 km at the limb, 41650 km distant from the instrument) and a cadence of 2 seconds per step. The two limb scans require 6 minutes to execute. Scans are interrupted when bright stars suitable for occultation measurements approach either limb.

To perform the occultation measurement, a slit mechanism inserts the 1° slit at the telescope focal plane, and the scan mirror slews the FOV center to a point ~ 225 km above the surface at the

latitude of the occultation (OCC mode). An occultation experiment duration is 6 minutes including time for setup and ~ 4 minutes for observation.

Nighttime scans commence at 17:00 local time, beginning $\sim 15^\circ$ in longitude east of the terminator and extend eastward. A single nightside sequence consists of a pair of ~ 15 -minute swaths, one of the north and one of the south, each with a fixed 0.149° (92.8 km at nadir) step size, which is slightly less than the 0.153 mm LR slit. The number of steps for the first pair are 20 and 24, the dwell times are 42 seconds and 36 seconds, and the longitude scan ranges at the equator are $\sim 26.8^\circ$ and 24.7° , respectively. Times and scan lengths are adjusted as the terminator rotates westward.

3 Level 0 Science Data

The Level 0 GOLD Science data consists of the raw binary CCSDS packets received on the ground. The packets contains both instrument telemetry and science measurements. The format and organization of the science packets is described below.

3.1 Level 0 Science Data Format

The breakdown of the L0 data format (Figure 3-1) is separated in multiple parts: from the raw data received by the ground stations Channel Access Data Unit (CADU) to the Consultative Committee for Space Data Systems (CCSDS) Science data packet format. The CADUs have a constant size of 250 bytes of which 206 bytes contains the actual telemetry data fields. We receive 300 CADU frames in 100 msec for a transfer rate of 750,000 bytes per seconds.

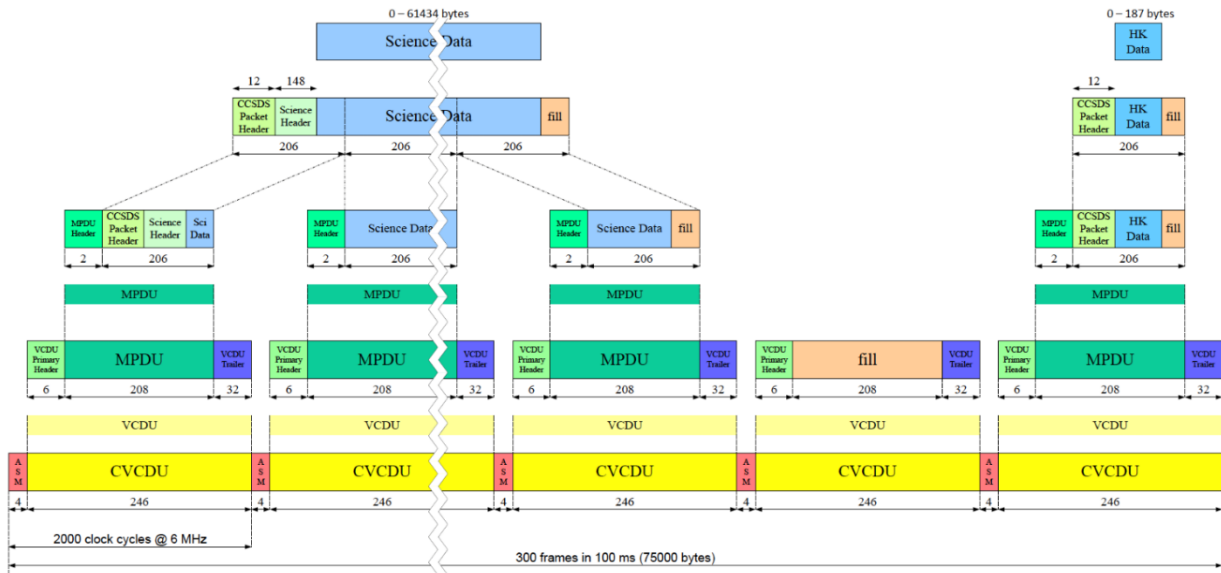


Figure 3-1 Level 0 Data Structure

The description below gives a more detailed breakdown of the data volumes and corresponding maximum science data volumes.

300 frames in 100 ms = 75000 bytes

75000 total bytes

-1200 ASM bytes (300 frames × 4 bytes/frame)

-1800 VCDU header bytes (300 frames × 6 bytes/frame)

-9600 VCDU check bytes (300 frames × 32 bytes/frame)

- 600 MPDU header bytes (300 frames × 2 bytes/frame)
- 12 science packet CCSDS header bytes/frame
- 148 science header bytes (eng. data required for science processing)
- 61640 data bytes per 100 ms (max) - 17.7% overhead
 - 206 housekeeping packet bytes
 - 61434 science data bytes per 100 ms (max)
 - 15358 photons (4 bytes) per 100 ms

3.2 Level 0 CCSDS Packet Description

The telemetry and science data are packed in CCSDS packets as shown in the figures below.

| | | | |
|---------------------------------------|-------------------------------------|---------------------|---------------------------------------|
| version (2:0) | type | sec hdr flag | APID (11:8) |
| APID (7:0) | | | |
| sequence flag (1:0) | source sequence count (13:8) | | |
| source sequence count (7:0) | | | |
| packet length (15:8) | | | |
| packet length (7:0) | | | |
| 1 second tick count (31:24) | | | |
| 1 second tick count (23:16) | | | |
| 1 second tick count (15:8) | | | |
| 1 second tick count (7:0) | | | |
| spare (6 bits) | | | 1 millisecond tick count (9:8) |
| 1 millisecond tick count (7:0) | | | |

Figure 3-2 CCSDS Packet Header (12)

| | | |
|------------------------------------|------------------------------------|------------------|
| spare (3 bits) | event counter A (20:16) | |
| event counter A (15:8) | | |
| event counter A (7:0) | | |
| spare (7 bits) | | tot phot A (16) |
| total photons A (15:8) | | |
| total photons A (7:0) | | |
| spare (2 bits) | packet photons A (13:8) | |
| packet photons A (7:0) | | |
| spare (4 bits) | window Ymin A (11:8) | |
| window Ymin A (7:0) | | |
| spare (4 bits) | window Ymax A (11:8) | |
| window Ymax A (7:0) | | |
| spare (7 bits) | | phot oow A (16) |
| photons out of window A (15:8) | | |
| photons out of window A (7:0) | | |
| spare (7 bits) | | phot dbuf A (16) |
| photons dropped at buffer A (15:8) | | |
| photons dropped at buffer A (7:0) | | |
| spare (2 bits) | photons written to buffer A (13:8) | |
| photons written to buffer A (7:0) | | |
| spare (8 bits) | | |
| spare (8 bits) | | |
| spare (8 bits) | | |
| spare (8 bits) | | |
| spare (8 bits) | | |
| spare (8 bits) | | |
| spare (8 bits) | | |
| spare (8 bits) | | |
| spare (8 bits) | | |
| spare (8 bits) | | |
| spare (8 bits) | | |
| spare (2 bits) | packet photons A limit (13:8) | |
| packet photons A limit (7:0) | | |

Figure 3-3 Det A photons – FPGA (32)

| | |
|------------------------------------|------------------------------------|
| spare (3 bits) | event counter B (20:16) |
| event counter B (15:8) | |
| event counter B (7:0) | |
| spare (7 bits) | tot phot B (16) |
| total photons B (15:8) | |
| total photons B (7:0) | |
| spare (2 bits) | packet photons B (13:8) |
| packet photons B (7:0) | |
| spare (4 bits) | window Ymin B (11:8) |
| window Ymin B (7:0) | |
| spare (4 bits) | window Ymax B (11:8) |
| window Ymax B (7:0) | |
| spare (7 bits) | phot oow B (16) |
| photons out of window B (15:8) | |
| photons out of window B (7:0) | |
| spare (7 bits) | phot dbuf B (16) |
| photons dropped at buffer B (15:8) | |
| photons dropped at buffer B (7:0) | |
| spare (2 bits) | photons written to buffer B (13:8) |
| photons written to buffer B (7:0) | |
| spare (8 bits) | |
| spare (8 bits) | |
| spare (8 bits) | |
| spare (8 bits) | |
| spare (8 bits) | |
| spare (8 bits) | |
| spare (8 bits) | |
| spare (8 bits) | |
| spare (8 bits) | |
| spare (8 bits) | |
| spare (8 bits) | |

Figure 3-4 Det B photons – FPGA (30)

| | |
|-------------------------------|--------------------------------|
| spare (5 bits) | scan mirror position A (18:16) |
| scan mirror position A (15:8) | |
| scan mirror position A (7:0) | |
| spare (5 bits) | scan mirror position B (18:16) |
| scan mirror position B (15:8) | |
| scan mirror position B (7:0) | |

Figure 3-5 Det A/B Scan Mirror – FPGA (6)

| |
|-----------------------------------|
| sync count (15:8) |
| sync count (7:0) |
| S/C time sync seconds (31:24) |
| S/C time sync seconds (23:16) |
| S/C time sync seconds (15:8) |
| S/C time sync seconds (7:0) |
| S/C time sync milliseconds (15:8) |
| S/C time sync milliseconds (7:0) |

Figure 3-6 S/C – SW (8)

| | |
|---|--|
| observation type A (3:0) | observation ID A (31:24) |
| observation ID A (23:16) | observation ID A (15:8) |
| observation ID A (7:0) | observation count A (31:24) |
| observation count A (23:16) | observation count A (15:8) |
| observation count A (7:0) | slit position A (2:0) |
| GYM position A (15:8) | GYM position A (7:0) |
| door position A (15:8) | door position A (7:0) |
| detector temp A (13:8) | detector temp A (7:0) |
| detector electronics temp A (13:8) | detector electronics temp A (7:0) |
| Z1 optical bench temp A (13:8) | Z1 optical bench temp A (7:0) |
| Z2 optical bench temp A (13:8) | Z2 optical bench temp A (7:0) |
| FFL current A (13:8) | FFL current A (7:0) |
| FRF voltage A (13:8) | FRF voltage A (7:0) |
| QEG voltage A (13:8) | QEG voltage A (7:0) |
| HV current A (13:8) | HV current A (7:0) |
| spare (8 bits) | spare (8 bits) |
| spare (8 bits) | spare (8 bits) |
| spare (8 bits) | spare (8 bits) |
| spare (8 bits) | spare (8 bits) |
| spare (8 bits) | spare (8 bits) |
| spare (8 bits) | spare (8 bits) |

Figure 3-7 Det A - SW (36)

| | |
|--|---|
| spare (4 bits) | observation type B (3:0) |
| observation ID B (31:24) | |
| observation ID B (23:16) | |
| observation ID B (15:8) | |
| observation ID B (7:0) | |
| observation count B (31:24) | |
| observation count B (23:16) | |
| observation count B (15:8) | |
| observation count B (7:0) | |
| spare (5 bits) | slit position B (2:0) |
| GYM position B (15:8) | |
| GYM position B (7:0) | |
| door position B (15:8) | |
| door position B (7:0) | |
| spare (2 bits) | detector temp B (13:8) |
| detector temp B (7:0) | |
| spare (2 bits) | detector electronics temp B (13:8) |
| detector electronics temp B (7:0) | |
| spare (2 bits) | Z1 optical bench temp B (13:8) |
| Z1 optical bench temp B (7:0) | |
| spare (2 bits) | Z2 optical bench temp B (13:8) |
| Z2 optical bench temp B (7:0) | |
| spare (2 bits) | FFL current B (13:8) |
| FFL current B (7:0) | |
| spare (2 bits) | FRF voltage B (13:8) |
| FRF voltage B (7:0) | |
| spare (2 bits) | QEG voltage B (13:8) |
| QEG voltage B (7:0) | |
| spare (2 bits) | HV current B (13:8) |
| HV current B (7:0) | |
| spare (8 bits) | |
| spare (8 bits) | |
| spare (8 bits) | |
| spare (8 bits) | |
| spare (8 bits) | |
| spare (8 bits) | |

Figure 3-8 Det A - SW (36)

4 Level 1 Data Products

There are four Level 1 Data Products: L1A, L1B, L1C, and L1D. These are discussed in the sections that follow.

4.1 Generating Level 1A data

The raw data coming from the ground station are compressed and bit-packed to minimize data volume. Science data packets are generated by the instrument at a 10 Hz cadence. On the ground, the various packets are extracted from the L0 data and L1A netCDF files are created at a 63-second cadence, one file per instrument channel. On average, L1A files contain 630 science data packets that are arranged sequentially in time. Minimal processing occurs to generate the L1A files. The steps are summarized in the upper left of Figure 4-1 and described below.

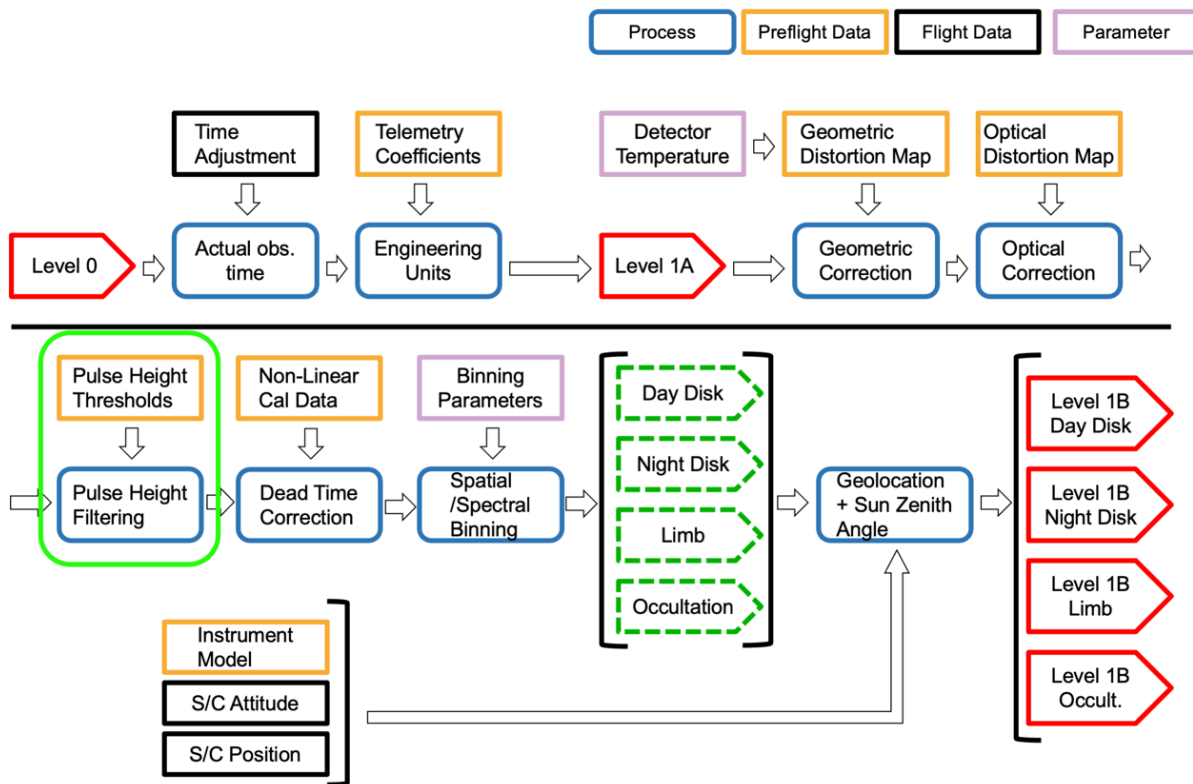


Figure 4-1 Level 0 to Level 1B Processing

4.1.1 Time Adjustment

The slowly drifting time from the instrument clock is inserted in the downloaded data packets. With the knowledge of the exact ground receipt time, an adjustment is made to the instrument clock through SPICE time kernels to generate UTC and Ephemeris Time (ET) used in the L1A files.

4.1.2 Telemetry Coefficients

Fixed conversions (polynomial coefficients, state conversions, etc.) are applied to the L0 data telemetry to convert from raw data numbers to engineering units (Volts, Amps, Degree C, etc.).

4.1.3 NetCDF File Format

Level 1A data are stored as a list of photon events with supporting engineering measurements in NetCDF-4 file format.

4.2 Generating Level 1B data

Figure 3-1 also shows a flow diagram for the process steps that generate L1B files from L1A files. For atmosphere observations, the nominal L1B file structure consists of spectral-spatial images that are accumulated for 2-second-long integration periods and contain data from 20 L1A packets, each covering a 0.1-second-long interval. These have an 800x600 element format. For occultation observations, the nominal structure contains spectral-spatial images that are constructed from individual packets. These have an 800x33 element format and a 0.1 second integration period.

4.2.1 Detector and Photon Event Data Description

Each GOLD detector is photon a locating device consisting of a z-stack of microchannel plates (MCPs) followed by a delay line anode. Photons arriving at the input side of the z-stack, which is located at the focal plane of an imaging spectrograph, produce photoelectrons at that surface. Each photoelectron is multiplied within the stack producing an $\sim 10^7$ -sized pulse of electrons (~ 1.6 picocoulombs of charge) at the stack output. This pulse impinges upon an anode that locates the position of the incident photon that initiated the pulse. Photon data in the L1A packets consist of a list of 32-bit words for the detected photons. The first 12 bits determine a photon location on the detector anode in the spectral (dispersion) dimension, the second 12 bits determine its location on the anode in the spatial dimension (position along the spectrograph entrance slit), and the last 8 bits provide a measure of the number of electrons in the pulse from the detector's microchannel plate stack (pulse height). Spatial scales for these locations are ~ 0.017 mm per DN (pixel) in X (dispersion) and ~ 0.019 mm per DN (pixel) in Y (cross dispersion). Each pulse height DN corresponds to ~ 0.02 picocoulombs of charge. The imaging area of the detector, which is 27 mm x 34 mm, is a rectangular region of the anode that is 1600 pixels wide x 1800 pixels tall.

4.2.2 Stim Pulse Location Correction

The location of a photon event on the detector is measured by a highly accurate timing electronics circuit attached to the anode. Because the response of this circuit varies slightly with temperature, the measured location of a fixed photon stream will appear to move on the detector

with temperature. This effect is corrected by tracking the location of fixed and electronically ingested stim pulses. Based on the location of these stim pulses, stretch and shift are applied to each detector photon event location to shift it into a standard reference frame.

4.2.3 Geometric Correction

Geometric distortion is caused by local variations in the plate scale of the detector. These variations are fixed in physical space and are caused by small differences in the propagation speed of the anode and the structure of the MCPs themselves. The variations in the propagation speed are in turn due to local differences in the anode substrate thickness, anode trace resistivity, and the behavior of a charge cloud propagating along a complex network of conductive traces. The correction is derived from images of an equal-spacing pinhole mask provided by Berkley SSL (detector manufacturer). A correction map in X and a correction map in Y are applied. Each detector has a unique set of maps.

4.2.4 Optical Correction

The GOLD spectrograph optical system produces slightly curved images of its entrance slit on the detector. To simplify processing and analysis, this effect is removed when generating L1B files. The correction forces the image of the slit to align with detector columns and for the spectra to align with its rows. This correction is based on ground calibration data. A correction map in X and a correction map in Y are applied. Each spectrograph has a unique set of maps.

4.2.5 Pulse Height Filtering

A configurable window is used to filter out non-photon-produced events identified by large pulse height values. These arise primarily from gamma rays produced when relativistic electrons are decelerated in shields that surround the detector. Pulse height values can range from 0 to 255. The current filtering window is set to remove all events with pulse height values of 0, 1, 2, or greater than 200 corresponding to maximum ~ 4 picocoulombs of charge.

4.2.6 Spatial/Spectral/Temporal Binning

After the spatial corrections are applied, the L1A pixel locations are placed into a 1600 x 1800 image array. These are then binned by 2 in X and 3 in Y to produce 800-pixel x 600-pixel L1B raw count image arrays that have spatial scales of ~ 0.034 mm (X) x ~ 0.057 mm (Y). The full 600-pixel tall image is retained in the final L1B images for disk and limb observations. Only 33 rows, centered on the star location in the entrance slit are telemetered and retained for occultation observations. L1B images are binned further during L1C processing to produce the various GOLD data products defined in Section 2. The temporal cadence for data in the L1B files is one image per 2-second interval except for occultations where the cadence is 0.1 seconds. L1C spatial, spectral and temporal binning are based on observation type (see Table 2-1 and Table 2-2). Each spatial – spectral pixel in an L1B raw count image is assigned an uncertainty equal to

the square root of the number of counts in that pixel (Poisson statistics - If the counts in pixel i,j,k are $C_{i,j,k}$, the $\text{raw_count_random_unc} = \text{square_root}(C_{i,j,k})$). Details are discussed in McClintock et al. 2020(b).

4.2.7 Global Dead Time Correction

The detector electronics have a finite response time and as the rate of photons events increases, the electronics can't keep pace and ignores an increasing fraction of them. This non-linearity effect has been well characterized on the ground, based on the Fast-Event-Counter (FEC) detector telemetry item. After a dead time correction is applied globally to binned image based on the FEC, the corrected counts are assembled into an L1B corrected count image. Each spatial – spectral pixel in an L1B corrected count image is assigned an uncertainty equal to the uncertainty in the dead time correction applied to that pixel. If the dead time correction is N , then $\text{corrected_count} = N * C_{i,j,k}$ and $\text{corrected_count_systematic_unc} = \sigma_N * C_{i,j,k}$ where σ_N is the uncertainty in the value of the correction parameter.

4.2.8 Local Dead Time Correction

Local dead time results from the limited ability of the MCPs to provide current to a locally-intense region of illumination. Local dead time affects both the measured count rate of individual bright sources and the shapes of those sources. Correction factors are based on ground calibration data taken at various detector irradiance levels. For GOLD, only the bright stars observed as part of the Occultations are impacted by this effect. This correction is not currently being applied.

4.2.9 Geolocation Information

A single L1B file can contain up to 30 disk or limb images and up to 600 occultation images (approximately 1 minute of data per file). It also contains the geolocation data for each image that is required for processing higher level data products.

Figure 4-2 defines the geometry for day and night disk observations.

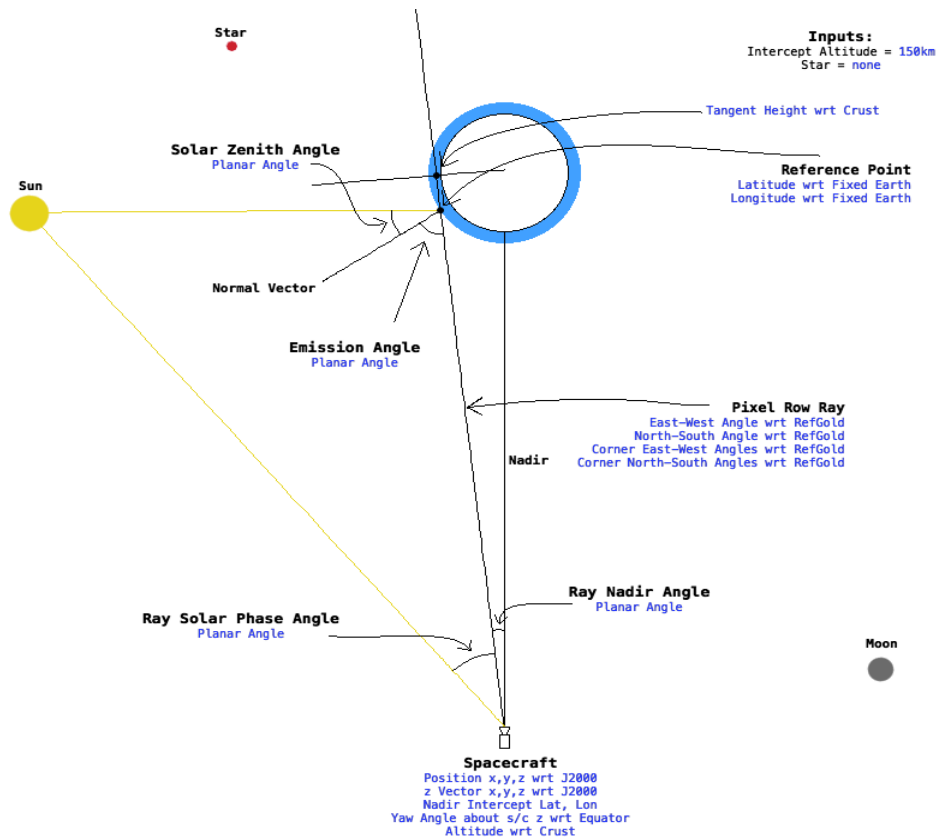


Figure 4-2 Geolocation geometry for day and night disk observations.

The Earth's ellipsoid is defined by WGS 84, giving radius values 6378.1370 km in x/y and 6356.7523 km in z. Latitude and longitude are defined using the geodetic coordinate system. For each scan mirror step and for each detector L1B pixel along the spectrograph, a viewing vector (ray) is projected toward the Earth with an origin at the spacecraft calculated from the spacecraft ephemeris and specified by its J2000 coordinates. Ray orientation relative to the spacecraft nadir direction, which is calculated using the angle of the instrument scan mirror and the orientation of the spacecraft and is specified in the J2000 coordinate system, is defined by two angles, `pixel_ray_ew` and `pixel_ray_ns`. The ray's angle relative to spacecraft nadir is also calculated.

Location of a ray as it intersects the Earth's atmosphere at a defined intercept altitude above the crust (150km for day disk observations and 300km for night disk observations) is referred to as the reference point and its latitude and longitude are calculated along with solar zenith angle and emission angle. The tangent height of the ray is also calculated. Latitude and longitude of the tangent point are not calculated. For a ray whose nadir angle is large enough that no intersection at the intercept altitude can occur, reference latitude and longitude, tangent altitude, solar zenith and emission angle are reported as not-a-number (NaN).

Figure 4-3 defines the geometry for limb scans.

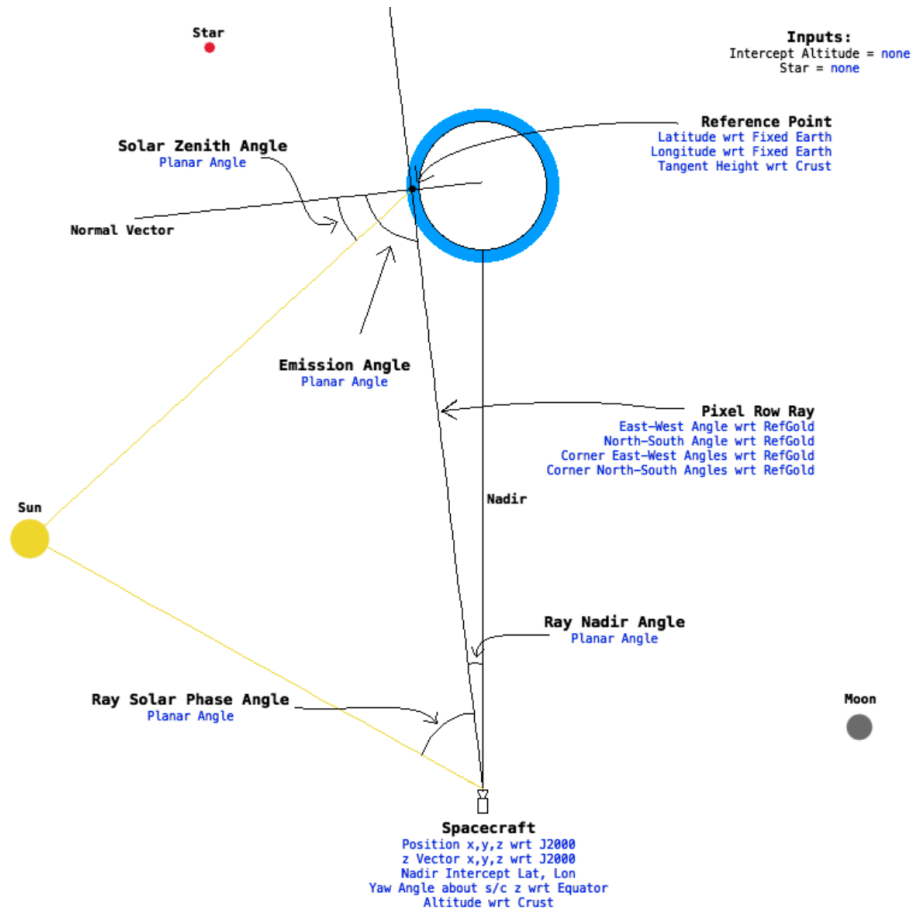


Figure 4-3 Geolocation geometry for limb scan observations.

Limb Scans do not use a fixed intercept altitude and the reference point and tangent point coincide, independent of where a ray intercepts the earth/atmosphere. In this case the tangent point = reference point for each ray is calculated along with its latitude and longitude, solar zenith angle and emission angle.

Figure 4-4 defines the geometry for occultations.

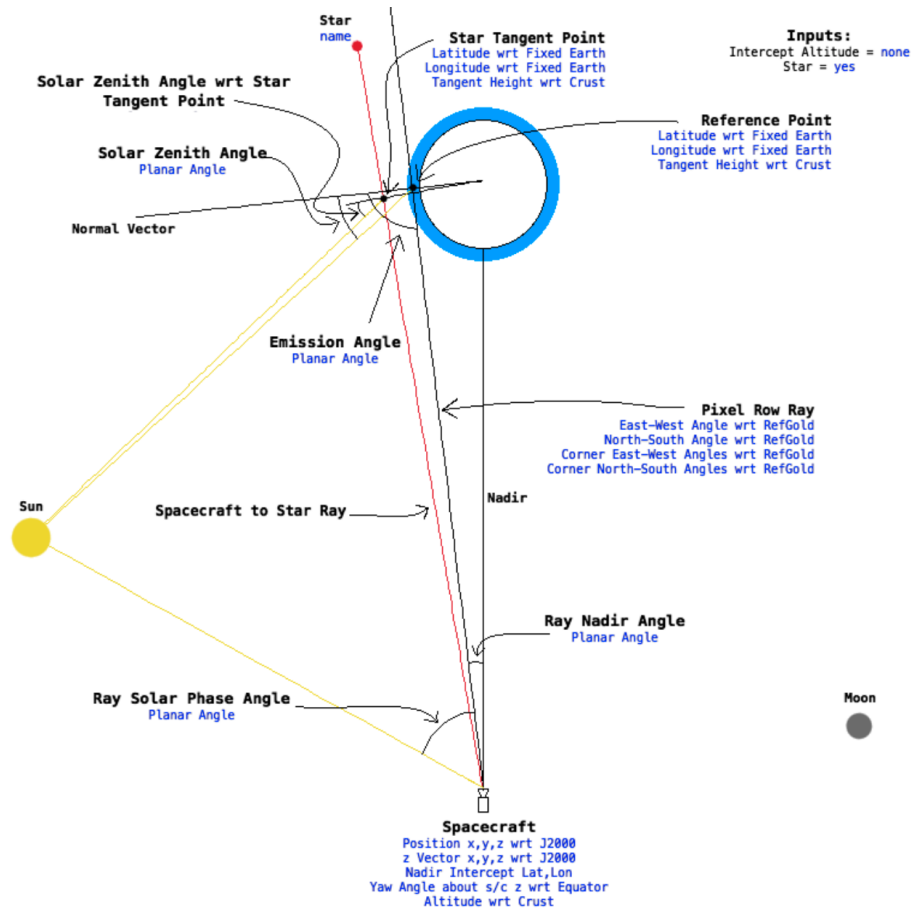


Figure 4-4 Geolocation geometry for occultation observations.

These observations are performed by slewing the instrument scan mirror so that the center of the 1° wide occultation slit intersects the atmosphere at an intercept altitude ~ 270 km at the latitude of the occultation. A detector windowing function is enabled such that only row with pixel_ray_ns closest to the star’s latitude and ±16 rows on either side of it are telemetered to the ground. The tangent point = reference point along with its latitude and longitude, solar zenith angle and emission angle is calculated for rays projected from each of the 33 L1B image rows. This slit geolocation is identical to that performed for the limb scans. Additionally, the spacecraft location and universal time of the observation are used to calculate the star’s tangent height, latitude, longitude, and solar zenith angle relative to the star for each time step (0.1 seconds) in an L1B data file.

4.3 L1B Data File Contents

4.3.1 Generic L1B Metadata

Each L1B file contains metadata for the file. Table 4-1 describes the general structure and content of the metadata for the observation type (atmosphere or occultation).

| Variable Name | Description |
|------------------------|--|
| ADID_Ref | NASA Contract > NNG12PQ28C |
| Conventions | SPDF ISTP/IACF Modified for NetCDF |
| Data_Level | L1B |
| Data_Type | APIDx0F > GOLD Application ID 0x0F: Level 1C XXX Science Data |
| Mirror_Hemisphere | Either 'N' (north) or 'S' (south) for the observed hemisphere |
| Observation_Type | <i>DAY_DISK, LIMB, NIGHT_DISK_ARCS, or STELLAR_OCCULTATION</i> |
| OBS_TYPE | 1 (DAY_DISK), 2 (LIMB), 8 (NIGHT_DISK) or 3 (OCCULTATION) |
| OBS_ID | Observation sequence number |
| Observation_Complete | 1 if this is the last l1b file in the current observation type otherwise 0 to continue |
| Last_obs_Count_In_File | Identifies the number of packets in the current science observation type |
| Channel_ID | 0 = CHANNEL A 1 = CHANNEL B |
| Data_Version | Version sequence number |
| Data_Revision | Revision sequence number |
| Data_Cycle | Data cycle sequence number |
| Minimum_PHD | Lower limit for the pulse height filter (typical value = 2) |
| Maximum_PHD | Upper limit for the pulse height filter (typical values range from 200 to 254) |
| Spatial_Binning | 3 (Fixed L1A – L1B binning) |
| Spectral_Binning | 2 (Fixed L1A – L1B binning) |
| Detector_Window_Ymin | minimum row selected from the detector anode readout 0 for atmosphere observations selected to place the star in center of a 96-row L1A image for stars |
| Detector_Window_Ymax | maximum row selected from the detector anode readout 4095 for atmosphere observations selected to place the star in center of a 96-row L1A image for stars |
| Window_Row_Min | L1B row corresponding to Detector_Window_Ymin |
| Window_Row_Max | L1B row corresponding to Detector_Window_Ymax |
| Slit_Name | OCC, HI_RES or LO_RES Observation type dependent |
| GYM_Position | Step position of the grating yaw mechanism |
| Detector_Door | Position of the detector door 0 for closed 450 for fully open |
| Reference_Altitude | 150km (DAY_DISK), 300km (NIGHT_DISK), -1km (LIMB and OCCULTATION) |

| Variable Name | Description |
|----------------------------|--|
| OCC_STAR | Common name for observed star (e.g., eps Ori) specified only for occultations |
| OCC_STAR_ID | Henry Draper Star Catalog number (e.g., HD37128) specified only for occultations |
| OCC_STAR_RA | Star right ascension (degrees) specified only for occultations |
| OCC_STAR_DEC | Star declination (degrees) specified only for occultations |
| OCC_STAR_BRIGHTNESS | Stan ultraviolet flux ranking relative to all stars observed by GOLD (1-30) |
| SC_Ref_Altitude | 35785.9 km relative to Earth's surface at spacecraft nadir nominal S/C altitude |
| Date_Processed | Processing date for this file (e.g., '2019-09-18T16:06:41.000Z') |
| Date_Start | Start of the observation for this file (e.g., '2016-11-17 08:26:45.000Z') |
| Date_End | End of the observation for this file (e.g., '2016-11-17 08:31:45.000Z') |
| SC_Reference_Alt | Median spacecraft altitude (km) during the observation relative to Earth's surface |
| SC_Reference_Lon | -47.5° relative to Earth's center at spacecraft nadir nominal S/C longitude |
| SC_Reference_Lat | 0° relative to Earth's center at spacecraft nadir nominal S/C latitude |
| Description | 'GOLD L1B binned photon count image' |
| Descriptor | 'CHA photon list > GOLD L1B photon count image' |
| Discipline | 'Space Physics > Ionospheric Science' |
| File | GOLD_L1C_CHB_2016_016_18_45_v01.nc |
| Discipline | 'Space Physics > Ionospheric Science' |
| File | File name (e.g., 'GOLD_L1C_CHB_2016_016_18_45_v01.nc') |
| File_Date | Process date (e.g., '2019-09-18T16:06:41.000Z') |
| Generated_By | e.g., 'GOLD SOC > GOLD L1B Processor v1.0.0 Process version can update' |
| History | e.g., 'Version 1, Created by GOLD L1C Processor v1.0.0 on 2016-11-17 08:26:45.000Z. Version number can update' |
| HTTP_LINK | 'http://gold.cs.ucf.edu' |
| Instrument | 'CHA' or 'CHB' |
| Instrument_Type | 'UV Imaging Spectrograph (Space)' |
| Link_Text | 'All GOLD information and data can be found at the HTTP_LINK' |
| Link_Title | 'GOLD Website' |
| Logical_File_ID | e.g., 'GOLD_L1B_CHA_DAY_2016_016_18_45_v01_r01' |
| Logical_Source | e.g., 'GOLD_L1B_CHA_DAY_2016_016_18_45' |
| Logical_Source_Description | GOLD Channel-A L1B binned photon count image |
| Mission_Group | 'Thermospheric and Ionospheric Investigations' |
| PI_Affiliation | 'University of Colorado / LASP' |
| PI_Name | 'Richard Eastes' |

| Variable Name | Description |
|------------------|--|
| Project | 'NASA > GOLD' |
| Rules_of_Use | 'Public Data for Scientific Use' |
| Software_Version | e.g. 'GOLD SOC > heads/release/GOLD-686-release-12-11-flat-field-0-ga0bda2e 2021-02-09 20:54:51 -0500' |
| Source_Name | 'GOLD > Global-scale Observations of the Limb and Disk (GOLD) Heliophysics Explorer mission of opportunity' |
| Spacecraft_ID | 'SES > GOLD – 518' |
| Text | The GOLD mission of opportunity flies an ultraviolet (UV) imaging spectrograph on a geostationary satellite to measure densities and temperatures in Earth's thermosphere and ionosphere and to understand the global-scale response to forcing in the integrate Sun-Earth system. Visit ' http://www.gold-mission.org/ ' for more details. |
| Time_Resolution | '100 milliseconds' |
| Title | GOLD Level 1B binned photon count image |
| Stim_Lx0 | Mean X value for the left stim pulses before the thermal correction is applied |
| Stim_Ly0 | Mean Y value for the left stim pulses before the thermal correction is applied |
| Stim_Rx0 | Mean X value for the right stim pulses before the thermal correction is applied |
| Stim_Ry0 | Mean Y value for the right stim pulses before the thermal correction is applied |
| Stim_FWHM_Lx | X value of the FWHM of the left stim pulses received for this data file |
| Stim_FWHM_Ly | Y value of the FWHM of the left stim pulses received for this data file |
| Stim_FWHM_Rx | X value of the FWHM of the right stim pulses received for this data file |
| Stim_FWHM_Ry | Y value of the FWHM of the right stim pulses received for this data file |
| Stim_Lx | Mean X value for the left stim pulses after the thermal correction is applied |
| Stim_Ly | Mean Y value for the left stim pulses after the thermal correction is applied |
| Stim_Rx | Mean X value for the right stim pulses after the thermal correction is applied |
| Stim_Ry | Mean Y value for the right stim pulses after the thermal correction is applied |
| Stim_Lcount | Number of left stim pulses for this data file |
| Stim_Rcount | Number of right stim pulses for this data file |
| Num_Trim | Number of events in the perimeter of the detector 4096 x 4092 window that have $x < 10$ plus $x > 4085$ plus $y < 10$ plus $y > 4085$ |
| Ph_Min | Lower limit for the pulse height filter (typical value = 2) |
| Ph_Max | Upper limit for the pulse height filter (typical values range from 200 to 254) |
| Num_Trim_Ph | Number of events removed by the pulse height filter |
| Tc_Date | Date for the current thermal correction (e.g., '2021-02-14T06:22:37.000Z') |
| Tc_Ver | Thermal correction version number (e.g., 3) |
| Gc_Date | Date for the current geometric correction (e.g., '2021-02-14T06:22:37.000Z') |

| Variable Name | Description |
|---------------|--|
| Gc_Ver | Geometric correction version number (e.g., 1) |
| Oc_Date | Date for the current optical correction (e.g., '2021-02-14T06:22:37.000Z') |
| Oc_Ver | Optical correction version number (e.g., 1) |
| Pixel_Width | Detector pixel width in micrometers (e.g., 17.2 μ m) |
| Pixel_Height | Detector pixel height in micrometers (e.g., 18.7 μ m) |
| Origin_X | X location on the pixel array for extraction of science image (e.g., 995) |
| Origin_Y | Ylocation on the pixel array for extraction of science image (e.g., 900) |
| Size_X | Number of x pixels in a science image (columns) (e.g., 1600) |
| Size_Y | Number of ypixels in a science image (rows) (e.g., 1800) |

Table 4-1 Generic L1B Metadata

4.3.2 L1B File Content for Atmosphere Observations

The file structure for L1B atmosphere observations typically span 60 seconds in time and contain 30 spectral-spatial images with detector count data accumulated during successive 2-second integration periods, assembled from 20 successive L1A science packets. Some L1B atmosphere files, assembled for times near the end of specific observation types, span less than 60 seconds and have fewer than 30 images. Some images are also constructed from fewer than 20 L1A packets. These can be identified using the Packets_Per_Dwell variable in their data files.

For each nominal 2 sec integration period, there are four 800x600 spectral-spatial images containing (separately) the raw detector counts, associated random uncertainty (square root of the number raw counts), detector counts corrected for dead time and the systematic uncertainty in corrected counts that is proportional to the estimated error in the dead time correction factor (10%).

In addition to the count-images, each L1B file contains the ancillary data required for generating L1C data products. These include statistics associated with the total detector events and detector events excluded from the spectral-spatial images, detector and temperature engineering data, and pointing and spacecraft position data. Averages and standard deviations (when appropriate) are provided for each set of 4 count images. Variables associated with occultations (star observations) are not defined and have not-a-number (NAN) entries in the data files.

Table 4-2 summarizes the contents of L1B files for atmosphere observations.

| Variable Name | Units | Type/Dim | Description |
|---------------|---------|-----------|---|
| Time_ET | seconds | Double/30 | TDB seconds from January 1, 2000, 11:58:55.816 UTC at start of L1B time bin |

| Variable Name | Units | Type/Dim | Description |
|---------------------------|---------|-----------|--|
| Time.UTC | | String/30 | ISO 8601 formatted UTC timestamp at start of integration) |
| FEC | counts | Float/30 | Average of the detector Fast Event Counter values from the L1A packets during the ~2 sec integration period (~20 L1A packets, each 0.1 sec long) |
| FEC_STDV | counts | Float/30 | Standard deviation of detector Fast Event Counter values during the ~2 sec integration period |
| Total_Events | counts | Float/30 | Average of the detector Total Events values from the L1A packets during the ~2 sec integration period (~20 L1A packets, each 0.1 sec long) |
| Total_Events_STDV | counts | Float/30 | Standard deviation of the detector Total Events values during the ~2 sec integration period |
| Nevents_Outside | counts | Float/30 | Average of the detector Number Events Outside of the window defined by Detector_Window_YMIN and Detector_Window_YMAX values from the L1A packets during the ~2 sec integration period (~20 L1A packets, each 0.1 sec long) |
| Nevents_Outside_STDV | counts | Float/30 | Standard deviation of the detector Number Events Outside of detector window values during the ~2 sec integration period |
| Nevents_Dropped | counts | Float/30 | Average of the detector Number Events Dropped because of limited output buffer size values from the L1A packets during the ~2 sec integration period (~20 L1A packets, each 0.1 sec long) |
| Nevents_Dropped_STDV | counts | Float/30 | Standard deviation of the detector Number of Events Dropped because of limited output buffer size values during the ~2 sec integration period |
| Nevents_Buffer | counts | Float/30 | Average of the detector Number Events written to Buffer values from the L1A packets during the ~2 sec integration period (~20 L1A packets, each 0.1 sec long) |
| Nevents_Buffer_STDV | counts | Float/30 | Standard deviation of the detector Number Events written to Buffer values during the ~2 sec integration period |
| Mirror_Radians | radians | Float/30 | Average Mirror Radians position values from the L1A packets during the ~2 sec integration period (~20 L1A packets, each 0.1 sec long) |
| Mirror_Radians_STDV | radians | Float/30 | Standard deviation of the Mirror Radians position values during the ~2 sec integration period |
| Packets_Per_Dwell | | int/30 | The number of L1A packets during the ~2sec integration period (~20 L1A packets, each 0.1 sec long) |
| Detector_Temperature | Deg. C | Float/30 | Average of the Detector Temperature values from the L1A packets during the ~2 sec integration period (20 L1A files, each 0.1 sec long) |
| Detector_Temperature_STDV | Deg. C | Float/30 | Standard deviation of the Detector Temperature values during the ~2sec integration period |

| Variable Name | Units | Type/Dim | Description |
|--------------------------------|------------|------------|--|
| Detector_Elec_Temperature | Deg. C | Float/30 | Average of the Detector Electronics Temperature values from the L1A packets during the ~2 sec integration period (20 L1A files, each 0.1 sec long) |
| Detector_Elec_Temperature_STDV | Deg. C | Float/30 | Standard deviation of the Detector Electronics Temperature values during the ~2sec integration period |
| Bench_Z1_Temperature | Deg. C | Float/30 | Average of the Optical Bench Zone 1 Temperature (front) values from the L1A packets during the ~2 sec integration period (20 L1A files, each 0.1 sec long) |
| Bench_Z1_Temperature_STDV | Deg. C | Float/30 | Standard deviation of the Optical Bench Zone 1 Temperature (front) values during the ~2sec integration period |
| Bench_Z2_Temperature | Deg. C | Float/30 | Average of the Optical Bench Zone 2 Temperature (rear) values from the L1A packets during the ~2 sec integration period (20 L1A files, each 0.1 sec long) |
| Bench_Z2_Temperature_STDV | Deg. C | Float/30 | Standard deviation of the Optical Bench Zone 2 Temperature (rear) values during the ~2sec integration period |
| FFL_Current | Amps | Float/30 | Average of the Flat Field Lamp Current values from the L1A packets during the ~2 sec integration period (20 L1A files, each 0.1 sec long) |
| FFL_Current_STDV | Amps | Float/30 | Standard deviation of the Flat Field Lamp Current values during the ~2sec integration period |
| FRF_Voltage | Volts | Float/30 | Average of the detector Fixed Rear-Field Voltage values from the L1A packets during the ~2 sec integration period (20 L1A files, each 0.1 sec long) |
| FRF_Voltage_STDV | Volts | Float/30 | Standard deviation of the Fixed Rear-Field Voltage values during the ~2sec integration period |
| QEG_Voltage | Volts | Float/30 | Average of the detector QE-Grid Voltage values from the L1A packets during the ~2 sec integration period (20 L1A files, each 0.1 sec long) |
| QEG_Voltage_STDV | Volts | Float/30 | Standard deviation of the QE-Grid Voltage values during the ~2sec integration period |
| HV_Current | μ Amps | Float/30 | Average of the detector High Voltage Current values from the L1A packets during the ~2 sec integration period (20 L1A files, each 0.1 sec long) |
| HV_Current_STDV | μ Amps | Float/30 | Standard deviation of the High Voltage Current values during the ~2sec integration period |
| SC_ALT | Km | Float/30 | Altitude of spacecraft above reference Earth ellipsoid |
| SC_POS | Km | Float/30x3 | Position of spacecraft relative to Earth center in J2000 coordinates |
| SC_Z_Dir | unit | Float/30x3 | Unit vector of spacecraft nadir- pointing direction in J2000 |
| SC_Nadir_Lat | Degrees | Float/30 | Latitude intercept of spacecraft nadir- pointing direction |

| Variable Name | Units | Type/Dim | Description |
|-----------------------------|---------|------------------|---|
| SC_Nadir_Lon | Degrees | Float/30 | Longitude intercept of spacecraft nadir- pointing direction |
| SC_Yaw | Degrees | Float/30 | The yaw angle of the spacecraft relative to the Earth's equator |
| Pixel_Ray_EW | Degrees | Float/30x600 | The E/W angle relative to spacecraft nadir for rays projected from the center of each row of an L1B spectral-spatial image (pixel rays) |
| Pixel_Ray_NS | Degrees | Float/30x600 | The N/S angle relative to spacecraft nadir for rays projected from the center of each row of an L1B spectral-spatial image (pixel rays) |
| Reference_Point_Lat | Degrees | Float/30x600 | Latitude at which rays projected from the center of each L1B row ((pixel rays)) intercept the atmosphere at the reference altitude (e.g., 150 km for Day disk observations and 300 km for night disk) |
| Reference_Point_Lon | Degrees | Float/30x600 | Longitude at which rays projected from the center of each L1B row (pixel rays) intercept the atmosphere at the reference altitude (e.g., 150 km for Day disk observations and 300 km for night disk) |
| Tangent_Height | Km | Float/30x600 | Altitude above the Earth's crust at which rays projected from the center of each L1B row (pixel rays) intercept a perpendicular vector projected from Earth's center |
| Ray_Solar_Phase_Angle | Degrees | Float/30x600 | The planar angle between pixel rays and a vector from the sun to the reference point |
| Ray_Nadir_Angle | Degrees | Float/30x600 | The planar angle between pixel rays and the spacecraft nadir vector |
| Emission_Angle | Degrees | Float/30x600 | The planar angle between pixel rays and the normal vector at the reference point |
| Solar_Zenith_Angle | Degrees | Float/30 | The planar angle between a vector from the sun to the reference point and the normal vector at the reference point |
| Solar_Zenith_Angle_Wrt_Star | NAN | NAN/30 | Set to not-a-number (NAN) for atmosphere observations |
| Star_Tangent_Height | NAN | NAN/30 | Set to not-a-number (NAN) for atmosphere observations |
| Star_Tangent_Lat | NAN | NAN/30 | Set to not-a-number (NAN) for atmosphere observations |
| Star_Tangent_Lon | NAN | NAN/30 | Set to not-a-number (NAN) for atmosphere observations |
| Quality_Flag | | int64/30 | Any saved quality flags |
| PHD | | Float/30x256 | Histogram distribution of the photon events Pulse Heights during an integration period |
| Raw_Count | counts | Float/30x800x600 | Spectral x spatial image of GOLD L1B raw photon counts accumulated during an integration period |

| Variable Name | Units | Type/Dim | Description |
|--------------------------------|--------|------------------|---|
| Raw_Count_Random_Unc | counts | Float/30x800x600 | Spectral x spatial image of the random uncertainty of GOLD L1B raw photon counts accumulated during an integration period |
| Corrected_Count | counts | Float/30x800x600 | Spectral x spatial image of GOLD L1B photon counts accumulated during an integration period and corrected for dead time |
| Corrected_Count_Systematic_Unc | counts | Float/30x800x600 | Spectral x spatial image of systematic uncertainty in GOLD L1B photon counts accumulated during an integration period and corrected for dead time |

Table 4-2 L1B File Content for Atmosphere Observations

4.3.3 L1B File Content for Occultation Observations

The file structure for L1B occultation observations typically span 60 seconds in time and contain 600 spectral-spatial images with detector count data accumulated during successive 0.1-second L1A packet integrations. Occultation duration is ~ 4.9 minutes and comprise 4 60-second L1B files plus one that has slightly fewer than 600 images. The Packets_Per_Dwell = 1 for occultations.

The detector windowing variables, Detector_Window_Ymin and Detector_Window_Ymax are set to acquire only 97 L1A detector rows. These are binned by 3 to produce 33 L1B detector rows that are identified in the Window_Row_Min and Window_Row_Max variables in the L1B metadata. For each 0.1 sec integration period, four 800x33 spectral-spatial images contain the raw detector counts, associated random uncertainty (square root of the number raw counts), detector counts corrected for dead time and the systematic uncertainty in corrected counts that is proportional to the estimated error in the dead time correction factor (10%).

In addition to the count-images, each L1B file contains the ancillary data required for generating L1C data products. These include statistics associated with the total detector events and detector events excluded from the spectral-spatial images, detector and temperature engineering data, and pointing and spacecraft position data. Variable values are provided for each set of 4 count images. Variables associated with standard deviations of engineering data are not defined and have not-a-number (NAN) entries in the data files.

Table 4-3 summarizes the contents of L1B files for occultation observations.

| Variable Name | Units | Type/Dim | Description |
|---------------|---------|------------|--|
| Time_ET | seconds | Double/600 | TDB seconds from January 1, 2000, 11:58:55.816 UTC at start of L1B time bin |
| Time_UTC | | String/600 | ISO 8601 formatted UTC timestamp at start of integration) |
| FEC | counts | Float/600 | Detector Fast Event Counter values during each 0.1 sec L1A packet integration period |

| Variable Name | Units | Type/Dim | Description |
|--------------------------------|---------|-----------|--|
| FEC_STDV | NAN | NAN/600 | Set to NAN (not a number) for occultations |
| Total_Events | counts | Float/600 | Detector Total Events values during each 0.1 sec L1A packet integration period |
| Total_Events_STDV | NAN | NAN/600 | Set to NAN (not a number) for occultations |
| Nevents_Outside | counts | Float/600 | Detector Number Events Outside of the window defined by Detector_Window_YMIN and Detector_Window_YMAX values during each 0.1 sec L1A packet integration period |
| Nevents_Outside_STDV | NAN | NAN/600 | Set to NAN (not a number) for occultations |
| Nevents_Dropped | counts | Float/600 | Detector Number Events Dropped because of limited output buffer size values during each 0.1 sec L1A packet integration period |
| Nevents_Dropped_STDV | NAN | NAN/600 | Set to NAN (not a number) for occultations |
| Nevents_Buffer | counts | Float/600 | Detector Number Events written to Buffer values during each 0.1 sec L1A packet integration period |
| Nevents_Buffer_STDV | NAN | NAN/600 | Set to NAN (not a number) for occultations |
| Mirror_Radians | radians | Float/600 | Mirror Radians position values during each 0.1 sec L1A packet integration period |
| Mirror_Radians_STDV | NAN | NAN/600 | Set to NAN (not a number) for occultations |
| Packets_Per_Dwell | | int/600 | The number of L1A packets = 1 |
| Detector_Temperature | Deg. C | Float/600 | Detector Temperature values during each 0.1 sec L1A packet integration period |
| Detector_Temperature_STDV | NAN | NAN/600 | Set to NAN (not a number) for occultations |
| Detector_Elec_Temperature | Deg. C | Float/600 | Detector Electronics Temperature values during each 0.1 sec L1A packet integration period |
| Detector_Elec_Temperature_STDV | NAN | NAN/600 | Set to NAN (not a number) for occultations |
| Bench_Z1_Temperature | Deg. C | Float/600 | Optical Bench Zone 1 Temperature (front) values during each 0.1 sec L1A packet integration period |
| Bench_Z1_Temperature_STDV | NAN | NAN/600 | Set to NAN (not a number) for occultations |
| Bench_Z2_Temperature | Deg. C | Float/600 | Optical Bench Zone 2 Temperature (rear) values during each 0.1 sec L1A packet integration period |
| Bench_Z2_Temperature_STDV | NAN | NAN/600 | Set to NAN (not a number) for occultations |
| FFL_Current | Amps | Float/600 | Flat Field Lamp Current values during each 0.1 sec L1A packet integration period |
| FFL_Current_STDV | NAN | NAN/600 | Set to NAN (not a number) for occultations |
| FRF_Voltage | Volts | Float/600 | Detector Fixed Rear-Field Voltage values during each 0.1 sec L1A packet integration period |
| FRF_Voltage_STDV | NAN | NAN/600 | Set to NAN (not a number) for occultations |
| QEG_Voltage | Volts | Float/600 | Detector QE-Grid Voltage values during each 0.1 sec L1A packet integration period |

| Variable Name | Units | Type/Dim | Description |
|-----------------------------|---------|---------------|---|
| QEG_Voltage_STDV | NAN | NAN/600 | Set to NAN (not a number) for occultations |
| HV_Current | μAmps | Float/600 | Detector High Voltage Current values during each 0.1 sec L1A packet integration period |
| HV_Current_STDV | NAN | NAN/600 | Set to NAN (not a number) for occultations |
| SC_ALT | Km | Float/600 | Altitude of spacecraft above reference Earth ellipsoid |
| SC_POS | Km | Float/600x3 | Position of spacecraft relative to Earth center in J2000 coordinates |
| SC_Z_Dir | unit | Float/600x3 | Unit vector of spacecraft nadir- pointing direction in J2000 |
| SC_Nadir_Lat | Degrees | Float/600 | Latitude intercept of spacecraft nadir- pointing direction |
| SC_Nadir_Lon | Degrees | Float/600 | Longitude intercept of spacecraft nadir- pointing direction |
| SC_Yaw | Degrees | Float/600 | The yaw angle of the spacecraft relative to the Earth's equator |
| Pixel_Ray_EW | Degrees | Float/600x33 | The E/W angle relative to spacecraft nadir for rays projected from the center of each row of an L1B spectral-spatial image (pixel rays) |
| Pixel_Ray_NS | Degrees | Float/600x33 | The N/S angle relative to spacecraft nadir for rays projected from the center of each row of an L1B spectral-spatial image (pixel rays) |
| Reference_Point_Lat | Degrees | Float/6600x33 | Latitude at which rays projected from the center of each L1B row ((pixel rays)) intercept the atmosphere at the reference altitude (e.g., 150 km for Day disk observations and 300 km for night disk) |
| Reference_Point_Lon | Degrees | Float/600x33 | Longitude at which rays projected from the center of each L1B row (pixel rays) intercept the atmosphere at the reference altitude (e.g., 150 km for Day disk observations and 300 km for night disk) |
| Tangent_Height | Km | Float/600x33 | Altitude above the Earth's crust at which rays projected from the center of each L1B row (pixel rays) intercept a perpendicular vector projected from Earth's center |
| Ray_Solar_Phase_Angle | Degrees | Float/600x33 | The planar angle between pixel rays and a vector from the sun to the reference point |
| Ray_Nadir_Angle | Degrees | Float/600x33 | The planar angle between pixel rays and the spacecraft nadir vector |
| Emission_Angle | Degrees | Float/600x33 | The planar angle between pixel rays and the normal vector at the reference point |
| Solar_Zenith_Angle | Degrees | Float/600 | The planar angle between a vector from the sun to the reference point and the normal vector at the reference point |
| Solar_Zenith_Angle_Wrt_Star | Degrees | Float/600 | The planar angle between a vector from the sun to the star tangent point and the normal vector at the star tangent point (Figure 4-4) |

| Variable Name | Units | Type/Dim | Description |
|--------------------------------|---------|------------------|---|
| Star_Tangent_Height | Km | Float/600 | Altitude of the star tangent point above the Earth's crust (Figure 4-4) |
| Star_Tangent_Lat | Degrees | Float/600 | Latitude of the star tangent point above the Earth's crust (Figure 4-4) |
| Star_Tangent_Lon | Degrees | Float/600 | Longitude of the star tangent point above the Earth's crust (Figure 4-4) |
| Quality_Flag | | int64/600 | Any saved quality flags |
| PHD | | Float/600x256 | Histogram distribution of the photon events Pulse Heights during an integration period |
| Raw_Count | | Float/600x800x33 | Spectral x spatial image of GOLD L1B raw photon counts accumulated during an integration period |
| Raw_Count_Random_Unc | | Float/600x800x33 | Spectral x spatial image of the random uncertainty of GOLD L1B raw photon counts accumulated during an integration period |
| Corrected_Count | | Float/600x800x33 | Spectral x spatial image of GOLD L1B photon counts accumulated during an integration period and corrected for dead time |
| Corrected_Count_Systematic_Unc | | Float/600x800x33 | Spectral x spatial image of systematic uncertainty in GOLD L1B photon counts accumulated during an integration period and corrected for dead time |

Table 4-3 L1B File Content for Occultation Observations

4.4 Generating Level 1C data

Disk and limb observations share common steps for L1B – L1C processing. Occultations are processed differently for binning, background subtraction and wavelength registration.

4.4.1 Disk and Limb Observations

L1C files for disk and limb observations contain geolocated data sampled on fixed spatial grids in both counts and radiance (calibrated) units. Equation 3.1 describes the conversion of L1B detector raw count images to fully calibrated radiances in Rayleighs/nm (One Rayleigh is a radiance unit equal to 10^6 photons emitted into 4π steradians from an area of 1 cm^2).

$$L(\lambda_j, h_k) = \frac{[C(\lambda_j, h_k) \cdot N(C(\lambda_j, h_k)) - S'_l(\lambda_j, h_k) - D'(\lambda_j, h_k)] / \Delta t}{R_c(\lambda_j) \cdot r(\lambda_j, h_k)}$$

$$R_c(\lambda_j) = A_T \cdot \Omega_c \cdot \Delta\lambda_j \cdot QT_c(\lambda_j)$$

- L = Atmosphere radiance
- C = Detector counts for (spectral, spatial) pixel (j,k)
- N = Detector linearity correction
 - MCP gain sag (System measurement, MOBI calibration facility)
 - Detector electronics dead time (Component measurement, bench test)
- S'_l = Stray plus scattered light correction ($S_{stray} + S_l$) (System measurement, MOBI calibration facility)
- D' = Total dark counts collected during an integration period,
 - Detector internal dark count (D) (Component measurement, MOBI calibration facility)
 - Background counts (B) that arise from bremsstrahlung radiation emitted by the detector particle radiation shields (model estimates. Measure on orbit)
- Δt = Integration time (GOLD E-Box Test)
- R_c = Responsivity at FOV center (System measurement, MOBI Calibration Facility)
- r = Responsivity for pixel j,k relative to that for pixel j, k_c ($r(j,k)=1$ for $k=k_c$) (System measurement, MOBI calibration facility, flat field lamp)
- A_T = Telescope area (Optical design, component measurement)
- Ω_c = Spectrograph entrance slit solid angle = $W_s \cdot H_s / F_T^2$ is the slit width
 - W_s = Slit width (Component mechanical measurement)
 - H_s = Slit height imaged onto the central row of the detector (Component mechanical measurement)
 - F_T = Telescope focal length at the center of the FOV (Optical design, component measurement)
- $\Delta\lambda_j$ = Spectral passband (System measurement, MOBI calibration facility)
- QT_c = Quantum throughput (QT) of the optics and detector at the center of the FOV (System measurement, MOBI calibration facility)

Green = Calibration Activity
 Blue = Metrology, electrical test
 Orange = Flight only

Equation 3.1 Radiometric Calibration Equation

The first term in the numerator is raw counts corrected for dead time (performed at L1A – L1B processing) and then further corrected at L1C processing for flat field (Section 4.4.1.1) and for 2-D sensitivity ($r(\lambda_j, h_k)$ (Section 4.4.1.2)). The second and third terms in the numerator are particle backgrounds and scattered light contributions to the raw counts. These are also corrected for flat field and 2-D sensitivity. Corrected total count (numerator) spectra for all the valid spatial elements in the assembled L1C image cube are divided by Δt and by $R_c(\lambda_j)$ to produce radiance.

Figure 4-5 summarize the L1B – L1C flow. The processing of the Level 1B into L1C data requires:

- current Flat-Field data
- pixel-to-pixel relative sensitivity matrix ($r(\lambda_j, h_k)$)
- measured values for the background counts and scattered light
- wavelength solution along the length of the current slit and the GYM position

- current radiometric sensitivity as a function of wavelength at detector central row ($Rc(\lambda_j)$)

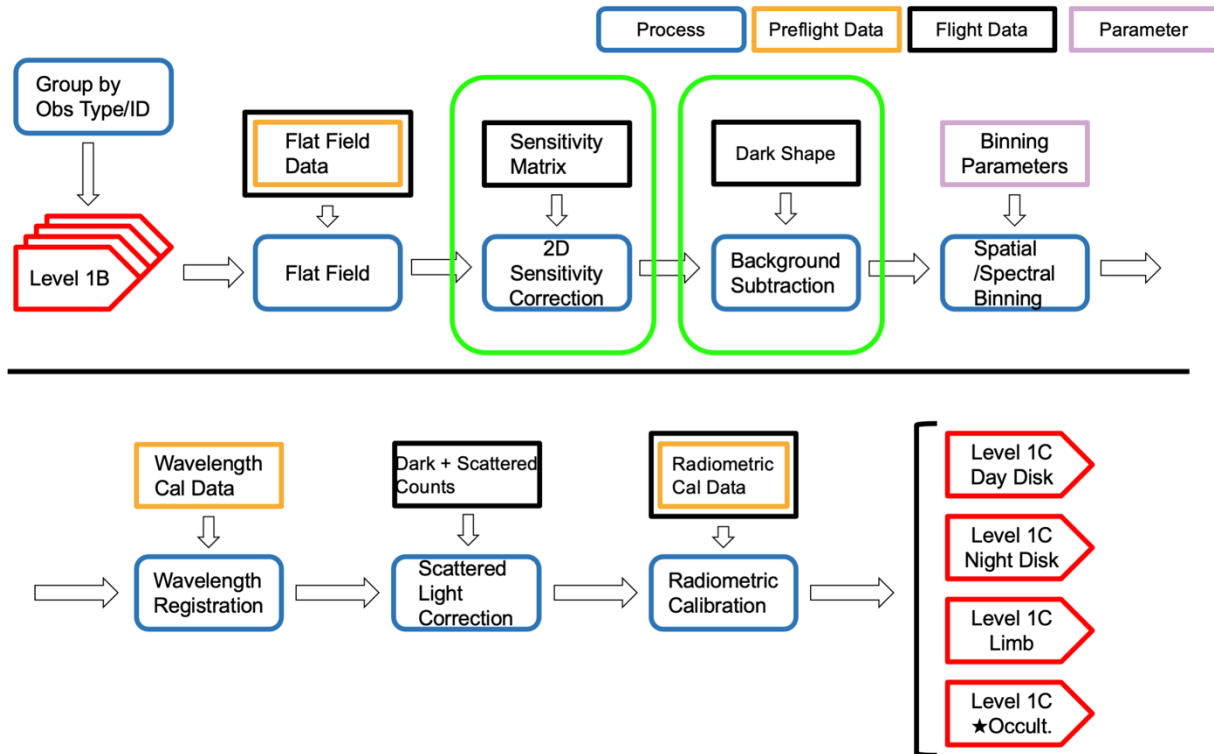


Figure 4-5 Level 1B to Level 1C Processing

4.4.1.1 Flatfield Correction

A flatfield image is used to measure and correct relative changes in detector sensitivity since the start of the mission resulting from a reduction in the MCPs pulse height (often referred to as burn in) after cumulative illumination by bright emissions (The brighter component of the OI 135.6 nm doublet is the emission primarily affected by this burn in). It is applied to the L1B images before they are assembled to produce the L1C image cubes. A flatfield image is taken once per day. Seven days of flatfield data are then combined to generate a daily calibration file. The daily flatfield calibration file is then applied to the current day’s data. Its name is recorded in the metadata.

4.4.1.2 2-D Sensitivity Correction

Equation 3.1 describes how we convert the detector raw count rates to fully calibrated radiances in Rayleighs/nm. Its denominator contains the product of two terms, $Rc(\lambda_j) * r(\lambda_j, h_k)$, the product of Responsivity at the center of the field of view and the relative responsivity of pixel (j, k) relative to pixel (j, k_0) where k_0 is the central row of an L1B image. $r(\lambda_j, h_k)$ is applied to L1B images after flat field correction before they are assembled to produce the L1C files. $Rc(\lambda_j)$ is applied as the last step in processing. This correction is currently applied to Channel A only.

4.4.1.3 Particle Background Subtraction

Particle backgrounds can vary significantly on time scales of minutes. This is accommodated in L1B – L1C processing using unilluminated areas of the detector to measure the background rate for each two-second L1B detector image. This background rate is used to scale a reference dark image, which is subtracted from each L1B image before L1C binning occurs. In addition to this time-dependent correction, a flag indicating the presence of high particle background during an observation has been added in the global attributes of the L1C files named “High_Background”. This processing is only applied to DAY, DLR, LIM, and NI1 observations. The file containing the reference dark image is bookkept in the metadata “Dark_image_file”.

4.4.1.4 Spatial Binning

Spatial binning sorts spectra from the rows of the L1B raw count and corrected count images (spatial location along the spectrograph slit) into the elements of fixed spatial grids as described in Sections 4.6 – 4.9 for each L1C data product. Variables are created for both the total L1B raw counts (processed as described in Section 4.2) and total corrected counts (processed as described in Sections 4.4.1.1 - 4.4.1.6 and 4.4.2.1 - 4.4.2.4) at each grid location. Typically, four scan mirror steps and ~ nine L1B rows are coadded at each L1C spatial bin for the DAY and DLR images. The number of rows and steps that are summed in each L1C spatial element is bookkept in a variable named ‘L1B_pixels_per_grid’. Divide raw_count by L1B_pixels_per_grid and by integration time (2 sec for Day and Limb observations, variable multiple of 2 sec for Night observations) to obtain raw_count rate. Binning for LIM and NI1 are described in Sections 4.7 and 4.8 respectively.

4.4.1.5 Wavelength Registration

The location of spectra on the detector is controlled by the GYM position, which is adjusted periodically to mitigate detector burn in. Wavelength registration is performed after summing all of the spatial bins in a single L1C image cube to produce a spectrum with high signal-to-noise. This spectrum is then aligned to a reference spectrum consisting of only the OI 135.6 and NI 149.6nm atomic lines whose wavelength locations and shapes are independent from changes in atmospheric conditions. Currently a single wavelength vector is supplied for all the valid spatial elements of each L1C image cube.

4.4.1.6 Residual Background and Scattered Light Subtraction

Any residual particle background + spectrograph scattered light is removed based on the principle that there should be essentially 0 emission at wavelengths between the LBH bands. These regions are shown in Figure 4-6.

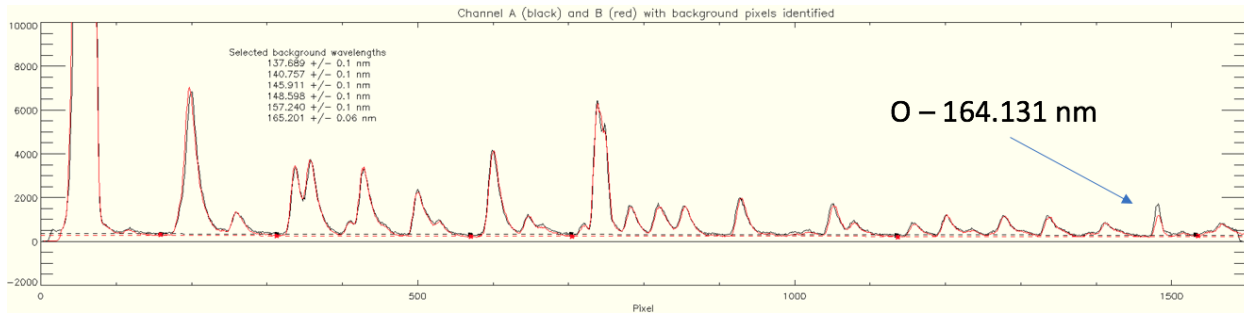


Figure 4-6 Reference Wavelengths for Background

A typical spectrum from an L1C spatial bin, shown in Figure 4-7, exhibits very little wavelength dependence and a constant background correction is currently applied at all wavelengths.

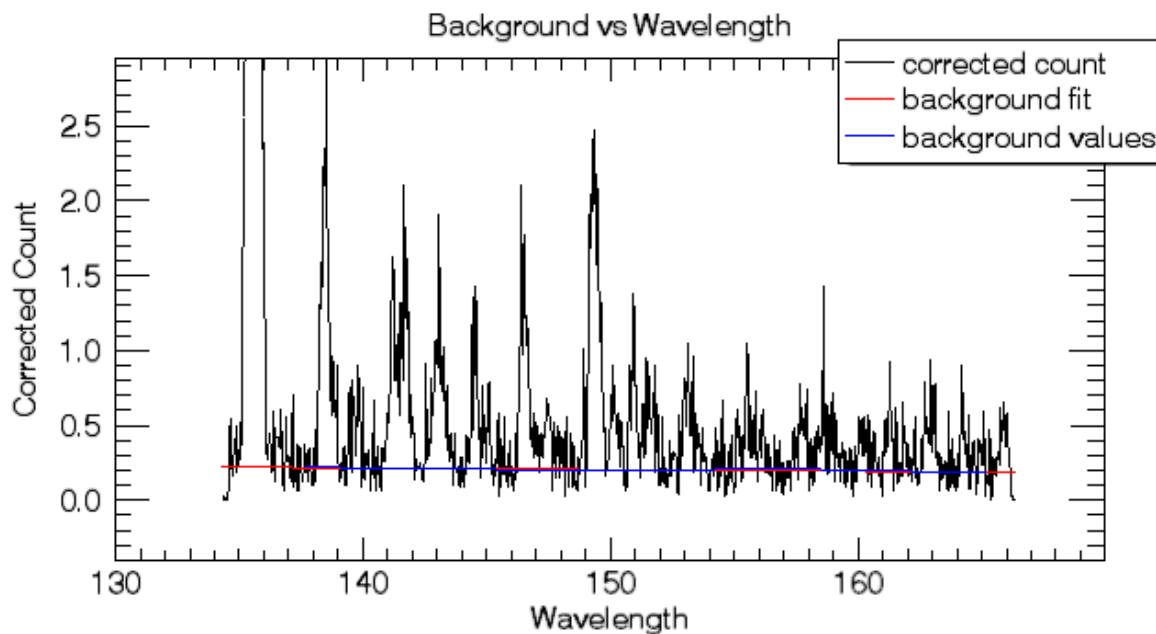


Figure 4-7 Wavelength Dependence of Background at one 1C Spatial Location

Because the counts in these ‘zero emission’ regions are low, calculating a background at each L1C spatial location directly from them alone, introduces considerable noise to the final corrected count values. Instead, a fourth-order smoothed surface is fit over the L1C spatial grid of pixels that contain valid counts. Additionally, contributions due to the presence of stars are removed. The background is multiplied by the `L1B_pixels_per_grid` before subtraction to produce the variable labeled ‘Corrected_count’ in the L1C data files. Divide this variable by `L1B_pixels_per_grid` and by Δt (0.1 sec for occultations and 2.0 sec for all other observation types) to compute corrected count rates. The `Background_counts` variable in the L1C data file contains the sum of the residual background fit at this step and the backgrounds subtracted from the L1B images (Section 4.4.1.3). Divide this variable by `L1B_pixels_per_grid` and by integration time (either 2 sec or 0.1 sec for occultations) to obtain the background count rate.

4.4.1.7 Radiometric Calibration

The final step in L1B – L1C processing is division of total corrected counts in an L1C spatial element by $L1B_pixels_per_grid$, by Δt and by $Rc(\lambda_j)$ to convert corrected count rate to radiance (Rayleighs/nm).

4.4.1.8 Uncertainty Definitions

Raw counts in each i,j,k pixel, $C_{i,j,k}$ of an L1C data cube is the total counts from all the L1B pixels that are binned for that location and $raw_count_random_unc = square_root(C_{i,j,k})$. $corrected_count$ and radiance have both systematic and random components that are bookkept separately. Details are described in McClintock et. al., 2020b. Note that data released after March 1, 2021 have updated values for error estimated for flat field, nonlinearity, and 2-D responsivity ($\sigma_{ff}=0.1$, $\sigma_N=0.1$ and $\sigma_r=0.1$). Previous releases had $\sigma_{ff}=0.0$, $\sigma_N=0.0$ and $\sigma_r=0.0$. Additionally $r(\lambda_i, h_k)$ is now variable.

4.4.2 Occultation Observations

Whereas Disk and Limb image cubes are built up by scanning an image of the Earth across a narrow spectrograph entrance slit, Occultation observations are implemented by slewing a 1° wide slit, which has an approximate 750 km wide field of view at the equator, to the limb. The slit remains motionless while the star drifts through it. L1B occultation files consist of image cubes with up to 600 spectral x spatial (800 x 33) images, sampled at 10 Hz (one minute of time per image cube).

4.4.2.1 Flatfield Correction

The flatfield correction process is identical to that for disk and limb observations.

4.4.2.2 2-D Sensitivity Correction

The 2-D sensitivity correction process is identical to that for disk and limb observations.

4.4.2.3 Particle Background Subtraction

No particle backgrounds are subtracted from the L1B files before spatial – spectral binning, wavelength scale assignment, and background subtraction.

4.4.2.4 Background Subtraction

The primary background contributions to occultation observations made on the sunlit limb of the Earth arise from atmospheric emission that enters the slit while it remains motionless during the occultation. Figure 4-8 illustrates the geometry for a western-limb occultation observation (star set) where the spectral dimension of the L1B files that comprise the occultation (total of 5) are summed to produce an image of total spectral counts (intensity values in the image) that is a function of time with 0.1 sec intervals (x axis) and 33 L1B spatial pixels (y axis).

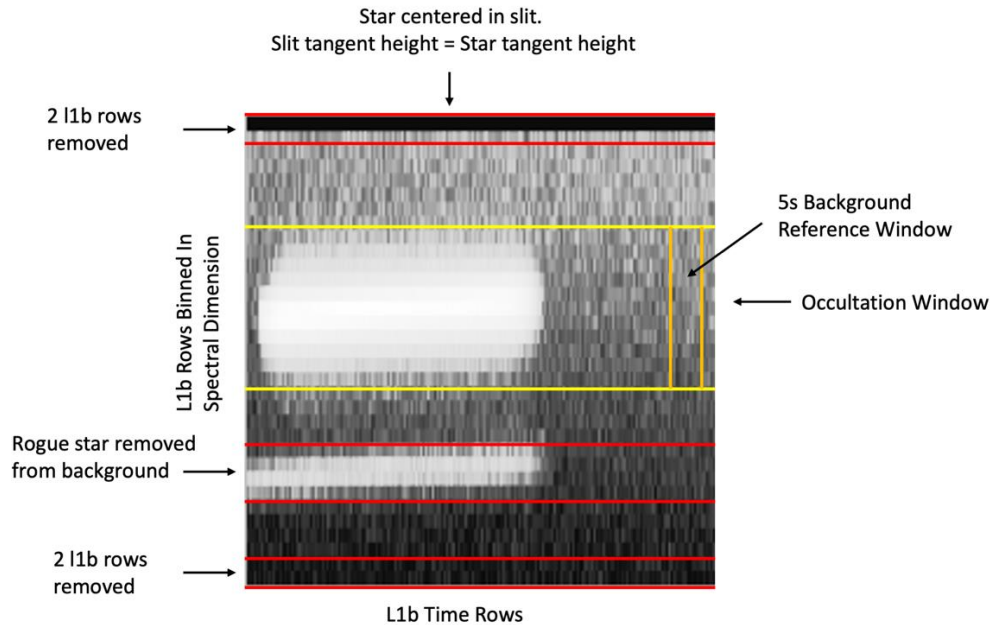


Figure 4-8 Occultation background subtraction algorithm. The image is total spectral counts as a function of time for a total of 300 seconds and of L1B row.

For the 240 seconds that the star is within the occultation slit, each spectrum in an L1B image cube is the sum of the stellar spectrum and emission from the atmosphere plus any particle backgrounds. Spectra averaged during a 5 second interval after (before for east-limb occultations) the star is completely occulted are used to calculate reference atmosphere emission plus backgrounds spectrum for the 11 rows that contain the stellar image. Experience has shown that actual atmosphere emission plus background can vary in time throughout the course of an occultation. This is mitigated by using the rows above and below the stellar image to compute a normalization factor that is applied to the reference spectra at each time step during the subtraction. Occasionally (and predictably) emission from a faint star appears in the normalization rows and must be removed from the normalization function. For night side occultations (solar zenith angle greater than 110 degrees) a linear fit is used to smooth the reference atmosphere emission spectrum. This is done because the background counts during night side occultations are too low to make reliable fits with higher wavelength resolution.

4.4.2.5 Wavelength Registration

As the star moves across the occultation slit, the light path through the instrument changes, and therefore the spectrum moves relative to the detector must be calculated for each time step in the L1C file. This is done by using a nominal wavelength solution for the high resolution slit and offsetting it to account for the stellar position as calculated from the spacecraft location and instantaneous universal time of the observation.

The wavelength returned is a function of the star's calculated position and so the solution is not applicable when the star is outside the view of the occultation slit. For the time steps outside of

the occultation slit, the default high resolution slit wavelength solution is used. This can add an discontinuity in the wavelength data when the star enters and exits the slit. This is intentional until a better approach is agreed on.

4.4.2.6 Radiometric Calibration

For stellar observations, corrected count rate in Equation 3-1 is divided by $R_c(\lambda_j)/Q_c$ rather than $R_c(\lambda_j)$ in order to convert count rate to irradiance expressed in photons/cm²/sec/nm.

4.5 Generic L1C Metadata

Each L1C file contains metadata for the file. Table 4-4 describes the general structure and content of the metadata for each type of observation, DAY, DLR, LIM, NI1 and OCC. Entries that vary from observation type to observation type are denoted by an 'XXX' in the Description column. Table 4-5 tabulates the entries for these variances.

| Variable Name | Description |
|------------------|--|
| ADID_Ref | NASA Contract > NNG12PQ28C |
| Conventions | SPDF ISTP/IACF Modified for NetCDF |
| Data_Level | L1C |
| Data_Type | APIDx0F > GOLD Application ID 0x0F: Level 1C XXX Science Data |
| Observation_Type | <i>DAY_DISK</i> , <i>LIMB</i> , <i>NIGHT_DISK_ARCS</i> , or <i>STELLAR_OCCULTATION</i> |
| OBS_TYPE | 1 (DAY_DISK), 2 (LIMB), 8 (NIGHT_DISK) or 3 (OCCULTATION) |
| OBS_ID | Observation sequence number |
| Channel_ID | 0 = CHANNEL A 1 = CHANNEL B |
| Data_Version | Version sequence number |
| Data_Revision | Revision sequence number |
| Data_Cycle | Data cycle sequence number |
| TC_VER | Version number for the detector thermal correction stim positions |
| GC_VER | Version number for the detector geometric correction files |
| OC_VER | Version number for the spectrograph optical correction files |
| Minimum_PHD | Lower limit for the pulse height filter (typical value = 2) |
| Maximum_PHD | Upper limit for the pulse height filter (typical values range from 200 to 254) |
| Spatial_Binning | 3 (Fixed L1A – L1B binning) |
| Spectral_Binning | 2 (Fixed L1A – L1B binning) |
| Slit_Position | OCC, HI_RES or LO_RES Observation type dependent |
| GYM_Position | Step position of the grating yaw mechanism |

| Variable Name | Description |
|----------------------|---|
| Mirror_Hemisphere | N or S for northern or southern hemisphere scan |
| Limb | "EAST or WEST" Specified for limb observations only |
| Reference_Altitude | 150km (DAY_DISK), 300km (NIGHT_DISK), -1km (LIMB and OCCULTATION) |
| OCC_STAR | Common name for observed star (e.g., eps Ori) specified only for occultations |
| OCC_STAR_ID | Henry Draper Star Catalog number (e.g., HD37128) specified only for occultations |
| OCC_STAR_RA | Star right ascension (degrees) specified only for occultations |
| OCC_STAR_DEC | Star declination (degrees) specified only for occultations |
| OCC_STAR_BRIGHTNESS | Star ultraviolet flux ranking relative to all stars observed by GOLD (1-30) |
| SC_Ref_Altitude | 35785.9 km relative to Earth's surface at spacecraft nadir nominal S/C altitude |
| SC_Ref_Lon | -47.5° relative to Earth's center at spacecraft nadir nominal S/C longitude |
| SC_Alt | Median spacecraft altitude (km) during the observation relative to Earth's surface |
| SC_Alt_min_max | Range of spacecraft altitudes (km) during the observation |
| SC_Pos | Median spacecraft position (km) in J2000 coordinate system during the observation |
| SC_Pos_x_min_max | Range of spacecraft x axis positions (km) during the observation |
| SC_Pos_y_min_max | Range of spacecraft y axis positions (km) during the observation |
| SC_Pos_z_min_max | Range of spacecraft z axis positions (km) during the observation |
| SC_Z_Dir | Median direction cosines of spacecraft z axis in J2000 coordinate system |
| SC_Z_Dir_x_min_max | Range of x direction cosines of spacecraft z axis in J2000 coordinate system |
| SC_Z_Dir_y_min_max | Range of y direction cosines of spacecraft z axis in J2000 coordinate system |
| SC_Z_Dir_z_min_max | Range of z direction cosines of spacecraft z axis in J2000 coordinate system |
| SC_Nadir_lat | Median latitude of the spacecraft nadir vector during the observation |
| SC_Nadir_lat_min_max | Range of latitudes of the spacecraft nadir vector during the observation |
| SC_Nadir_lon | Median longitude of the spacecraft nadir vector during the observation |
| SC_Nadir_lon_min_max | Range of longitudes of the spacecraft nadir vector during the observation |
| SC_Yaw | Median yaw of the spacecraft nadir vector rel to equator during the observation |
| SC_Yaw_min_max | Range of yaw angles of the spacecraft nadir vector relative to the equator |
| Date_Processed | Processing date for this file (e.g., 2019-09-18T16:06:41.000Z) |
| Date_Start | Start of the observation for this file (e.g., 2016-11-17 08:26:45.000Z) |
| Date_End | End of the observation for this file e.g. (2016-11-17 08:31:45.000Z) |
| Date_Start_ET | Start of the observation for this file in Ephemeris Time (seconds from January 1, 2000, 11:58:55.816 UTC) |
| Description | GOLD L1C spectral radiance image in XXX |
| Descriptor | CHA > GOLD L1C spectral radiance image in XXX |

| Variable Name | Description |
|----------------------------|--|
| Discipline | Space Physics > Ionospheric Science |
| File | GOLD_L1C_CHB_2016_016_18_45_v01.nc |
| Discipline | Space Physics > Ionospheric Science |
| File | File name (e.g., GOLD_L1C_CHB_2016_016_18_45_v01.nc) |
| File_Date | Process date (e.g., 2019-09-18T16:06:41.000Z) |
| Generated_By | e.g., GOLD SOC > GOLD L1C Processor v1.0.0 Process version can update |
| History | e.g., Version 1, Created by GOLD L1C Processor v1.0.0 on 2016-11-17 08:26:45.000Z. Version number can update |
| HTTP_LINK | http://gold.cs.ucf.edu |
| Instrument | CHA or CHB |
| Instrument_Type | UV Imaging Spectrograph (Space) |
| Link_Text | All GOLD information and data can be found at the HTTP_LINK |
| Link_Title | GOLD Website |
| Logical_File_ID | e.g., GOLD_L1C_CHC_2016_016_18_45_v01_r01 |
| Logical_Source | e.g., GOLD_L1C_CHC_2016_016_18_45 |
| Logical_Source_Description | GOLD Channel-A L1C spectral XXX |
| Flatfield_Correction_File | Data file for ff correction (e.g., GOLD_FF7_CHA_2020_305_v02_r01.nc) |
| Dark_Image_File | Data file for particle background subtraction (e.g., GOLD_DRKTOTAL_CHA_2020_306_v02_r01.nc) |
| N_Dark_Images_In_file | Number of images in the Dark_Image_file (e.g., 50) |
| High_background | High background flag |
| Mission_Group | Thermospheric and Ionospheric Investigations |
| PI_Affiliation | University of Colorado > LASP |
| PI_Name | Richard Eastes |
| Project | NASA > GOLD |
| Rules_of_Use | Public Data for Scientific Use |
| Software_Version | e.g., GOLD SOC > GOLD L1C Processor v1.0.0 Software version can update |
| Source_Name | GOLD > Global-scale Observations of the Limb and Disk (GOLD) Heliophysics Explorer mission of opportunity |
| Spacecraft_ID | SES > GOLD – 518 |
| Text | The GOLD mission of opportunity flies an ultraviolet (UV) imaging spectrograph on a geostationary satellite to measure densities and temperatures in Earth's thermosphere and ionosphere and to understand the global-scale response to forcing in the integrate Sun-Earth system. Visit ' http://www.gold-mission.org/ ' for more details. |

| Variable Name | Description |
|-----------------|--|
| Time_Resolution | Fixed with integration time at each Scan Mirror Position |
| Title | GOLD Level 1C spectral XXX |

Table 4-4 L1C Generic Metadata

| Variable Name | Description Variance |
|----------------------------|---|
| Data_Type | XXX = Day Disk, Limb, Night Disk, or Occultation |
| Description | XXX = Rayleighs/nm for atmosphere XXX= Photons.cm ² /nm/sec for stars |
| Descriptor | XXX = Rayleighs/nm for atmosphere XXX= Photons.cm ² /nm/sec for stars |
| Logical_Source_Description | XXX = radiance image in Rayleighs/nm for atmosphere XXX = irradiance image in Photons.cm ² /nm/sec for stars |
| Title | XXX = radiance image in Rayleighs/nm for atmosphere XXX = irradiance image in Photons.cm ² /nm/sec for stars |

Table 4-5 Variances from the generic metadata

4.6 L1C and L1D Day Disk Scan Data Products

4.6.1 Day Disk Scan Observations

Dayside disk and dayside limb scans are performed with channel A (CHA) operating in the High Resolution (HR) mode.

For the Dayside Disk scan, the channel A scan mirror steps the 10.8° tall image of its spectrometer entrance slit across the sunlit portions of the disk in two swaths, one covers the northern hemisphere and the other covers the southern hemisphere, as shown in Figure 4-9. Each swath requires 12 minutes to complete including setup (24 minutes for a complete disk image) at a fixed rate of 0.05214° per step (nadir ground speed of 32.56 km per step at the sub spacecraft point) for 346 scan mirror positions (17.87°). It scans the disk +150 km on each side with (+/- 0.073°) margin for spacecraft pointing. All disk scans are performed scanning from East to West. Figure 4-10 shows the GOLD field of view for disk pixels.

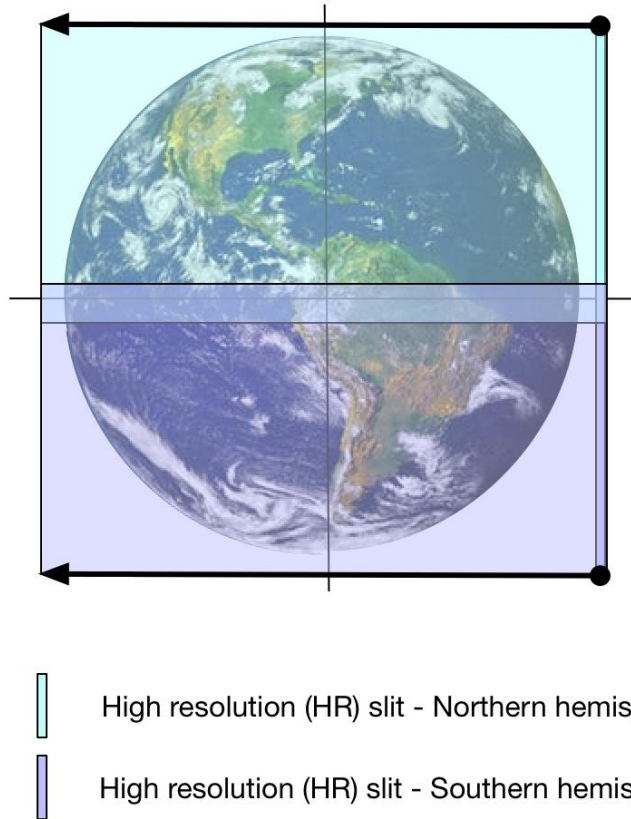


Figure 4-9 Day Disk Scan Observation

GOLD Field of View for Disk Pixels

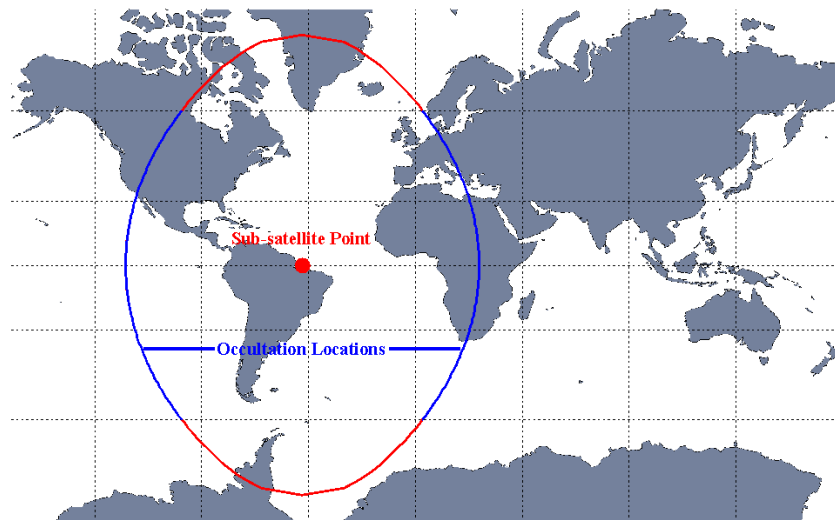


Figure 4-10 GOLD Field of View

4.6.2 Level 1C Data File Structure and Content

The Level 1C Day Disk data is sampled on a uniform satellite look angle grid of 0.2° , referred to as ‘super pixels’ (Table 4-6, Figure 4-11), in both the Longitude and Latitude directions. The data is resampled as follows:

- Approximately 4 scan mirror positions that fall within the 0.2° L1C bin
- Approximately 9 L1B image rows that fall within the 0.2° L1C bin
- Image displacement per scan mirror step: 0.05214
- HR slit width: 0.075°
- Accumulate counts in an L1C bin for all 1B pixels whose centers falls within the bin (nearest neighbor)
- Spectral data is combined within a L1C bin WITHOUT applying any wavelength adjustment to each L1B sample
- 92 bins E-W
- 104 bins N-S

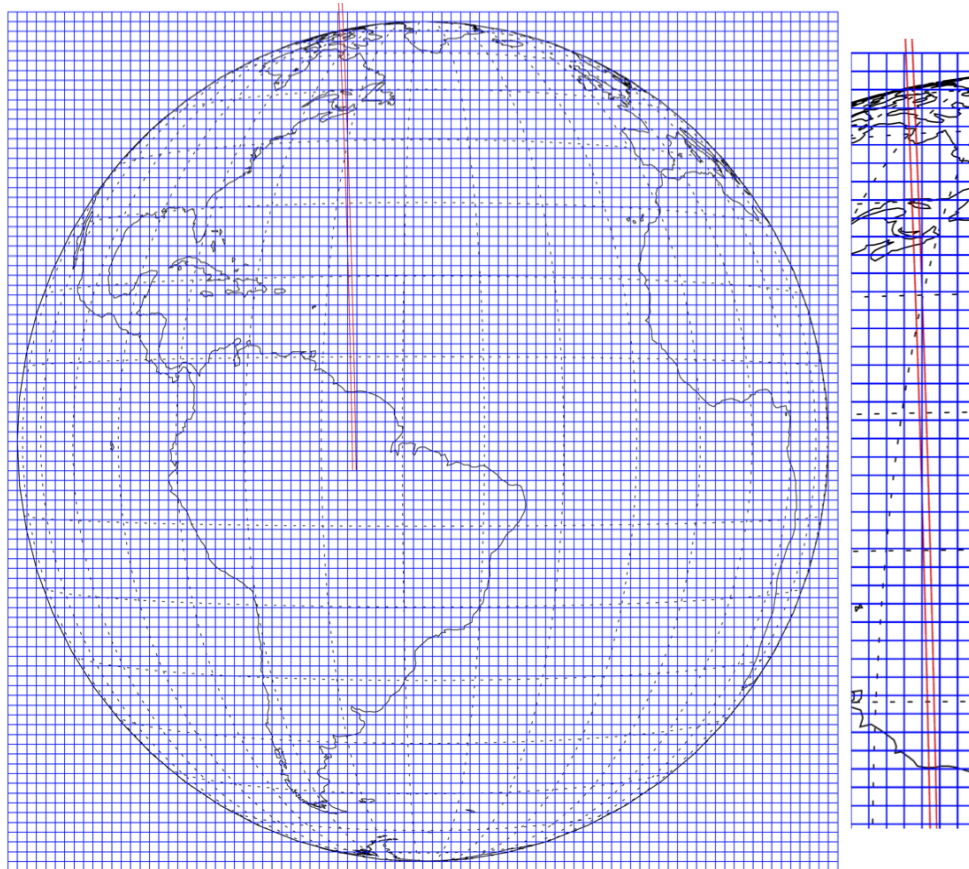


Figure 4-11 Level 1C Bins

Table 4-6 summarizes the contents of L1C_DAY disk scans

| Variable Name | Units | Type/Dim | Description |
|--------------------------------|------------------|------------------|--|
| Grid_EW | Degrees | Float/92 | East-West grid location (center of pixel). |
| Grid_NS | Degrees | Float/104 | North-South grid Location (center of pixel). |
| Grid_LAT | Degrees | Float/104x92 | The fixed L1C pixel center latitude location. |
| Grid_LON | Degrees | Float/104x92 | The fixed L1C pixel center longitude location. |
| Time_ET | seconds | Double/104x92 | TDB seconds from January 1, 2000, 11:58:55.816 UTC. The average ET of all the L1B bins coadded in each L1C spatial pixel. |
| Time_UTC | date/time | Char/104x92x24 | UTC date/time string: "2017-06-21T23:46:38.015Z" The average UTC of all the L1B bins coadded in each L1C spatial pixel. |
| L1b_Time_Bins_Per_Grid | count | int/104x92 | The number of L1B scan mirror steps in each L1C spatial pixel. |
| L1b_Pixels_Per_Grid | count | int/104x92 | The number of L1B pixels coadded in each L1C spatial pixel. |
| Quality_FLAG | | uint64/104x92 | Per pixel quality flags |
| Wavelength | Nm | Float/104x92x800 | The wavelength vector at each spatial pixel |
| Raw_Count | counts | Float/104x92x800 | The co-added raw count data from the L1B records. |
| Raw_Count_Random_Unc | counts | Float/104x92x800 | The random uncertainty of the raw counts (Poisson). |
| Corrected_Count | counts | Float/104x92x800 | The co-added L1B raw counts corrected for dead time, flat field, and 2-D sensitivity |
| Corrected_Count_Systematic_Unc | counts | Float/104x92x800 | Systematic uncertainty of the corrected counts. |
| Corrected_Count_Random_Unc | counts | Float/104x92x800 | Random uncertainty of the corrected counts. |
| Radiance | Rayleighs/ nm | Float/104x92x800 | The spectral radiance at each grid position. |
| Radiance_Systematic_Unc | Rayleighs/ nm | Float/104x92x800 | The spectral radiance systematic uncertainty. |
| Radiance_Random_Unc | Rayleighs/ nm | Float/104x92x800 | The spectral radiance random uncertainty. |
| Background_Counts | Counts | Float/104x92x800 | The particle + scattered light background counts subtracted in the background correction. |
| Reference_Point_Lat | Degrees | Float/104x92 | Mean latitude of all L1B pixels in L1C superpixel. |
| Reference_Point_Lon | Degrees | Float/104x92 | Mean longitude of all L1B pixels in L1C superpixel. |
| Tangent_Height | Km | Float/104x92 | The tangent height of the pixel center ray from the Earth's crust. |
| Ray_Solar_Phase_Angle | Degrees | Float/104x92 | The planar angle between the pixel ray from center and the sun direction. |

| Variable Name | Units | Type/Dim | Description |
|--------------------|---------|--------------|--|
| Ray_Nadir_Angle | Degrees | Float/104x92 | The planar angle between the pixel ray from center and the spacecraft nadir. |
| Emission_Angle | Degrees | Float/104x92 | The planar angle between the pixel ray from center and the normal to the reference point. |
| Solar_Zenith_Angle | Degrees | Float/104x92 | The planar angle between the sun direction to the reference point and the normal to the reference point. |

Table 4-6 Level 1C Day Disk File Content

4.6.3 Level 1D Data File Structures

Level 1D files contain a thumbnail image (PNG) for individual disk scans. There are individual thumbnail files created for 135.6 nm (Atomic Oxygen), for total Lyman-Birge-Hopfield (LBH), and for Solar Zenith Angle (SZA). There is also a combined thumbnail image file created that contains 4 images: 135.6 nm, LBH Short (denoted LBH1), LBH Long (denoted LBH2), and SZA (see example in Figure 4-12). Radiance values are calculated by integrating over the wavelength intervals specified in Table 4-7. Separate files are created for Channel A and Channel B data. A new L1D file is generated for each new L1C file. These correspond to either a Northern or Southern hemisphere scan.

Combined file definition (image size = 1024 x 1024 pixels)

- € Header information (at the top of the set of 4 images)
 - Date of image
 - Time of image
 - File name
- € 1356 radiance map (in Rayleighs).
- € LBH band 1 radiance map (in Rayleighs).
- € LBH band 2 radiance map (in Rayleighs).
- € 1493 radiance map (in Rayleighs).
- € SZA solar zenith angle map is at the reference altitude of 150 km.

Individual file definitions (image size = 512 x 512 pixels)

- € 1356 radiance map (in Rayleighs).
- € Total LBH radiance map (in Rayleighs).
- € SZA solar zenith angle map is at the reference altitude of 150 km.

| Feature Name | Wavelength integration intervals [nm] |
|--------------|---------------------------------------|
|--------------|---------------------------------------|

| | |
|------|--|
| 1356 | [135.0, 137.0] |
| LBH | [137.7, 140.1], [140.9, 142.2], [142.5, 143.7], [144.2, 145.4], [146.1, 148.0], [149.9, 152.0], [152.8, 154.0] |
| LBH1 | [140.8, 142.1], [142.6, 143.7], [144.2, 145.2], [146.1, 147.8] |
| LBH2 | [149.9, 152.0], [152.8, 154.0], [155.2, 156.6], [157.4, 160.6] |
| 1493 | [149.0, 149.8] |

Table 4-7 L1D Radiance Band Definitions

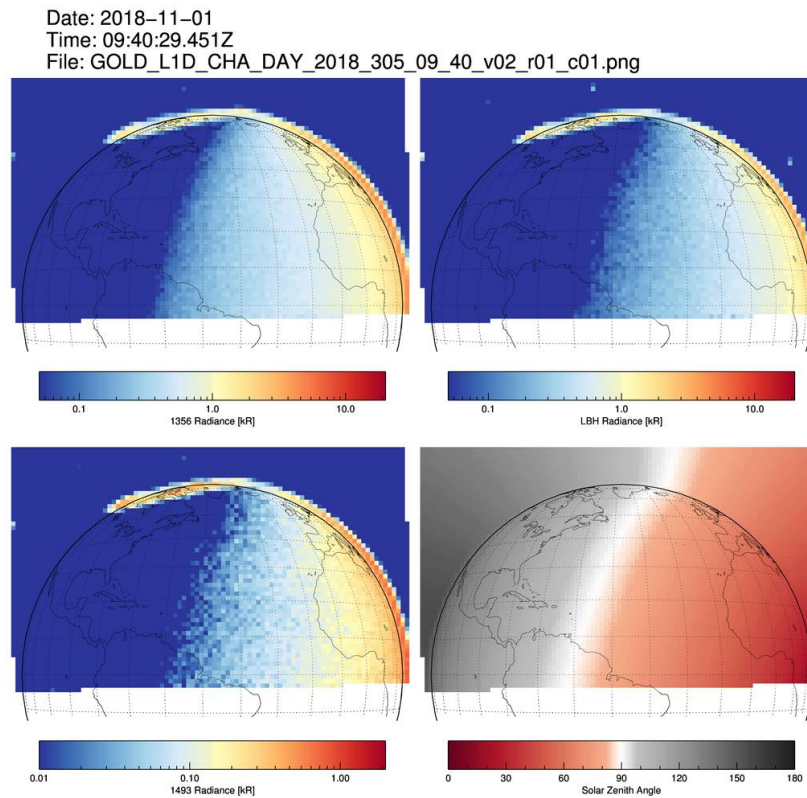


Figure 4-12 Example Level 1D Combined Day Disk File

4.7 L1C and L1D Limb Scan Data Products

4.7.1 Limb Scan Observations

Following the disk observation (if an occultation observation is not available within the 30-minute block), Channel A scans both the north and south hemispheres of the dayside limb, as shown in Figure 4-13. The limb scans begin on the disk at a limb-height of -50 km at the equator and scan to a limb height of 430 km with a step size of 8 km at the equator and a cadence of 2.0

seconds per step with a total of 59 steps (for 60 positions). These two scans require a total of 6 minutes to complete. Detector dark counts are measured with the scan mirrors turned inward for 18 seconds, once per hemisphere, in order to monitor particle backgrounds. The entire sequence of dayside disk image and limb scan, without occultations, requires 30 minutes to execute.

Limb scans: distance to the limb = 41650 km

-step time = 2 sec

-image motion = 8.0 km/step at nadir

-angular coverage = 486 km at limb

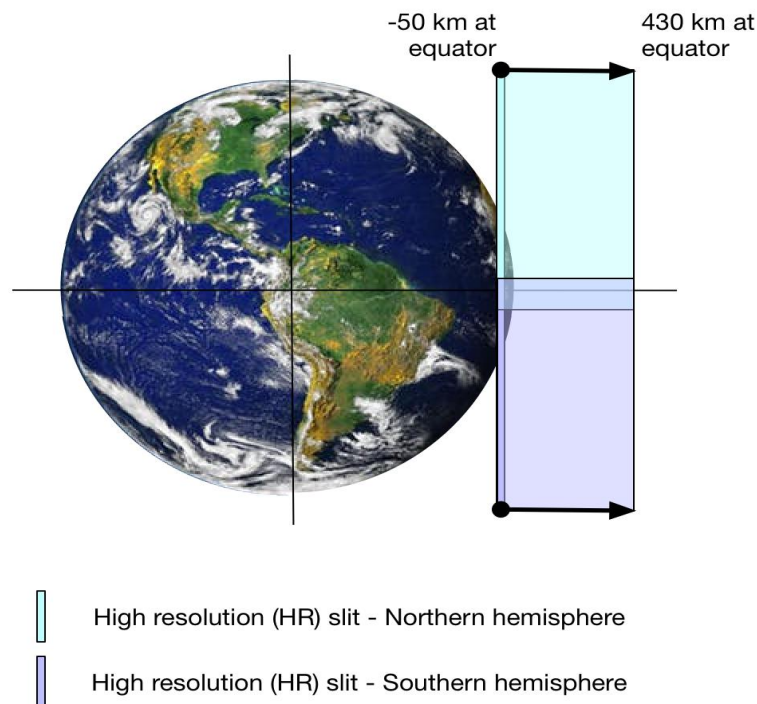


Figure 4-13 Limb Scan

4.7.2 Level 1C Data File Structure and Contents

The Level 1C Limb data is sampled on a radial grid of 1.25° in Latitude and 16 Km in tangent altitude from -44 Km to 435 Km above the surface (Figure 4-14). The data is resampled as follows:

- Image displacement per scan mirror step: 0.011°
- 2 scan mirror positions to cover the 16 Km at the equator for L1C bin.

- HR slit width: 0.075°
- Accumulate counts in an L1C bin for all 1B pixels whose centers falls within the bin (nearest neighbor)
- Spectral data is combined within a L1C bin WITHOUT doing any wavelength adjustment for each L1B sample
- Going from -20 to $+20$ degree latitudes

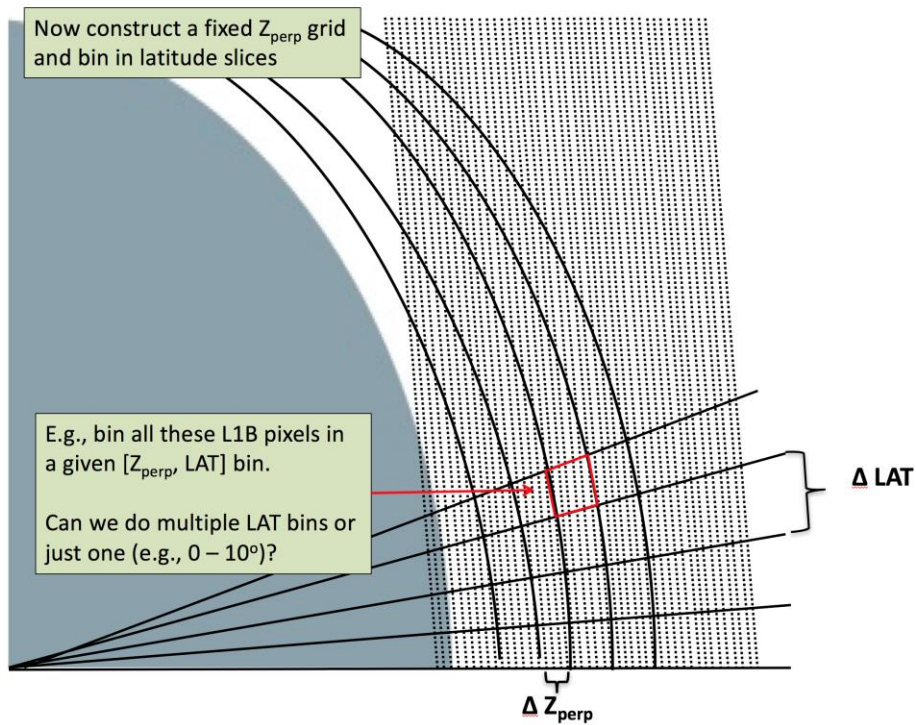


Figure 4-14 Grid for Limb Scan

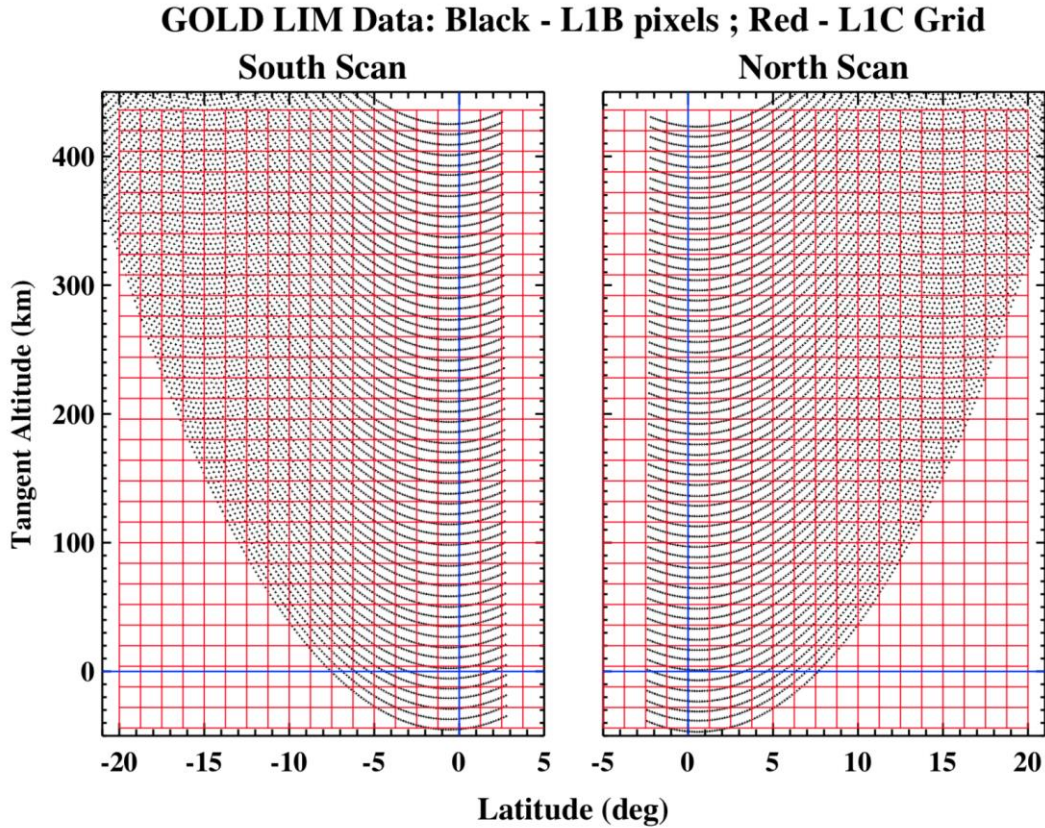


Figure 4-15 Fixed Grid for Limb Scan

Table 4-8 summarizes the contents of L1C_LIM

| Variable Name | Units | Type/Dim | Description |
|------------------------|---------------|-----------------|---|
| Grid_ALT | Km | Float/30 | The Tangent Height Altitude grid values. |
| Grid_LAT | Degrees | Float/32 | The Radial Latitude grid values. |
| Time_ET | seconds | Double/32x30 | TDB seconds from January 1, 2000, 11:58:55.816 UTC. The average ET of all the L1B bins coadded in each L1C spatial pixel. |
| Time_UTC | date/time UTC | Char/32x30x24 | UTC date/time string: "2017-06-21T23:46:38.015Z" The average UTC of all the L1B bins coadded in each L1C spatial pixel. |
| L1b_Time_Bins_Per_Grid | count | int/32x30 | The number of L1B scan mirror steps in each L1C spatial pixel. |
| L1b_Pixels_Per_Grid | count | int/32x30 | The number of L1B pixels coadded in each L1C spatial pixel. |
| Quality | | uint64/32x30 | The per pixel quality flags. |
| Wavelength | nm | Float/32x30x800 | The wavelength vector at each spatial pixel |
| Raw_Count | counts | Float/32x30x800 | The co-added raw count data from the L1B records. |

| Variable Name | Units | Type/Dim | Description |
|--------------------------------|------------------|-----------------|--|
| Raw_Count_Random_Unc | counts | Float/32x30x800 | The random uncertainty of the raw counts (Poisson). |
| Corrected_Count | counts | Float/32x30x800 | The co-added L1B raw counts corrected for dead time, flat field, and 2-D sensitivity |
| Corrected_Count_Systematic_Unc | counts | Float/32x30x800 | Systematic uncertainty of the corrected counts. |
| Corrected_Count_Random_Unc | counts | Float/32x30x800 | Random uncertainty of the corrected counts. |
| Radiance | Rayleighs/n m | Float/32x30x800 | The spectral radiance at each grid position. |
| Radiance_Systematic_Unc | Rayleighs/n m | Float/32x30x800 | The spectral radiance systematic uncertainty. |
| Radiance_Random_Unc | Rayleighs/n m | Float/32x30x800 | The spectral radiance random uncertainty. |
| Background_Counts | counts | Float/32x30x800 | The particle + scattered light background counts subtracted in the background correction. |
| Reference_Point_Lat | Degrees | Float/32x30 | Mean latitude of all L1B pixels in L1C superpixel. |
| Reference_Point_Lon | Degrees | Float/32x30 | Mean longitude of all L1B pixels in L1C superpixel. |
| Tangent_Height | km | Float/32x30 | The tangent height of the pixel center ray from the Earth's crust. |
| Ray_Solar_Phase_Angle | Degrees | Float/32x30 | The planar angle between the pixel ray from center and the sun direction. |
| Ray_Nadir_Angle | Degrees | Float/32x30 | The planar angle between the pixel ray from center and the spacecraft nadir. |
| Emission_Angle | Degrees | Float/32x30 | The planar angle between the pixel ray from center and the normal to the reference point. |
| Solar_Zenith_Angle | Degrees | Float/32x30 | The planar angle between the sun direction to the reference point and the normal to the reference point. |

Table 4-8 Level 1C Limb File Content

4.7.3 Level 1D Data File Structures

Level 1D files contain a thumbnail image (PNG) for individual limb scans. There are individual thumbnail files created for 135.6 nm (Atomic Oxygen), for total Lyman-Birge-Hopfield (LBH), stack of 8 slices for different latitudes of radiance as a function of wavelength and tangent altitude, and a single line plot with radiance of 135.6, LBH Short (denoted LBH1), and LBH Long (denoted LBH2) as a function of tangent altitude. There is also a combined thumbnail image file created that contains 4 images: 135.6 nm (Atomic Oxygen), total Lyman-Birge-Hopfield (LBH), stack of 8 slices for different latitudes of radiance as a function of wavelength and tangent altitude, and a single line plot with radiance of 135.6, LBH Short (denoted LBH1), and LBH Long (denoted LBH2) as a function of tangent altitude (see example in Figure 4-16).

Radiance values are calculated by integrating over the wavelength intervals specified in Table 4-7. Separate files are created for Channel A and Channel B data. A new L1D file is generated for each new L1C file. These correspond to either the Northern or Southern hemisphere.

Combined file definition (image size = 1024 x 1024 pixels)

- € Header information (at the top of the set of 4 images)
 - Date of image
 - Time of image
 - File name
 - Mean Solar Zenith Angle (SZA)
- € 1356 radiance map (in Rayleighs).
- € Total LBH radiance map (in Rayleighs).
- € Single line plot of the lowest latitude radiance in (kilo-Rayleighs) as a function of tangent altitude (in kilometers) with the following 3 lines
 - 135.6
 - LBH band 1
 - LBH band 2
- € Stack of 8 slices for different latitudes of intensity as a function of wavelength and altitude
 - Use the 8 latitudes that correspond to the scan hemisphere (since there are 16 latitudes per hemisphere, 2 latitude bins are co-added to get to 8 latitudes)
 - Latitudes are +/- [0.625, 1.875, 3.125, 4.375, 5.625, 6.875, 8.125, 9.375]

Individual file definitions (image size = 512 x 512 pixels)

- € 135.6 radiance map (in Rayleighs).
- € Total LBH radiance map (in Rayleighs)..
- € Single line plot of the lowest latitude radiance in (kilo-Rayleighs) as a function of tangent altitude (in kilometers) with the following 3 lines
 - 135.6
 - LBH band 1
 - LBH band 2
- € Stack of 8 slices for different latitudes of intensity as a function of wavelength and altitude
 - Use the 8 latitudes that correspond to the scan hemisphere (since there are 16 latitudes per hemisphere, 2 latitude bins are co-added to get to 8 latitudes)

- Latitudes are +/- [0.625, 1.875, 3.125, 4.375, 5.625, 6.875, 8.125, 9.375]

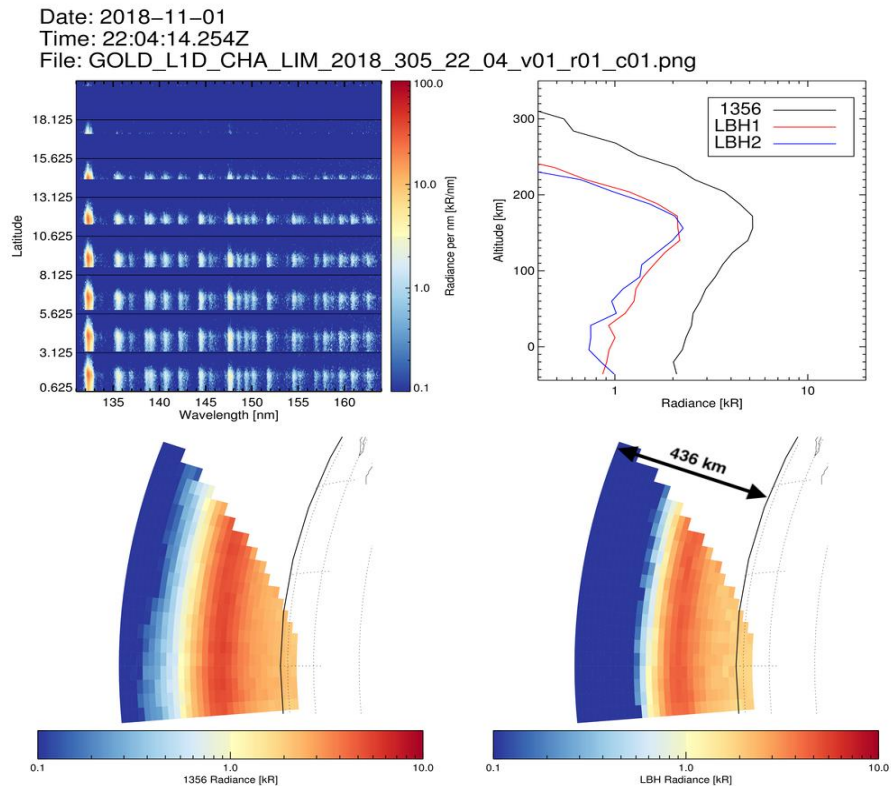


Figure 4-16 Example Level 1D Combined Limb File

4.8 L1C and L1D Night Disk Scan Data Products

4.8.1 Night Disk Scan Observations

Night disk scans may be performed independently on each channel (CHA and CHB).

For the Night Disk Scan (Figure 4-17), each channel may use the low-resolution slit (observation type = NI1) or the occultation slit (observation type = NI2). Each swath requires 15 minutes to complete including setup using a variable number of steps and variable step time, depending on time of day and day of year.

Night Disk scans - Low Resolution Slit: 35786 km

-step time = variable (increments of 2 sec)

-image motion = 92.73 km/step at nadir

-angular coverage = variable

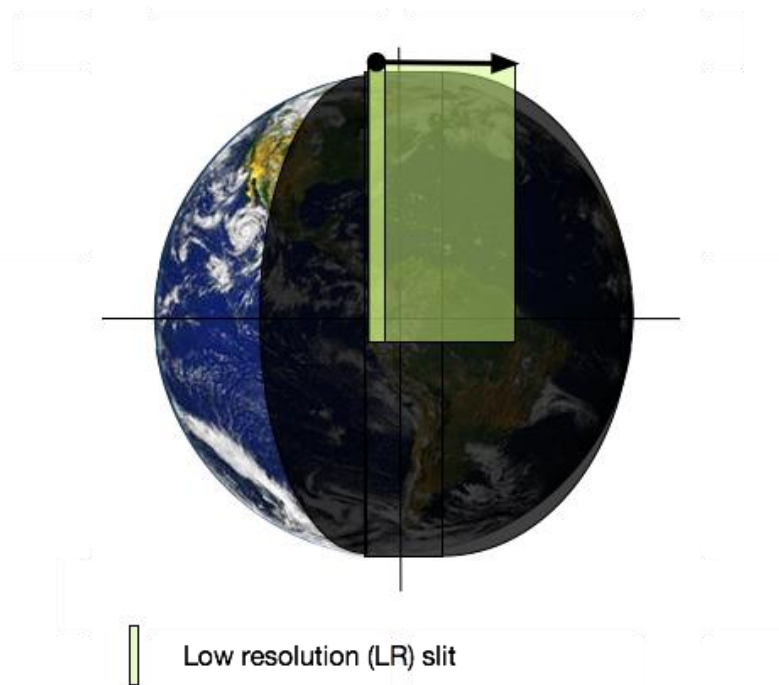


Figure 4-17 Night Disk Scan - Low Resolution Slit (NI1)

4.8.2 Level 1C Data File Content

Table 4-9 summarizes the contents of L1C_NI1 Disk scans

| Variable Name | Units | Type/Dim | Description |
|------------------------|-----------|-------------------------|---|
| Grid_EW | Degrees | Float/n_ns x n_ew | East-West grid location (center of pixel). |
| Grid_NS | Degrees | Float/n_ns x n_ew | North-South grid Location (center of pixel). |
| Time_ET | seconds | Double/n_ew | TDB seconds from January 1, 2000, 11:58:55.816 UTC. The average ET of all the L1B bins coadded in each L1C spatial pixel. |
| Time_UTC | date/time | Char/n_ew x 24 | UTC date/time string: "2017-06-21T23:46:38.015Z" The average UTC of all the L1B bins coadded in each L1C spatial pixel. |
| Wavelength | nm | Float/n_ns x n_ew x 800 | The wavelengths vector for each spatial pixel |
| L1b_Time_Bins_Per_Grid | counts | int/n_ns x n_ew | The number of L1B time steps in each L1C spatial pixel. |
| L1b_Pixels_Per_Grid | counts | int/n_ns x n_ew | The number of L1B pixels coadded in each L1C spatial pixel. |
| Quality_Flag | | int64/n_ew | |
| Reference_Point_Lat | Degrees | Float/n_ns x n_ew | Latitude of the reference point. |
| Reference_Point_Lon | Degrees | Float/n_ns x n_ew | Longitude of the reference point. |

| Variable Name | Units | Type/Dim | Description |
|--------------------------------|--------------|-------------------------|--|
| Tangent_Height | Km | Float/n_ns x n_ew | The tangent height of the pixel center from the Earth's crust. |
| Ray_Solar_Phase_Angle | Degrees | Float/n_ns x n_ew | The planar angle between the pixel from center and the sun direction. |
| Ray_Nadir_Angle | Degrees | Float/n_ns x n_ew | The planar angle between the pixel from center and the spacecraft nadir. |
| Emission_Angle | Degrees | Float/n_ns x n_ew | The planar angle between the pixel from center and the normal to the reference point. |
| Solar_Zenith_Angle | Degrees | Float/n_ns x n_ew | The planar angle between the sun direction to the reference point and the normal to the reference point. |
| Raw_Count | counts | Float/n_ns x n_ew x 800 | The random uncertainty of the raw counts (Poisson). |
| Raw_Count_Random_unc | counts | Float/n_ns x n_ew x 800 | The co-added L1B raw counts corrected for dead time, flat field, and 2-D sensitivity |
| Corrected_Count | counts | Float/n_ns x n_ew x 800 | Systematic uncertainty of the corrected counts. |
| Corrected_Count_Systematic_Unc | counts | Float/n_ns x n_ew x 800 | Random uncertainty of the corrected counts. |
| Corrected_Count_Random_Unc | counts | Float/n_ns x n_ew x 800 | The random uncertainty of the raw counts (Poisson). |
| Radiance | Rayleighs/nm | Float/n_ns x n_ew x 800 | The spectral radiance at each grid position. |
| Radiance_Systematic_Unc | Rayleighs/nm | Float/n_ns x n_ew x 800 | The spectral radiance systematic uncertainty. |
| Radiance_Random_Unc | Rayleighs/nm | Float/n_ns x n_ew x 800 | The spectral radiance random uncertainty. |
| Background_Counts | counts | Float/600 x 800 | The particle + scattered light background counts subtracted in the background correction. |

Table 4-9 Level 1C Night Disk Scan File Content

4.8.3 Level 1D Data File Structures

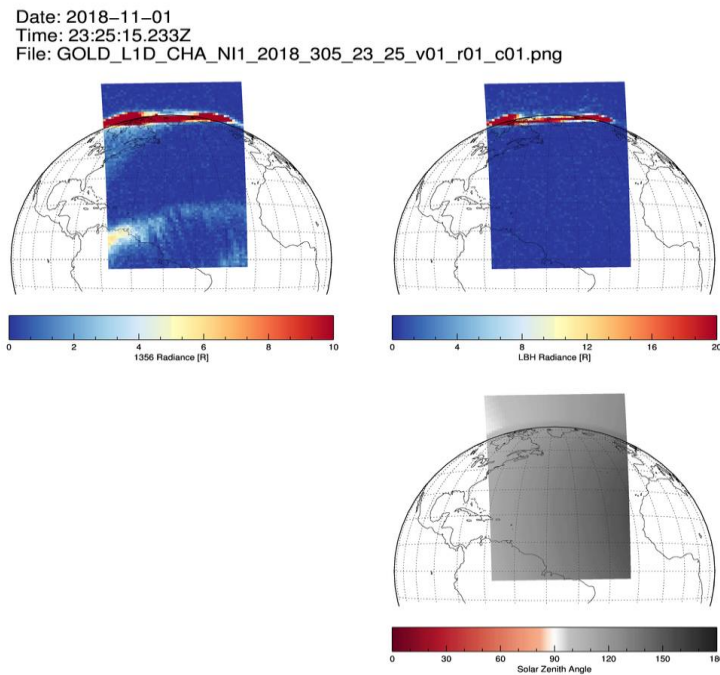
Level 1D files contain a thumbnail image (PNG) for individual night scans. There are individual thumbnail files created for 135.6 nm (Atomic Oxygen), for total Lyman-Birge-Hopfield (LBH), and for Solar Zenith Angle (SZA). There is also a combined thumbnail image file created that contains 3 images: 135.6 nm, Total LBH, and SZA (see example in Figure 4-18). Radiance values are calculated by integrating over the wavelength intervals specified in Table 4-7. Separate files are created for Channel A and Channel B data. A new L1D file is generated for each new L1C file. These correspond to either the Northern or Southern hemisphere.

Combined file definition (image size = 1024 x 1024 pixels)

- € Header information (at the top of the set of 3 images)
 - Date of image
 - Time of image
 - File name
- € 135.6 radiance map (in Rayleighs).
- € Total LBH radiance map (in Rayleighs).
- € SZA solar zenith angle map is at the reference altitude of 150 km.

Individual file definitions (image size = 512 x 512 pixels)

- € 135.6 radiance map (in Rayleighs).
- € Total LBH radiance map (in Rayleighs).
- € SZA solar zenith angle map is at the reference altitude of 150 km.

**Figure 4-18 Example Level 1D Combined Night 1 File**

4.9 LIC and L1D Stellar Occultation Data Products

4.9.1 Stellar Occultation Observations

Dayside Disk Images are interrupted via stored instrument commands when target stars suitable for occultation measurements approach either limb, as shown in Figure 4-19. To perform the occultation measurement, the slit mechanism inserts the 1° wide occultation (OCC) slit at the spectrometer focal plane, and the scan mirrors slew the Field of View to the star. The mirror is centered at a 225 km tangent point altitude. Occultations require 6 minutes to execute (30 seconds to configure the instrument, 30 seconds for uncertainty in timing and pointing, 4 minutes for the actual occultation, 30 seconds for uncertainty in timing and pointing, and 30 seconds to return to HR slit). Once the occultation is complete, the HR slit is inserted, the scan mirror returns to its departure point in the original mapping observation, and Dayside Disk Image is resumed. By choice, GOLD is limited to performing ~10 occultations a day for most of the year. Since occultation observations replace limb scans, this reduces the number of daily limb scans by ~5%.

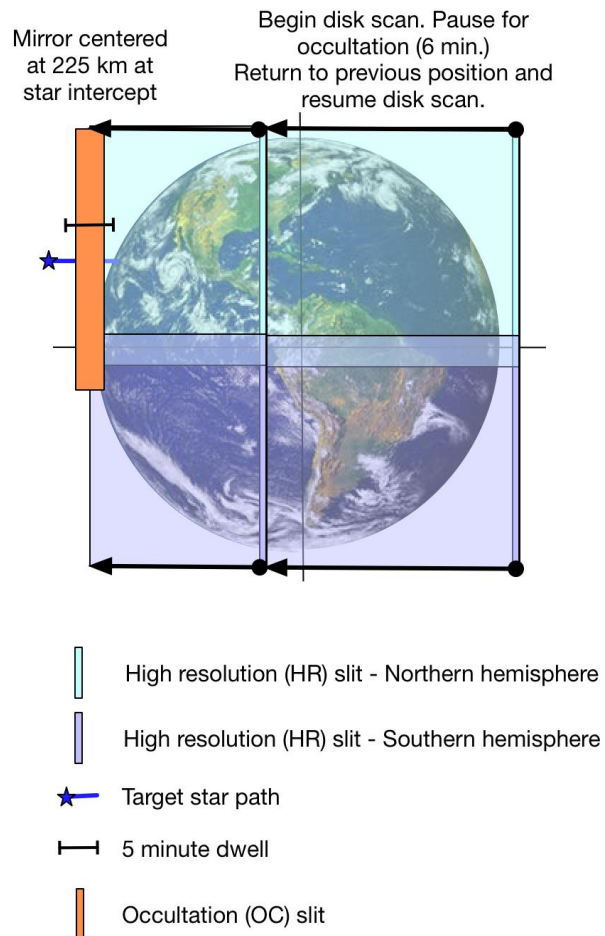


Figure 4-19 Occultation Observation

4.9.2 Level 1C Data File Structures

Table 4-10 summarizes the contents of L1C_OCC files

| Variable Name | Units | Type/Dim | Description |
|--------------------------------|--------------------------------|---------------|---|
| Time_ET | seconds | Double/980 | TDB seconds from January 1, 2000, 11:58:55.816 UTC. The average ET of all the L1B bins coadded in each L1C spatial pixel. |
| Time_UTC | date/time UTC | Char/980x24 | UTC date/time string: "2017-06-21T23:46:38.015Z" The average UTC of all the L1B bins coadded in each L1C spatial pixel. |
| L1b_Time_Bins_Per_Grid | count | int/980 | The number of L1B time steps in each L1C spatial pixel. |
| L1b_Pixels_Per_Grid | count | int/980 | The number of L1B pixels coadded in each L1C spatial pixel. |
| Quality_Flag | | uint64/980 | The per pixel quality flags. |
| Wavelength | nm | Float/980x266 | The wavelengths vector each time step |
| Raw_Count | counts | Float/980x266 | The co-added L1B raw counts corrected for dead time, flat field, and 2-D sensitivity |
| Raw_Count_Random_Unc | counts | Float/980x266 | Systematic uncertainty of the corrected counts. |
| Corrected_Count | counts | Float/980x266 | Random uncertainty of the corrected counts. |
| Corrected_Count_Systematic_Unc | counts | Float/980x266 | The spectral radiance at each grid position. |
| Corrected_Count_Random_Unc | counts | Float/980x266 | The spectral radiance systematic uncertainty. |
| Irradiance | Ph/cm ² /sec/ nm | Float/980x266 | The spectral irradiance at each time step |
| Irradiance_Systematic_Unc | Ph/cm ² /sec/ nm | Float/980x266 | The spectral irradiance systematic uncertainty at each time step |
| Irradiance_Random_Unc | Ph/cm ² /sec/ nm | Float/980x266 | The spectral irradiance random uncertainty at each time step |
| Background_Counts | counts | Float/600x800 | The background counts subtracted in the background correction. |
| Reference_Point_Lat | Degrees | Float/980 | Latitude of the reference point. |
| Reference_Point_Lon | Degrees | Float/980 | Longitude of the reference point. |
| Tangent_Height | km | Float/980 | The tangent height of the star from the Earth's crust. |
| Ray_Solar_Phase_Angle | Degrees | Float/980 | The planar angle between the pixel ray from center and the sun direction. |
| Ray_Nadir_Angle | Degrees | Float/980 | The planar angle between the pixel ray from center and the spacecraft nadir. |
| Emission_Angle | Degrees | Float/980 | The planar angle between the pixel ray from center and the normal to the reference point. |

| Variable Name | Units | Type/Dim | Description |
|-----------------------------|---------|-----------|--|
| Solar_Zenith_Angle | Degrees | Float/980 | The planar angle between the sun direction to the reference point and the normal to the reference point. |
| Star_Tangent_Height | km | Float/980 | The tangent height of the star with respect to GOLD. |
| Solar_Zenith_Angle_Wrt_Star | Degrees | Float/980 | The planar angle between the sun direction to the star tangent point normal. |
| Star_Tangent_Lat | Degrees | Float/980 | Tangent point Latitude relative to fixed Earth frame of line to star. |
| Star_Tangent_Lon | Degrees | Float/980 | Tangent point Longitude relative to fixed Earth frame of line to star. |

Table 4-10 Level 1C Stellar Occultation Disk File Contents

4.9.3 Level 1D Data File Structures

Level 1D files contain a thumbnail image (PNG) for individual occultations. There are individual thumbnail files created for a 2D image of counts vs. wavelength and tangent altitude, and line plots of counts vs. time, tangent altitude, and wavelength. There is also a combined thumbnail image file created that contains all 4 of these images (see example in Figure 4-20). The line plots show counts from three separate spectral bins, which are defined in Table 4-11 and Table 4-12. Separate files are created for Channel A and Channel B data. A new L1D file is generated for each new L1C file.

| Spectral Bin Center [nm] | Bin Width [# of L1C Pixels] |
|--------------------------|-----------------------------|
| 140 | 12 |
| 152 | 12 |
| 159 | 12 |

Table 4-11 Occultation L1D Spectral Bins

| Altitude Bin Center [km] | Bin Width [# of L1C Pixels] |
|--------------------------|-----------------------------|
| 140 | 10 |
| 180 | 10 |
| 250 | 10 |

Table 4-12 Occultation L1D Altitude Bins

Combined file definition (image size = 1024 x 1024 pixels)

€ Header information (at the top of the set of 4 images)

- Date of image
 - Time of image
 - File name
 - Star name, HD and brightness rank
 - RA and declination
 - Latitude, longitude, SZA
- ∄ Wavelength vs. Tangent altitude over full wavelength range in counts.
- ∄ Counts vs. time for each spectral bin (see Table 4-11).
- ∄ Counts vs. tangent altitude for each spectral bin (see Table 4-11).
- ∄ Counts vs. wavelength for each altitude bin (see Table 4-12).

Individual file definitions (image size = 512 x 512 pixels)

- ∄ Wavelength vs. Tangent altitude over full wavelength range in counts.
- Name:
- ∄ Counts vs. time for each spectral bin (see Table 4-11).
- ∄ Counts vs. tangent altitude for each spectral bin (see Table 4-11).
- ∄ Counts vs. wavelength for each altitude bin (see Table 4-12).

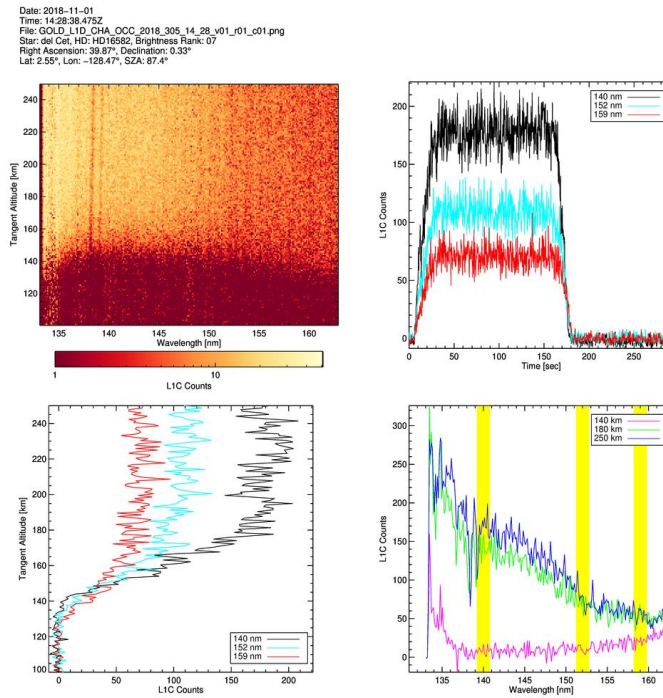


Figure 4-20 Example Level 1D Combined Occultation File

5 Level 2 Data Products

There are six GOLD Level 2 (L2) data products. The physical descriptions, L2 data product names, and mapping back to the four primary GOLD measurement modes and L1C data products are shown in Table 5-1:

| Measurement mode/L1C data product | Derived L2 data products |
|--|---|
| Dayside disk measurements (L1C DAY) | Disk neutral temperature - TDISK |
| | O/N ₂ column density ratio - ON2 |
| | Solar EUV flux proxy - QEUV |
| Limb measurements (L1C LIM) | Limb exospheric temperature - TLIMB |
| Stellar occultation measurements (L1C OCC) | O ₂ density profile - O2DEN |
| Nightside disk measurements (L1C NI1) | Peak electron density - NMAX |

Table 5-1 Level 2 data products and L1C dependence

In routine daily processing, the Level 2 algorithms operate on each individual L1C file as soon as they are created by the GOLD data processing pipeline. Each application of the algorithms produces an individual L2 file for each event. Thus, for example, there are individual TDISK, ON2 and QEUV files created for each dayside disk scan during the day, individual O2DEN files for each occultation, and so forth. At the end of the day (after midnight satellite local time) all individual files of the same type are combined into a single file containing all data of that type for the day. These daily summary files are the publicly released L2 data products.

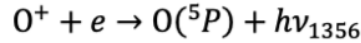
5.1 NMAX Data Product

The GOLD night disk scan (NI1) measurements are used to derive the peak electron density (NMAX, electrons/cm³) on the disk. GOLD performs NI1 scans in both hemispheres from 17:00 to 21:00 hours spacecraft local time each night. NMAX is retrieved on a 2D rectangular (latitude vs. longitude) grid of fixed dimensions for each scan. However, the actual latitude and longitude values in the grid vary from scan to scan as the NI1 sequence of images progresses from east to west across the disk throughout the evening (see Section 4.8.1).

5.1.1 Algorithm Description

There are two primary sources of the O I 135.6 nm nightglow emission: radiative recombination and ion-ion mutual neutralization. In addition, there is a small enhancement in the radiance due to multiple scattering from lower altitudes. The complexity of the algorithm depends on the extent to which each of these components are accounted for.

The primary source is radiative recombination, which is due to the recombination of O^+ ions with electrons to produce O atoms in an excited state that decays via various channels, including the emission of a photon at 135.6 nm:



A secondary source is ion-ion mutual neutralization, which involves the interaction of an O^+ ion with an O^- ion that results in two O atoms, one or both of which may be in an excited state, which can result in the emission of a photon at 135.6 nm. The O^- ion comes from the attachment of an electron to a neutral O atom, and it can also interact with a neutral O atom to produce an O_2 molecule and an electron. This competes with ion-ion neutralization, resulting in a very low ambient density of O^- , but the throughput of production and loss is sufficient to produce an observable amount of 135.6 radiation.

Finally, although both of these sources of 135.6 nm radiation occur at high altitudes where the atmosphere is optically thin at 135.6 nm, the downward directed photons encounter increasing densities of O so they can be resonantly scattered back in the upward direction. Preliminary AURIC runs indicate that, depending on geometry, this multiple scattering can result in an enhancement of the radiance by 10% or more.

The algorithm used for Version 2 of the NMAX data product is the simplest possible implementation, and makes the following assumptions:

1. Ignore ion-ion mutual neutralization
2. Neglect multiple scattering
3. Assume the electron and O^+ densities are identical, $N_e = N_{O^+}$
4. Assume a Chapman layer profile for the electron density profile, $N_e(z)$.

Given these assumptions one can derive the following formula relating the peak of the electron density profile, N_{max} , directly to the measured 135.6 nm intensity, I_{1356} :

$$N_{max} = \sqrt{\frac{4\pi I_{1356}}{\alpha_{1356} e H}}$$

Here α_{1356} is the radiative recombination rate, H is the Chapman function scale height and e is the base of natural logarithms. The bandpass used to derive I_{1356} is taken to be 133-137 nm. The value of $\alpha_{1356} = 7.3 \times 10^{-13} \text{ cm}^3 \text{ s}^{-1}$ is taken from Melendez-Alvira et al. [1999]. The scale height

is essentially a free parameter in this formula, as it is unknown *a priori*. We have assumed a value of 100 km in the Version 1 algorithm.

References

Melendez-Alvira et al. (1999), Analysis of the oxygen nightglow measured by the Hopkins Ultraviolet Telescope: Implications for ionospheric partial radiative recombination rate coefficients, *J. Geophys. Res.*, 104, 14,901-14,913.

5.1.2 Data File Structures

5.1.2.1 NMAX File Contents

| Variable Name | Units | Type/Dim | Description |
|--|-----------|------------------------------|--|
| Parameters defined per day/file | | | |
| NSCANS | | Long/1 | Number of scans in file. |
| NLATS | | Long/1 | Latitude grid dimension. |
| NLONS | | Long/1 | Longitude grid dimension. |
| NMASK | | Long/1 | Spectral mask dimension. |
| Parameters defined per scan | | | |
| DQI | | Long/[NSCANS] | NMAX data quality index (see table below). |
| HEMISPHERE | | String/[NSCANS] | Hemisphere scanned ('N' or 'S'). |
| INPUT_LIC_FILE | | String/[NSCANS] | LIC file for each scan. |
| CHANNEL | | String/[NSCANS] | GOLD channel ('A' or 'B'). |
| SCAN_START_TIME | | String/[NSCANS] | UTC start time of scan, e.g., "2017-06-21T23:46:38.015Z". |
| SCAN_STOP_TIME | | String/[NSCANS] | UTC end time of scan, e.g., "2017-06-21T23:46:38.015Z". |
| TIME.UTC | | String/[NLONS, NSCANS] | UTC time for each slit position, e.g., "2017-06-21T23:46:38.015Z". |
| LATITUDE | Degrees | Float/[NLONS, NLATS, NSCANS] | Pixel latitude. |
| LONGITUDE | Degrees | Float/[NLONS, NLATS, NSCANS] | Pixel longitude. |
| SOLAR_ZENITH_ANGLE | Degrees | Float/[NLONS, NLATS, NSCANS] | Pixel solar zenith angle. |
| EMISSION_ANGLE | Degrees | Float/[NLONS, NLATS, NSCANS] | Pixel emission angle (relative to zenith). |
| COUNTS_OI_1356 | Counts | Float/[NLONS, NLATS, NSCANS] | Counts in Oxygen 135.6-nm bandpass. |
| RADIANCE_OI_1356 | Rayleighs | Float/[NLONS, NLATS, NSCANS] | Radiance in Oxygen 135.6-nm bandpass. |
| OI_1356_UNC_RAN | Rayleighs | Float/[NLONS, NLATS, NSCANS] | Random uncertainty in 135.6-nm radiance. |
| OI_1356_UNC_SYS | Rayleighs | Float/[NLONS, NLATS, NSCANS] | Systematic uncertainty in 135.6-nm radiance. |

| | | | |
|-----------------|---------------------------|------------------------------|--|
| OI_1356_UNC_MOD | Rayleighs | Float/[NLONS, NLATS, NSCANS] | Model uncertainty in 135.6-nm radiance. |
| NMAX | electrons/cm ³ | Float/[NLONS, NLATS, NSCANS] | Retrieved peak electron density. |
| NMAX_DQI | | Long/[NLONS, NLATS, NSCANS] | NMAX data quality index per pixel (see table below). |
| NMAX_UNC_RAN | electrons/cm ³ | Float/[NLONS, NLATS, NSCANS] | Random uncertainty in retrieved peak electron density. |
| NMAX_UNC_SYS | electrons/cm ³ | Float/[NLONS, NLATS, NSCANS] | Systematic uncertainty in retrieved peak electron density. |
| NMAX_UNC_MOD | electrons/cm ³ | Float/[NLONS, NLATS, NSCANS] | Model uncertainty in retrieved peak electron density. |
| MASK_OI_1356 | | Long/[NMASK] | Wavelength mask defining the 135.6-nm emission passband. |
| MASK_WAVELENGTH | | Float/[NMASK] | Wavelength grid for 1356 mask. |

Table 5-2 NMAX File Content

5.1.2.2 NMAX Data Quality Index

| Value | Description |
|--------------------|---|
| File Level | |
| 0 | No known data quality issues. |
| 1 | Solar zenith angle out of bounds. |
| 2 | Invalid O I 135.6 nm counts. |
| 4 | Invalid O I 135.6 nm radiance. |
| 8 | Invalid O I 135.6 nm radiance random uncertainties. |
| 16 | Invalid O I 135.6 nm radiance systematic uncertainties. |
| 32 | Invalid emission angle. |
| 64 | Algorithm failure. |
| 128 | Invalid wavelength. |
| 256 | No valid input. |
| 512 | High background. |
| 1024 | No valid output. |
| Pixel Level | |
| 0 | No known data quality issues. |
| 1 | Solar zenith angle out of bounds. |
| 2 | Invalid O I 135.6 nm counts. |
| 4 | Invalid O I 135.6 nm radiance. |
| 8 | Invalid O I 135.6 nm radiance random uncertainties. |
| 16 | Invalid O I 135.6 nm radiance systematic uncertainties. |
| 32 | Invalid emission angle. |
| 64 | Algorithm failure. |
| 128 | High background. |

Table 5-3 NMAX Data Quality Index

5.2 O2DEN Data Product

The GOLD stellar occultation (OCC) measurements are used to derive the molecular oxygen (O₂) absolute density profile (mol/cm³) on the limb. Of the six GOLD Level 2 data products this is the only one that provides altitude-resolved geophysical information. GOLD performs approximately 10 occultation measurements per day in nominal operation, sampling from a set of thirty bright type O and B target stars. Stars are observed to rise (set) on the East (West) limbs relative to the satellite's fixed position in geosynchronous orbit. Occultations occur at latitudes from 60° S to 45° N and at all local times during the day.

5.2.1 Algorithm Description

Algorithm heritage

The O2DEN algorithm is based on the Polar Ozone and Aerosol Measurement (POAM) solar occultation algorithms (Lumpe et al., [2002]). These algorithms were used to generate operational retrievals of aerosol and trace gas densities in the polar stratosphere from the POAM II and III instruments between 1993 and 2005. The algorithm was subsequently modified and used to retrieve thermospheric O₂ density profiles from both SUSIM/UARS solar occultation measurements (Lumpe et al., [2007]) and SOLSTICE/SORCE stellar occultation measurements (Lumpe et al., [2006]).

Algorithm theoretical basis

O₂ is derived from measurements of stellar occultation in the Shumann Runge continuum. As the star rises or sets relative to the satellite position the stellar spectrum is measured across the GOLD spectral bandpass, from ~134 to ~162 nm. Geolocation of the OCC L1B data provides the line-of-sight tangent altitude vs. time during the occultation. This results in a 2-dimensional map of the stellar signal, in counts or calibrated geophysical units (irradiance), vs. wavelength and tangent altitude. A sample of this image is represented in the top left panel of the OCC L1D image in Figure 4-20 .

The measured counts profile is then normalized by the unattenuated, exo-atmospheric spectrum, yielding the slant path transmission profile vs. wavelength at the native L1C spectral sampling of 0.12 nm. The defining characteristic of the atmospheric transmission is that it is completely independent of instrument calibration or absolute accuracy. The full transmission spectrum is binned into a small number of 2-nm spectral channels for use in the retrievals. These retrieval channels are chosen to span the spectral dependence of the O₂ absorption cross-section in order to maximize the O₂ retrieval altitude range (approximately 120-240 km). In the current O2DEN data set two spectral channels are used, centered at 142- and 159-nm.

Since stars rise or set at approximately 3 km/sec, as observed from orbit, the 100-msec occultation cadence results in a measurement of extremely high (sub-km) vertical resolution. The

data are binned to enhance signal-to-noise, producing an effective vertical resolution of 10 km or less, which is sufficient to easily resolve the scale height of the O₂ profile.

The algorithm uses an optimal estimation routine, which provide a complete error analysis and retrieval diagnostics such as averaging kernels and information content. A data vector constructed from the multiple spectral channels of slant path transmission is used to derive the atmospheric state vector – O₂ density vs. geometric altitude – via a nonlinear, iterative inversion. The retrieved O₂ density profile is reported on a fixed altitude grid with 5-km spacing. The valid altitude range varies for each event, but generally ranges from ~120 – 240 km. A complete description of the GOLD O2DEN algorithm and data product can be found in Lumpe et al., [2020].

References

Lumpe, J. D., R. M. Bevilacqua, K. W. Hoppel, & C. E. Randall (2002), POAM III retrieval algorithm and error analysis, *J. Geophys. Res.*, 107(D21), 4575, 10.1029/2002JD002137.

Lumpe, J. D., L. Floyd, M. Snow, and T. Woods (2006), Thermospheric Remote Sensing by Occultation: Comparison of SUSIM and SOLSTICE O₂ Measurements, Presented at the Fall 2006 AGU meeting, San Francisco, CA.

Lumpe, J. D., L. E. Floyd, L. C. Herring, S. T. Gibson, and B. R. Lewis (2007), Measurements of thermospheric molecular oxygen from the Solar Ultraviolet Spectral Irradiance Monitor, *J. Geophys. Res.*, 112, D16308, doi:10.1029/2006JD008076.

Lumpe, J. D., McClintock, W. E., Evans, J. S., Correira, J., Veibell, V., Beland, S., & Eastes, R. (2020), A new data set of thermospheric molecular oxygen from the Global- scale Observations of the Limb and Disk (GOLD) mission, *J. Geophys. Res., Space Physics*, 125, e2020JA027812. doi:10.1029/2020JA027812.

5.2.2 Data File Structures

5.2.2.1 O2DEN File Contents

| Variable Name | Units | Type/Dim | Description |
|--|-------|----------|--|
| Parameters defined per day/file | | | |
| DQI | | Long/1 | File level Data Quality Index. |
| NEVENTS | | Long/1 | Number of occultations in file. |
| N_WAVELENGTH | | Long/1 | Number of spectral channels used in retrieval. |
| NZRET | | Long/1 | Number of levels in retrieval altitude grid. |

| | | | |
|---|---------------------|--------------------------------------|---|
| NZDAT | | Long/1 | Number of levels in data tangent altitude grid. |
| Parameters defined per occultation event | | | |
| DQI | | Long/[NEVENTS] | O ₂ data quality index (see table below). |
| TARGET_STAR | | String/[NEVENTS] | Name of target star. |
| INPUT_L1C_FILE | | String/[NEVENTS] | L1C file name for each occultation. |
| CHANNEL | | String/[NEVENTS] | GOLD channel (“A” or “B”) |
| TIME_UTC | | String/[NEVENTS] | UTC date/time string, e.g. "2017-06-21T23:46:38.015Z" |
| LAT_REF | Degrees | Float/[NEVENTS] | Latitude at 225 km tangent point. |
| LON_REF | Degrees | Float/[NEVENTS] | Longitude at 225 km tangent point. |
| SZA_REF | Degrees | Float/[NEVENTS] | Solar zenith angle at 225 km tangent point. |
| CONVERGENCE | | Long/[NEVENTS] | Retrieval convergence flag (= 1 if retrieval converged). |
| N_ITER | | Long/[NEVENTS] | Number of iterations to converge. |
| SPECTRAL_WIDTH | nm | Float/[NEVENTS] | Width of each data spectral channel. |
| ZRET | km | Float/[NZRET] | Retrieval geometric altitude grid. |
| O2_APRIORI | mol/cm ³ | Float/[NZRET, NEVENTS] | A priori O ₂ density used in retrieval. |
| O2DEN | mol/cm ³ | Float/[NZRET, NEVENTS] | Retrieved O ₂ density. |
| O2DEN_DQI | | Long/[NZRET, NEVENTS] | O ₂ data quality indicator per altitude (see table below). |
| O2DEN_UNC_RAN | mol/cm ³ | Float/[NZRET, NEVENTS] | Random uncertainty of retrieved O ₂ . |
| O2DEN_UNC_SYS | mol/cm ³ | Float/[NZRET, NEVENTS] | Systematic uncertainty of retrieved O ₂ . |
| O2DEN_UNC_MOD | mol/cm ³ | Float/[NZRET, NEVENTS] | Model uncertainty of retrieved O ₂ . |
| TEMPERATURE | K | Float/[NZRET, NEVENTS] | Assumed temperature profile. |
| CENTRAL_WAVELENGTH | nm | Float/[N_WAVELENGTH, NEVENTS] | Center wavelength of each data channel. |
| NORMALIZATION | Counts | Float/[N_WAVELENGTH, NEVENTS] | Transmission normalization factor (unattenuated stellar irradiance). |
| SIGNAL_TO_NOISE | | Float/[N_WAVELENGTH, NEVENTS] | Effective signal to noise (above atmosphere). |
| ZDAT | km | Float/[NZDAT] | Data tangent altitude grid. |
| TRANSMISSION | | Float/[NZDAT, N_WAVELENGTH, NEVENTS] | Measured slant path transmission profile. |
| TRANSMISSION_UNC | | Float/[NZDAT, N_WAVELENGTH, NEVENTS] | Transmission variance. |
| TRANSMISSION_FIT | | Float/[NZDAT, N_WAVELENGTH, NEVENTS] | Forward model fit to data. |

Table 5-4 O2DEN File Contents

5.2.2.2 O2DEN Data Quality Index Definitions

| Value | Description |
|--------------------|---|
| File Level | |
| 0 | No known data quality issues. |
| 2 | Dayside occultation. |
| 4 | Invalid NORMALIZATION value (max altitude not high enough). |
| 8 | Retrieval non-convergence. |
| 16 | Wavelengths out of bounds. |
| 32 | Invalid tangent altitude grid in input transmission data. |
| 64 | Counts array out of bounds |
| 128 | Counts random errors out of bounds. |
| 256 | Counts systematic errors out of bounds. |
| 512 | Transmission array out of bounds. |
| 1024 | O2DEN non-finite or out of bounds. |
| 2048 | O2DEN random error non-finite or out of bounds. |
| 8192 | Algorithm failure. |
| Pixel Level | |
| 0 | No known data quality issues. |
| 1 | O2DEN non-finite or out of bounds. |
| 2 | O2DEN random error non-finite or out of bounds. |

Table 5-5 O2DEN Data Quality Index

5.3 ON2 Data Product

GOLD daytime disk scan (DAY) measurements are used to derive the ratio of the column abundance of thermospheric O relative to N₂, conventionally referred to as O/N₂ or $\Sigma\text{O}/\text{N}_2$, but abbreviated to ON2 for the GOLD data product. ON2 is derived for each valid dayside Level 1C pixel for approximately 68 disk scan measurements performed per day by GOLD in nominal operation. Beginning with Version 3 of the ON2 data product, the L1C DAY pixels are first binned 2x2 spatially before application of the ON2 algorithm. The resulting ON2 data product therefore has a spatial (horizontal) resolution of 250 km x 250 km at spacecraft nadir

5.3.1 Algorithm Description

Algorithm heritage

The disk ON2 retrieval algorithm was originally developed by Computational Physics, Inc. (CPI) for use with GUVI and SSUSI radiance images (Strickland et al., 1995). The GOLD implementation of this algorithm takes advantage of GOLD's ability to transmit the full spectrum to maximize the signal-to-noise ratio and eliminate atomic emission lines that contaminate the N₂ LBH bands (e.g., N I 149.3 nm). This algorithm has been extensively documented and applied

over the past several decades (e.g., Evans et al. [1995]; Christensen et al. [2003]; Strickland et al. [2004]).

Algorithm theoretical basis

The geophysical parameter retrieved, O/N_2 , is the ratio of the vertical column density of O relative to N_2 , defined at a standard reference N_2 depth of 10^{17} cm^{-2} , which is chosen to minimize uncertainty in the derived O/N_2 . It is retrieved directly from the ratio of the O I 135.6 nm and N_2 LBH band intensities measured by GOLD on the dayside disk (DAY measurement mode). The AURIC atmospheric radiance model (Strickland et al. [1999]) is used to derive this relationship as a function of solar zenith angle and to create the look-up table (LUT) used by the algorithm. . A complete description of the GOLD ON2 algorithm and data product can be found in Correia et al., [2021].

References

Christensen, A. B., et al. (2003), Initial observations with the Global Ultraviolet Imager (GUVI) in the NASA TIMED satellite mission, *J. Geophys. Res.*, vol. 108, NO. A12, 1451, doi:10.1029/2003JA009918.

Evans, J. S., D. J. Strickland and R. E. Huffman (1995), Satellite remote sensing of thermospheric O/N_2 and solar EUV: 2. Data analysis, *J. Geophys. Res.*, vol. 100, NO. A7, pages 12,227-12,233.

Strickland, D. J., R. R. Meier, R. L. Walterscheid, J. D. Craven, A. B. Christensen, L. J. Paxton, D. Morrison, and G. Crowley (2004), Quiet-time seasonal behavior of the thermosphere seen in the far ultraviolet dayglow, *J. Geophys. Res.*, vol. 109, A01302, doi:10.1029/2003JA010220.

Strickland, D.J., J. Bishop, J.S. Evans, T. Majeed, P.M. Shen, R.J. Cox, R. Link, and R.E. Huffman (1999), Atmospheric Ultraviolet Radiance Integrated Code (AURIC): theory, software architecture, inputs and selected results, *JQSRT*, 62, 689-742.

Strickland, D. J., J. S. Evans, and L. J. Paxton (1995), Satellite remote sensing of thermospheric O/N_2 and solar EUV: 1. Theory, *J. Geophys. Res.*, 110, A7, pages 12,217-12,226.

Correia, J., J. S. Evans, A. Krywonos, J. D. Lumpe, V. Veibell, W. E. McClintock, and R. W. Eastes (2021), Thermospheric Composition and Solar EUV Flux from the Global-scale Observations of the Limb and Disk (GOLD) mission, to be submitted to *J. Geophys. Res.*.

5.3.2 Data File Structures

5.3.2.1 ON2 File Contents

| Variable Name | Units | Type/Dim | Description |
|--|-----------|-------------------------------|--|
| Parameters defined per day/file | | | |
| NSCANS | | Long/1 | Number of scans in file. |
| NLATS | | Long/1 | Latitude grid dimension. |
| NLONS | | Long/1 | Longitude grid dimension. |
| NMASK | | Long/1 | Spectral mask dimension. |
| Parameters defined per scan | | | |
| DQI | | Long/[NSCANS] | Overall data quality index per scan (see table below). |
| HEMISPHERE | | String/[NSCANS] | Hemisphere scanned ('N' or 'S'). |
| CHANNEL | | String/[NSCANS] | GOLD channel ('A' or 'B'). |
| INPUT_L1C_FILE | | String/[NSCANS] | L1C file for each scan. |
| SCAN_START_TIME | | String/[NSCANS] | UTC start time of scan, e.g., "2017-06-21T23:46:38.015Z". |
| SCAN_STOP_TIME | | String/[NSCANS] | UTC end time of scan, e.g., "2017-06-21T23:46:38.015Z". |
| LOOKUP_TABLE | | String/[NSCANS] | Lookup table filename. |
| LATITUDE | Degrees | Float/[NLONS, NLATS] | Pixel latitude. |
| LONGITUDE | Degrees | Float/[NLONS, NLATS] | Pixel longitude. |
| TIME.UTC | | String/[NLONS, NLATS, NSCANS] | UTC time for each pixel, e.g., "2017-06-21T23:46:38.015Z". |
| SOLAR_ZENITH_ANGLE | Degrees | Float/[NLONS, NLATS, NSCANS] | Pixel solar zenith angle. |
| EMISSION_ANGLE | Degrees | Float/[NLONS, NLATS, NSCANS] | Pixel emission angle (relative to zenith). |
| RADIANCE_OI_1356 | Rayleighs | Float/[NLONS, NLATS, NSCANS] | Oxygen 135.6 nm radiance used in retrieval. |
| OI_1356_UNC_RAN | Rayleighs | Float/[NLONS, NLATS, NSCANS] | Random uncertainty in oxygen 135.6 nm radiance. |
| OI_1356_UNC_SYS | Rayleighs | Float/[NLONS, NLATS, NSCANS] | Systematic uncertainty in oxygen 135.6 nm radiance. |
| RADIANCE_N2_LBH | Rayleighs | Float/[NLONS, NLATS, NSCANS] | N ₂ LBH radiance used in retrieval. |
| N2_LBH_UNC_RAN | Rayleighs | Float/[NLONS, NLATS, NSCANS] | Random uncertainty in N ₂ LBH radiance. |
| N2_LBH_UNC_SYS | Rayleighs | Float/[NLONS, NLATS, NSCANS] | Systematic uncertainty in N ₂ LBH radiance. |
| ON2 | | Float/[NLONS, NLATS, NSCANS] | Retrieved O/N ₂ column density ratio, per pixel. |
| ON2_DQI | | Long/[NLONS, NLATS, NSCANS] | ON2 data quality index per pixel (see table below). |
| ON2_UNC_RAN | | Float/[NLONS, NLATS, NSCANS] | Random uncertainty in retrieved O/N ₂ column density ratio. |
| ON2_UNC_SYS | | Float/[NLONS, NLATS, NSCANS] | Systematic uncertainty in retrieved O/N ₂ column density ratio. |

| | | | |
|-----------------|----|------------------------------|---|
| ON2_UNC_MOD | | Float/[NLONS, NLATS, NSCANS] | Model uncertainty in retrieved O/N ₂ column density ratio. |
| MASK_WAVELENGTH | nm | Float/[NMASK] | Wavelength grid for MASK_N2_LBH and MASK_OI_1356. |
| MASK_N2_LBH | | Long/[NMASK] | Wavelength mask defining LBH bandpass used in retrieval. |
| MASK_OI_1356 | | Long/[NMASK] | Wavelength mask defining OI 1356 bandpass used in retrieval. |

Table 5-6 ON2 File Content

5.3.2.2 ON2 Data Quality Index

| Value | Description |
|--------------------|--|
| File Level | |
| 0 | No known data quality issues. |
| 1 | Invalid wavelength mask. |
| 2 | No valid input. |
| 4 | No valid output. |
| 8 | Invalid lookup table. |
| Pixel Level | |
| 0 | No known data quality issues. |
| 1 | Invalid solar zenith angle. |
| 2 | Invalid intensity ratio 135.6 nm/N ₂ LBH. |
| 4 | Invalid 135.6 nm radiance random uncertainty. |
| 8 | Invalid N ₂ LBH radiance random uncertainty. |
| 16 | Invalid 135.6 nm radiance systematic random uncertainty. |
| 32 | Invalid N ₂ LBH radiance systematic random uncertainty. |
| 64 | Algorithm failure. |

Table 5-7 ON2 Data Quality Index

5.4 QEUV Data Product

Q_{EUUV} is a proxy for the integrated solar EUV irradiance below 45 nm, which can be derived directly from far ultraviolet (FUV) radiance measurements. Q_{EUUV} is a dayside disk data product, derived from the GOLD DAY measurement mode.

5.4.1 Algorithm Description

Algorithm heritage

The disk Q_{EUUV} retrieval algorithm was originally developed for use with GUVI and SSUSI images (Strickland et al., [1995]). The GOLD implementation of this algorithm takes advantage

of GOLD's ability to transmit the full spectrum to maximize the signal-to-noise ratio and eliminate atomic emission lines that contaminate the N₂ LBH bands (e.g., N I 149.3 nm). This algorithm has been extensively documented and applied (e.g., Strickland et al. [2004]; Evans et al., [1995]). The associated GOLD Level 2 data product is called QEUV.

Algorithm theoretical basis

Like ON2, the QEUV data product is also produced via a look-up-table (LUT) approach, and depends on the observed O I 135.6 nm radiance, the solar zenith angle, and the derived O/N₂ ratio. The AURIC airglow model is used to derive this relationship as a function of solar zenith angle in order to create the LUT used by the algorithm.

In order to avoid contamination of O I 135.6 nm by sources other than photoelectron impact, QEUV is only calculated for a row of pixels from DAY disk scans corresponding to mid-latitudes. This avoids both low latitude contamination from O⁺ recombination in the EIA and energetic particle precipitation in the auroral region at polar latitudes. Due to the asymmetry of the magnetic equator and EIA, the latitude used for the northern and southern hemispheres differs: 30° N latitude and -37.5° S latitude, respectively. O I 135.6 nm and N₂ LBH intensities are calculated from LIC spectra at these latitudes and used as inputs for the QEUV algorithm. Temporal sampling is approximately 5 seconds. A complete description of the GOLD QEUV algorithm and data product can be found in Correira et al., [2021]

References

Evans, J. S., D. J. Strickland and R. E. Huffman (1995), Satellite remote sensing of thermospheric O/N₂ and solar EUV: 2. Data analysis, *J. Geophys. Res.*, Vol. 100, NO. A7, pages 12,227-12,233.

Strickland, D. J., J. S. Evans, and L. J. Paxton (1995), Satellite remote sensing of thermospheric O/N₂ and solar EUV: 1. Theory, *J. Geophys. Res.*, 110, A7, pages 12,217-12,226.

Strickland, D. J., J. L. Lean, R. R. Meier, A. B. Christensen, L. J. Paxton, D. Morrison, J. D. Craven, R. L. Walterscheid, D. L. Judge, and D. R. McMullin, (2004), Solar EUV irradiance variability derived from terrestrial far ultraviolet dayglow observations, Vol. 31, L03801, doi:10.1029/2003GL018415.

Correira, J., J. S. Evans, A. Krywonos, J. D. Lumpe, V. Veibell, W. E. McClintock, and R. W. Eastes (2021), Thermospheric Composition and Solar EUV Flux from the Global-scale Observations of the Limb and Disk (GOLD) mission, to be submitted to *J. Geophys. Res.*.

5.4.2 Data File Structures

5.4.2.1 QEUV File Contents

| Variable Name | Units | Type/Dim | Description |
|--|------------------------|-------------------------|---|
| Parameters defined per day/file | | | |
| NSCANS | | Long/1 | Number of scans in file. |
| NTIMES | | Long/1 | Time grid dimension. |
| NMASK | | Long/1 | Spectral mask dimension. |
| Parameters defined per scan | | | |
| DQI | | Long/[NSCANS] | Overall data quality index per scan (see table below). |
| CHANNEL | | String/[NSCANS] | GOLD channel ('A' or 'B'). |
| HEMISPHERE | | String/[NSCANS] | Hemisphere scanned ('N' or 'S'). |
| INPUT_LIC_FILE | | String/[NSCANS] | LIC file for each scan. |
| SCAN_START_TIME | | String/[NSCANS] | UTC start time of scan, e.g., "2017-06-21T23:46:38.015Z". |
| SCAN_STOP_TIME | | String/[NSCANS] | UTC end time of scan, e.g., "2017-06-21T23:46:38.015Z". |
| QEUV_LOOKUP_TABLE | | String/[NSCANS] | QEUV lookup table filename. |
| ON2_LOOKUP_TABLE | | String/[NSCANS] | ON2 lookup table filename. |
| TIME.UTC | | String/[NTIMES, NSCANS] | UTC time for each QEUV value e.g., "2017-06-21T23:46:38.015Z". |
| SOLAR_ZENITH_ANGLE | Degrees | Float/[NTIMES, NSCANS] | Solar zenith angle. |
| EMISSION_ANGLE | Degrees | Float/[NTIMES, NSCANS] | Emission angle (relative to zenith). |
| RADIANCE_OI_1356 | Rayleighs | Float/[NTIMES, NSCANS] | Oxygen 135.6 nm radiance used in retrieval. |
| OI_1356_UNC_RAN | Rayleighs | Float/[NTIMES, NSCANS] | Random uncertainty in oxygen 135.6 nm radiance. |
| OI_1356_UNC_SYS | Rayleighs | Float/[NTIMES, NSCANS] | Systematic uncertainty in oxygen 135.6 nm radiance. |
| RADIANCE_N2_LBH | Rayleighs | Float/[NTIMES, NSCANS] | N ₂ LBH radiance used in retrieval. |
| N2_LBH_UNC_RAN | Rayleighs | Float/[NTIMES, NSCANS] | Random uncertainty in N ₂ LBH radiance. |
| N2_LBH_UNC_SYS | Rayleighs | Float/[NTIMES, NSCANS] | Systematic uncertainty in N ₂ LBH radiance. |
| ON2 | | Float/[NTIMES, NSCANS] | Retrieved O/N ₂ column density ratio used in QEUV retrieval. |
| ON2_DQI | | Long/[NTIMES, NSCANS] | ON2 data quality index. |
| ON2_UNC_RAN | | Float/[NTIMES, NSCANS] | Random uncertainty in ON2. |
| ON2_UNC_SYS | | Float/[NTIMES, NSCANS] | Systematic uncertainty in ON2. |
| ON2_UNC_MOD | | Float/[NTIMES, NSCANS] | Model uncertainty in ON2. |
| QEUV | erg/cm ² /s | Float/[NTIMES, NSCANS] | Retrieved QEUV value. |
| QEUV_DQI | | Long/[NTIMES, NSCANS] | QEUV data quality index per pixel (see table below). |
| QEUV_UNC_RAN | erg/cm ² /s | Float/[NTIMES, NSCANS] | Random uncertainty in retrieved QEUV. |
| QEUV_UNC_SYS | erg/cm ² /s | Float/[NTIMES, NSCANS] | Systematic uncertainty in retrieved QEUV. |

| | | | |
|-----------------|------------------------|------------------------|--|
| QEUV_UNC_MOD | erg/cm ² /s | Float/[NTIMES, NSCANS] | Model uncertainty in retrieved QEUV. |
| MASK_WAVELENGTH | nm | Float/[NMASK] | Wavelength grid for MASK_N2_LBH and MASK_OI_1356. |
| MASK_N2_LBH | | Long/[NMASK] | Wavelength mask defining LBH bandpass used in retrieval. |
| MASK_OI_1356 | | Long/[NMASK] | Wavelength mask defining OI 1356 bandpass used in retrieval. |

Table 5-8 QEUV File Content

5.4.2.2 QEUV Data Quality Index

| Value | Description |
|---------------------------|--|
| File Level | |
| 0 | No known data quality issues. |
| 1 | Invalid wavelength mask. |
| 2 | No valid input. |
| 4 | No valid output. |
| 8 | Insufficient latitude coverage. |
| 16 | Invalid lookup table. |
| Pixel Level - ON2 | |
| 0 | No known data quality issues. |
| 1 | Invalid solar zenith angle. |
| 2 | Invalid intensity ratio 135.6 nm/N2 LBH. |
| 4 | Invalid 135.6 nm radiance random uncertainty. |
| 8 | Invalid N2 LBH radiance random uncertainty. |
| 16 | Invalid 135.6 nm radiance systematic random uncertainty. |
| 32 | Invalid N2 LBH radiance systematic random uncertainty. |
| 64 | Algorithm failure. |
| Pixel Level - QEUV | |
| 0 | No known data quality issues. |
| 1 | Invalid solar zenith angle. |
| 2 | Invalid 135.6 nm radiance. |
| 4 | Invalid 135.6 nm radiance random uncertainty. |
| 8 | Invalid 135.6 nm radiance sytematic uncertainty. |
| 16 | Invalid ON2. |
| 32 | Invalid ON2 random uncertainty. |
| 64 | Invalid ON2 systematic uncertainty. |
| 128 | Invalid ON2 model uncertainty. |
| 256 | Algorithm failure. |

Table 5-9 QEUV Data Quality Index

5.5 TDISK Data Product

The GOLD daytime disk scan measurements are used to derive the TDISK data product, which is the effective disk neutral temperature at a height of approximately 150 km. TDISK is derived for each valid dayside Level 1C pixel for approximately 68 disk scan measurements performed per day by GOLD in nominal operation. Beginning with Version 3 of the TDISK data product, the L1C DAY pixels are first binned 2x2 spatially before application of the TDISK algorithm. The resulting TDISK data product therefore has a spatial (horizontal) resolution of 250 km x 250 km at spacecraft nadir.

5.5.1 Algorithm Description

Algorithm heritage

The retrieval algorithm is an extension of those previously used to derive temperature from limb measurements of LBH intensity from the HITS instrument (Aksnes et al., [2006]; Krywonos et al. [2012]).

Algorithm theoretical basis

GOLD measurements have a higher signal-to-noise ratio than HITS and a spectral range that includes more of the total N₂ LBH emission (134–162 nm). Effective neutral temperatures near ~150 km altitude are retrieved by fitting the observed rotational structure of the N₂ LBH bands using an optimal estimation routine. Retrieved parameters also include the upper vibrational level ($v'=0-6$) relative intensities (i.e. populations), a constant background, wavelength shift, and wavelength dispersion (constant term). A complete description of the GOLD ON2 algorithm and data product can be found in Evans et al., [2021]

References

Aksnes, A., R. Eastes, S. Budzien, & K. Dymond (2006), Neutral temperatures in the lower thermosphere from N₂ Lyman-Birge-Hopfield (LBH) band profiles, *Geophys. Res. Lett.*, 33, L15103, doi:10.1029/2006GL026255.

Krywonos, A., D. J. Murray, R. W. Eastes, A. Aksnes, S. A. Budzien, and R. E. Daniell (2012), Remote sensing of neutral temperatures in the Earth's thermosphere using the Lyman-Birge-Hopfield bands of N₂: Comparisons with satellite drag data, *J. Geophys. Res.*, 117, A09311, doi:10.1029/2011JA017226.

Evans, J. S., J. D. Lumpe, J. Correia, V. Veibell, A. Krywonos, W. E. McClintock, S. C. Solomon, and R. W. Eastes (2021), Neutral disk temperatures from the GOLD mission, to be submitted to *J. Geophys. Res*

5.5.2 Data File Structures

5.5.2.1 TDISK File Contents

| Variable Name | Units | Type/Dim | Description |
|--|---------|-------------------------------|--|
| Parameters defined per day/file | | | |
| NSCANS | | Long/1 | Number of scans in file. |
| NLATS | | Long/1 | Latitude grid dimension. |
| NLONS | | Long/1 | Longitude grid dimension. |
| NMASK | | Long/1 | Spectral mask dimension. |
| NPOP | | Long/1 | Vibrational population grid dimension. |
| Parameters defined per scan | | | |
| DQI | | Long/[NSCANS] | NMAX data quality index (see table below). |
| HEMISPHERE | | String/[NSCANS] | Hemisphere scanned ('N' or 'S'). |
| INPUT_LIC_FILE | | String/[NSCANS] | LIC file for each scan. |
| CHANNEL | | String/[NSCANS] | GOLD channel ('A' or 'B'). |
| SCAN_START_TIME | | String/[NSCANS] | UTC start time of scan, e.g., "2017-06-21T23:46:38.015Z". |
| SCAN_STOP_TIME | | String/[NSCANS] | UTC end time of scan, e.g., "2017-06-21T23:46:38.015Z". |
| LOOKUP_TABLE | | String/[NSCANS] | Retrieval lookup table filename. |
| LATITUDE | Degrees | Float/[NLONS, NLATS] | Pixel latitude. |
| LONGITUDE | Degrees | Float/[NLONS, NLATS] | Pixel longitude. |
| TIME.UTC | | String/[NLONS, NLATS, NSCANS] | UTC time for each pixel, e.g., "2017-06-21T23:46:38.015Z". |
| SOLAR_ZENITH_ANGLE | Degrees | Float/[NLONS, NLATS, NSCANS] | Pixel solar zenith angle. |
| EMISSION_ANGLE | Degrees | Float/[NLONS, NLATS, NSCANS] | Pixel emission angle (relative to zenith). |
| EFFECTIVE_ALTITUDE | km | Float/[NLONS, NLATS, NSCANS] | Effective altitude of retrieved temperature. |
| TDISK | K | Float/[NLONS, NLATS, NSCANS] | Retrieved neutral temperature. |
| TDISK_DQI | | Long/[NLONS, NLATS, NSCANS] | TDISK data quality index per pixel (see table below). |
| TDISK_UNC_RAN | K | Float/[NLONS, NLATS, NSCANS] | Random uncertainty in retrieved neutral temperature. |
| TDISK_UNC_SYS | K | Float/[NLONS, NLATS, NSCANS] | Systematic uncertainty in retrieved neutral temperature. |
| TDISK_UNC_MOD | K | Float/[NLONS, NLATS, NSCANS] | Model uncertainty in retrieved neutral temperature. |

| | | | |
|-------------------------|--------|------------------------------|--|
| WAVELENGTH_STRETCH | nm | Float/[NLONS, NLATS, NSCANS] | Retrieved wavelength stretch parameter in each pixel. |
| WAVELENGTH_SHIFT | nm | Float/[NLONS, NLATS, NSCANS] | Retrieved wavelength stretch parameter in each pixel. |
| BACKGROUND | counts | Float/[NLONS, NLATS, NSCANS] | Retrieved background per pixel. |
| VIBRATIONAL_POPULATIONS | | Float/[NLONS, NLATS, NSCANS] | Retrieved temperature vibrational populations. |
| MASK_N2_LBH | | Long/[NMASK] | Wavelength mask defining LBH spectrum used in retrieval. |
| MASK_WAVELENGTH | nm | Float/[NMASK] | Wavelength grid for N2_LBH mask. |

Table 5-10 TDISK File Content

5.5.2.2 TDISK Data Quality Index

| Value | Description |
|--------------------|---|
| File Level | |
| 0 | No known data quality issues. |
| 1 | Invalid solar zenith angle. |
| 2 | Invalid N ₂ LBH counts. |
| 4 | Invalid N ₂ LBH counts random uncertainty. |
| 8 | Invalid emission angle. |
| 16 | Invalid wavelength. |
| 32 | No valid input. |
| 64 | No valid output. |
| Pixel Level | |
| 0 | No known data quality issues. |
| 1 | Invalid solar zenith angle. |
| 2 | Invalid N ₂ LBH counts. |
| 4 | Invalid N ₂ LBH counts random uncertainty. |
| 8 | Invalid emission angle. |
| 16 | Algorithm failure. |

Table 5-11 TDISK Data Quality Index

5.6 TLIMB Data Product

GOLD retrieves the exospheric temperature from the integrated N₂ LBH radiance profile obtained from atmospheric limb scans (LIM observation mode). This data product, referred to as TLIMB, is derived from limb scan data by fitting the shape of the LBH radiance profile between 100 and 300 km.

5.6.1 Algorithm Description

Algorithm heritage

An approach similar to the GOLD TLIMB retrieval has been used to analyze data from TIMED/GUVI, Cassini/UVIS and MAVEN/IUVS. The GOLD TLIMB algorithm is most similar to the operational algorithm used to retrieve exospheric temperature on Mars from MAVEN/IUVS CO₂ density retrievals. The GOLD algorithm follows the procedure outlined in Lo et al. [2015] as originally applied to the atmosphere of Mars. The operational code is implemented in IDL and has been generalized to be used with any species in any planetary atmosphere.

Algorithm theoretical basis

Limb profiles of thermospheric airglow emissions depend fundamentally on temperature, particularly the decay rate with altitude above the peak of the emission. This has been exploited in retrieval algorithms for analyzing far-ultraviolet limb emissions from low-Earth orbit (e.g., Picone and Meier [2000]). For GOLD, the low spatial resolution on the limb mandates that, rather than attempting to fit an entire temperature profile, we only infer a single parameter, the exospheric temperature (TLIMB), defined as the temperature of the atmosphere when in diffusion equilibrium.

We use daytime, non-auroral N₂ LBH emission limb radiance profiles where the only excitation mechanism is photoelectron impact on N₂. LBH emission bands in the 137-160 nm range are integrated spectrally, excluding the N I 149.3 nm line. The GOLD limb scan measurements are done in one hemisphere at a time, and the L1C LIMB data covers a latitude range from the equator to ~20 degree.

The specific steps involved in the TLIMB retrieval are as follows:

- Filter data using topside tangent height range (~100-300 km).
- Fit a Chapman function to the emission radiance profile.
- Obtain the N₂ scale height H (Z_0) from the Chapman fit.
- Obtain T_∞ from $H(Z_0) = kT/Mg$, where k is Boltzmann's constant, M is the molecular mass of N₂, and g is the gravitational acceleration.

Note that this fit is independent of the absolute radiance calibration of the airglow intensity, it depends only on the shape of the radiance profile. For this reason, it is necessary to detect stars in the field-of-view, since the emission from stars can produce a profile shape that can be very different from a profile produced solely by thermospheric airglow. A complete description of the GOLD TLIMB algorithm and data product can be found in Evans et al., [2020].

References

Picone and Meier (2000), Similarity transformations for fitting of geophysical properties: Application to altitude profiles of upper atmospheric species, *J. Geophys. Res.*, *105*, 18599, doi:10.1029/1999JA000385].

Lo, D. Y., et al. (2015), Nonmigrating tides in the Martian atmosphere as observed by MAVEN IUVS, *Geophys. Res. Lett.*, 42, 9057–9063, doi:10.1002/2015GL066268.

Snowden, D., R. V. Yelle, J. Cui, J.-E. Wahlund, N. J. T. Edberg, and K. Ågren (2013), The thermal structure of Titan’s upper atmosphere, I: Temperature profiles from Cassini INMS observations, *Icarus*, 226, 52–582.

Evans, J. S., J. Lumpe, J. Correira, V. Viebell, A. Kyrwonos, S. C. Solomon, and R. W. Eastes (2020), Neutral exospheric temperatures from the GOLD mission, *J. Geophys. Res. Space Physics*, doi:10.1029/2020JA027814.

5.6.2 Data File Structures

5.6.2.1 TLIMB File Contents

| Variable Name | Units | Type/Dim | Description |
|--|-----------|-------------------------------|---|
| Parameters defined per day/file | | | |
| NSCANS | | Long/1 | Number of scans in file. |
| NLATS | | Long/1 | Latitude grid dimension. |
| NLONS | | Long/1 | Longitude grid dimension. |
| NMASK | | Long/1 | Spectral mask dimension. |
| Parameters defined per scan | | | |
| DQI | | Long/[NSCANS] | TLIMB data quality index (see table below). |
| HEMISPHERE | | String/[NSCANS] | Hemisphere scanned ('N' or 'S'). |
| INPUT_LIC_FILE | | String/[NSCANS] | LIC file for each scan. |
| CHANNEL | | String/[NSCANS] | GOLD channel ('A' or 'B'). |
| SCAN_START_TIME | | String/[NSCANS] | UTC start time of scan, e.g., "2017-06-21T23:46:38.015Z". |
| SCAN_STOP_TIME | | String/[NSCANS] | UTC end time of scan, e.g., "2017-06-21T23:46:38.015Z". |
| TLIMB_LOOKUP_TABLE | | String/[NSCANS] | Retrieval lookup table filename. |
| TIME.UTC | | String/[NLONS, NLATS, NSCANS] | UTC time for each pixel, e.g., "2017-06-21T23:46:38.015Z". |
| TANGENT_POINT_ALTITUDE | km | Float/[NLONS, NLATS, NSCANS] | Tangent point altitude at each latitude/longitude grid point. |
| TANGENT_POINT_LATITUDE | Degrees | Float/[NLONS, NLATS, NSCANS] | Latitude at each tangent point. |
| TANGENT_POINT_LONGITUDE | Degrees | Float/[NLONS, NLATS, NSCANS] | Longitude at each tangent point. |
| TANGENT_POINT_SOLAR_ZENITH_ANGLE | Degrees | Float/[NLONS, NLATS, NSCANS] | Solar zenith angle at each tangent point. |
| RADIANCE_NH_LBH | Rayleighs | Double/[NLONS, NLATS, NSCANS] | N2 LBH slant path radiance. |
| N2_LBH_UNC_RAN | Rayleighs | Double/[NLONS, NLATS, NSCANS] | Random uncertainty in LBH slant path radiance. |

| | | | |
|-------------------------|-----------|-------------------------------|---|
| NH_LBH UNC_SYS | Rayleighs | Double/[NLONS, NLATS, NSCANS] | Systematic uncertainty in LBH slant path radiance. |
| N2_SCALE_HEIGHT | km | Float/[NLATS, NSCANS] | Top side scale height of N2 LBH radiance profile. |
| N2_SCALE_HEIGHT_UNC_RAN | km | Float/[NLATS, NSCANS] | Random uncertainty in top side LBH scale height. |
| N2_SCALE_HEIGHT_UNC_SYS | km | Float/[NLATS, NSCANS] | Systematic uncertainty in top side LBH scale height. |
| N2_SCALE_HEIGHT_UNC_MOD | km | Float/[NLATS, NSCANS] | Model uncertainty in top side LBH scale height. |
| TLIMB | K | Float/[NLATS, NSCANS] | Retrieved exospheric temperature. |
| TLIMB_DQI | | Long/[NLONS, NLATS, NSCANS] | TLIMB data quality index per pixel (see table below). |
| TLIMB_UNC_RAN | K | Float/[NLONS, NLATS, NSCANS] | Random uncertainty in retrieved exospheric temperature. |
| TLIMB_UNC_SYS | K | Float/[NLONS, NLATS, NSCANS] | Systematic uncertainty in retrieved exospheric temperature. |
| TLIMB_UNC_MOD | K | Float/[NLONS, NLATS, NSCANS] | Model uncertainty in retrieved exospheric temperature. |
| MASK_N2_LBH | | Long/[NMASK] | Wavelength mask defining LBH bandpass used in retrieval. |
| MASK_WAVELENGTH | nm | Float/[NMASK] | Wavelength grid for N2_LBH mask. |

Table 5-12 TLIMB File Contents

5.6.2.2 TLIMB Data Quality Index

| Value | Description |
|--------------------|--|
| File Level | |
| 0 | No known data quality issues. |
| 1 | Invalid solar zenith angle. |
| 2 | Degraded algorithm performance due to high solar zenith angle. |
| 4 | Invalid N ₂ LBH radiance. |
| 8 | Invalid N ₂ LBH radiance random uncertainty. |
| 16 | Invalid N ₂ LBH radiance systematic uncertainty. |
| 32 | Invalid or insufficient tangent altitude coverage. |
| 64 | Invalid wavelength. |
| 128 | No valid output. |
| Pixel Level | |
| 0 | No known data quality issues. |
| 1 | Invalid solar zenith angle. |
| 2 | Degraded algorithm performance due to high solar zenith angle. |
| 4 | Invalid N ₂ LBH radiance. |
| 8 | Invalid N ₂ LBH radiance random uncertainty. |
| 32 | Invalid or insufficient tangent altitude coverage. |

| | |
|-----|----------------------------|
| 64 | Algorithm failure. |
| 128 | Low signal-to-noise ratio. |
| 256 | Star in the field-of-view. |

Table 5-13 TLIMB Data Quality Index